WALLEYE POLLOCK (*THERAGRA CHALCOGRAMMA*) DISTRIBUTION IN THE EASTERN BERING SEA RELATED TO FISHERY AND ENVIRONMENTAL FACTORS

A

THESIS

Presented to the Faculty

of the University of Alaska Fairbanks

in Partial Fulfillment of the Requirements

for the Degree of

DOCTOR OF PHILOSOPHY

BY

Haixue Shen, B.A., M.S.

Fairbanks, Alaska

December 2009

WALLEYE POLLOCK (*THERAGRA CHALCOGRAMMA*) DISTRIBUTION IN THE EASTERN BERING SEA RELATED TO FISHERY AND ENVIRONMENTAL FACTORS

By

Haixue Shen

RECOMMENDED:

Advisory Committee Chair

Interim Director, Fisheries Division

APPROVED:

Dean, School of Fisheries and Ocean Sciences

Dean of the Graduate School

Nov 16, 2009

Date

Abstract

Walleye pollock (*Theragra chalcogramma*) in the eastern Bering Sea (EBS) support the largest single-species fishery in the world. Pollock also play an important role in the EBS ecosystem as an important prey species. The decline of the western population of Steller sea lions during the 1980s and 1990s raised concerns about the potential competition between the pollock fishery and the sea lion population. My research focused on pollock distribution related to the fishery and physical environment at different temporal and spatial scales using fisheries acoustic data and observer data in the winter fishing season during 2002–2006. Temperature and wind played important roles in determining the pollock distribution in winter, especially from late February to March. The changes in spatial structure during the fishing season suggested that the fishery probably influenced pollock distribution by removing some portion of the local population and perhaps even smoothing out the aggregated distribution of pollock. At a small scale, pollock schools became smaller and denser. At the meso-scale, the distances between schools increased. At a larger scale, range estimates from variography increased which indicated that the spatial correlation among pollock extended to greater distances after fishing. Fishing behavior was also studied using Levy flight theory and its relation to pollock distribution in the EBS. Fishing behavior was significantly correlated to the fractal dimension of fish which measures the degree of pollock clustering, rather than to pollock spatial concentration or density in the EBS. The observer data were also included to analyze the effect of fish distribution on fishing behavior at the school scale. The results indicated that school density rather than the school size played an important role in fishing behavior. Finally, catch depletion analysis was used to examine the potential local depletion. While frequentist and Bayesian methods confirmed that the fishery caused slight local depletion in some areas in the EBS, the magnitude was less than that before sea lion protection measures were put into place in 1999 to spread out the fishery in space and time.

Table of Contents

Page

Page

Page

Page

Page

List of Figures

Page

Chapter 1

Chapter 2

Page

Chapter 3

Chapter 4

Chapter 5

Page

List of Tables

Page

Page

Preface

With the increasing use of fisheries acoustics, a project started in 2001 to explore the feasibility of using commercial vessels to collect hydroacoustic data for investigating the spatiotemporal changes of walleye pollock abundance and distribution in the Bering Sea. This project was funded by the Pollock Conservation Cooperative Research Center between 2001 and 2007, and was a collaborative project between University of Alaska Fairbanks (UAF), Alaska Fisheries Science Center (AFSC), and the fishing industry. The principal investigator was Dr. Terrance J. Quinn II (UAF), the co-investigator was Dr. Martin Dorn (AFSC), and Dr. James Ianelli (AFSC), Mr. Steven Barbeaux (AFSC) and Dr. Vidar Wespestad (UAF) were collaborators.

In 2001, a prototype data logger was developed to interface with the 38 kHz echosounder onboard fishing vessels, and acoustic backscatter was captured. Since 2002, the data loggers have been installed on three to seven commercial vessels to collect fisheries acoustic data during fishing seasons. Since 2005, data analysis started to be the focus of this project and formed the basis of my dissertation. The initial data process included integrating the acoustic backscatter by layers and regions, identifying echo trace and extracting pollock schools. The overall goal of my dissertation is to show that the processed data can be successfully used to investigate the changes of pollock distribution at different spatiotemporal scales during the fishing season.

This dissertation is part of the project. It would not have been possible without the help of numerous people. First and foremost, I'd like to thank my graduate committee chair Terrance J. Quinn II. Without his support, I could not have come to the United States and studied fisheries at UAF. His fisheries wisdom brought me new insight about fisheries science. Martin W. Dorn is a committee member who gave me many suggestions on fishing behavior and fisheries acoustics. Vidar Wespestad is also a committee member, who inspired me with the overall insights about fisheries. Special thanks also go to William Smoker who helped edit my drafts. I also would like to thank Steven J. Barbeaux and Matthew Kookesh for their significant help on processing the

acoustic data, and Franz Mueter for help with R software. I would also like to thank students that have helped me along the way, including Sara Miller, Peter-John Hulson and William Bechtol. Finally, my husband, Lu Li, has provided me with support in all forms. This work was supported by a grant from the Pollock Conservation Cooperative Research Center to the University of Alaska Fairbanks, and a student fellowship by the Cooperative Institute for Arctic Research with funds from the Alaska Fisheries Science Center, National Oceanic and Atmospheric Administration under cooperative agreement NA17RJ1224 with the University of Alaska. I thank the Graduate School for a Thesis Completion Fellowship.

General Introduction

The walleye pollock (*Theragra chalcogramma*) fishery is one of the largest, representing about 5% of the world's fish harvest (Bailey et al. 1999) and about 40% of the global whitefish production (Ianelli et al. 2008). Pollock are typically caught by large mid-water trawls deployed close to the bottom. According to American Fisheries Act (AFA), there are three fishing sectors operating in the EBS pollock fishery. The catcher-processor sector both catches and processes fish. The mothership sector receives and processes fish from other vessels without harvesting fish. The third sector is the inshore vessel sector including the smaller catcher/processor less than 125ft in length and catcher vessels delivering to processors in the inshore sector.

Since the early 1990s, there have been mainly two fishing seasons. The first one ("A" season) is in winter on spawning aggregations and begins on January 20th and lasts about 4–6 weeks. The second season ("B" season), which mainly target sparser concentrations of fishes during feeding, opens on September 1st with a variable fishing period over years. Since 1998, both fishing seasons were markedly extended, due to the formation of cooperatives. The "A" season extended into March and even April in some years. The opening of the second season advanced to middle-late June (Ianelli et al. 2008). In the "A" season, the fishery concentrates to the north or west of Unimak Island. In warmer years, the fishery may extend to waters around the Pribilof Islands. The fishing ground is located more north and west in the "B" season.

In the EBS, about 70% of the groundfish biomass consists of pollock (Wespestad 1993). Walleye pollock, as a forage fish, are very important to the EBS ecosystem. This stock contributes much of the food component of the extensive groundfishes, marine mammals, and seabirds (Springer 1992). Since the western population of Steller sea lion (*Eumetopias jubatus*) was classified as an endangered species according to ESA (Endanger Species Act) in 1997, there were great concerns about the potential biological competition between commercial pollock fishery and Steller sea lions. Some groups associated commercial fishing with the removal of prey species of sea lion which would

cause the decrease of predation efficiency of Steller sea lions and then affect the rebuilding of the population. The seasonal pollock fishery may induce a disproportionately high seasonal harvest rate which can result in a low seasonal prey density for sea lions. On the other hand, fishermen tend to chase aggregations of fish. The aggregation behavior of pollock may exacerbate this kind of local or seasonal depletion when the overall abundance is stable. The localized depletion is difficult to evaluate because the impact of the fishery on the distribution of pollock is not well known at a small spatial scale and also how this distribution may affect the prey density of sea lions is not well known.

Fish is one of the most dynamic elements of aquatic ecosystems. Acoustic methods make it possible to remotely, continuously, and synoptically observe the fish *in situ*. In addition to investigation of fishing catchability, acoustics are also very useful in the study of individual behavior, aggregation behavior of fish and the effects of environmental and biological factors (Godlewska and Zalewski 2001). Fisheries acoustics have been used worldwide, but most of them are used in scientific research surveys with specialized scientific echosounders. Echosounders capable of collecting scientific-quality data have been recently available to fishing vessels and are used to collect acoustic data opportunistically from the commercial fishing vessels. Although the opportunistic acoustic data (OAD) are not as precise as the scientific acoustic data, they have their own merits. For example, the OAD can cover the same area several times by different ships at different times which are very important to study temporal fish behavior. The OAD have been successfully used in a broad range of worldwide fisheries research (Stephenson et al. 1999, Wyeth et al. 2000, Melvin et al. 2002, O'Driscoll and Macaulay 2005). In US fisheries, the results of our project demonstrated the use of OAD in the EBS pollock fishery (Dorn et al. 2002, Barbeaux et al. 2005, Shen et al. 2008, Shen et al. 2009). One large scale project initiated in 2006 also explored the potential to develop an annual index of pollock abundance in the EBS using acoustic data from commercial fishing vessels (Ressler et al. 2008).

Pollock is the main sound scatter at 38 kHz in the southeastern of Bering Sea in winter (Barbeaux et al. 2005). Since 1979, acoustics have been successfully used in the echo-integration trawl (EIT) survey approximately triennially to estimate pollock in midwater (Traynor and Nelson 1985, Barbeaux and Dorn 2003). However, there are few surveys conducted in winter which make it difficult to study the interaction between fishing and pollock aggregations in the winter fishing season. The echosounders aboard fishing vessels may provide a different way to investigate pollock distribution during the winter fishing season. The high spatial resolution makes it possible to study pollock aggregating behavior at a finer scale. On the other hand, acoustic data can provide some information about the fleet behavior and, combining with the observer data, how these kinds of fishing patterns are related to pollock distribution and catchability.

This work used fisheries acoustic data collected by commercial fishing vessels and observer data to investigate how pollock distribution is related to the fishery and some key environmental factors in the winter fishing season. In chapter 1, the changes in school characteristics during fishing were examined at different spatial scales. The changed spatial pattern may be due to commercial fishing or to biological changes in behavior and movement related to physical environment and biological environment. To examine the mechanism of pollock distribution, the relationship between pollock and environmental factors was investigated using model-based geostatistics in chapter 2. To further understand the relationship between pollock and harvesters, in chapter 3, the searching behavior was examined to understand its relation to pollock distribution at a large spatial scale. Chapter 4 describes the relationship between pollock and harvesters at the school scale. Finally, the DeLury (1947) depletion model was used to examine local depletion using frequentist and Bayesian methods in chapter 5 for the years 2002–2006. This work updates earlier work by Battalie and Quinn (2006) which covered the time period 1995–1999.

References

Bailey, K.M., Quinn, T.J., II, Bentzen, P., and Grant, W.S. 1999. Population structure and dynamics of walleye pollock, *Theragra chalcogramma*. Adv. Mar. Biol. 37: 179–255.

Barbeaux, S.J., and Dorn, M.W. 2003. Spatial and Temporal Analysis of Eastern Bering Sea Echo Integration-trawl Survey and Catch Data of Walleye Pollock, '*Theragra chalcogramma*', for 2001 and 2002. NOAA Technical Memorandum NMFS AFSC. no. 136.

Barbeaux, S.J., Dorn, M., Ianelli, J., and Horne, J. 2005. Visualizing Alaska pollock (*Theragra chalcogramma*) aggregation dynamics. ICES Document CM 2005/U: 01. 12 pp.

Battaile, B.C., and Quinn, T.J., II. 2006. A DeLury depletion estimator for walleye pollock (*Theragra chalcogramma*) in the eastern Bering Sea. Nat. Resour. Model. 19: 655–674.

DeLury, D.B. 1947. On the estimation of biological populations. Biometrics 3: 145–167.

Dorn, M.W., Karp, W.A., Wespestad, V.G., Ianelli, J., and Quinn, T.J., II. 2002. Using fishing vessels to collect acoustic data for scientific purposes: preliminary results from midwater trawlers in the eastern Bering Sea walleye pollock fishery. ICES Symposium on Acoustics in Fisheries and Aquatic Ecology, Montpellier, France, 10–14 June 2002, Contribution 67, 11 pp.

Godlewska, M., and Zalewski, M. 2001. Hydroacoustics as a tool for studying the impact of habitat modification (degradation) upon fish: a review. Ecohydrol. & Hydrobiol. 1: 393–399.

Ianelli, J.N., Barbeaux, S., Honkalehto, T., Kotwicki, S., Aydin, K., and Williamson, N. 2008. Assessment of walleye pollock stock in the eastern Bering Sea. In: Stock assessment and fishery evaluation report for the groundfish resources of the Bering Sea/Aleutian Islands regions. North Pac. Fish. Mgmt. Council, Anchorage, AK, section 1: 47–136.

Melvin, G., Li, Y., Mayer, L., and Clay, A. 2002. Commercial fishing vessels, automatic acoustic logging systems and 3D data visualization. ICES J. Mar. Sci. 59: 179–190.

O'Driscoll, R.L., and Macaulay, G.J. 2005. Using fish-processing time to carry out acoustic surveys from commercial vessels. ICES J. Mar. Sci. 62: 295–305.

Ressler, P., Honkalehto, T., Towler, R., and Wilson, C. 2008. Using Acoustic Data From Vessels of Opportunity to Estimate Walleye Pollock Abundance in the Eastern Bering Sea. Proceedings of the SEAFACTS Symposium, Bergen, Norway.

Shen, H., Dorn, M.W., Wespestad, V., and Quinn, T.J., II. 2009. Schooling pattern of eastern Bering Sea walleye pollock and its effect on fishing behaviour. ICES J. Mar. Sci. 66: 1284–1288.

Shen, H., Quinn, T.J., II, Wespestad, V., Dorn, M.W., and Kookesh, M. 2008. Using acoustics to evaluate the effect of fishing on school characteristics of walleye pollock. In: Resiliency of gadid stocks to fishing and climate change. Alaska Sea Grant, University of Alaska Fairbanks: 125–140.

Simmonds, J., and MacLennan, D. 2005. Fisheries Acoustics: Theory and Practice. 2nd ed. Blackwell Science, Oxford. 437 pp.

Springer, A.M. 1992. A review: walleye pollock in the North Pacific-how much difference do they really make? Fish. Oceanogr. 1: 80–96.

Stephenson, R.L., Rodman, K., Aldous, D.G., and Lane, D.E. 1999. An in-season approach to management under uncertainty: the case of the SW Nova Scotia herring fishery. ICES J. Mar. Sci. 56: 1005–1013.

Traynor, J.J., and Nelson, M.O. 1985. Results of the U.S. hydroacoustic survey of pollock on the continental shelf and slope. *In*: Bakkala, R.G., and Wakabayashi, K. (eds), Results of cooperative U.S.–Japan groundfish investigations in the Bering Sea during May–August 1979. Int. North Pac. Fish. Comm. Bull. 44: 192–199.

Wespestad, V.G. 1993. The status of Bering Sea pollock and the effect of the "Donut Hole" fishery. Fisheries 18: 18–24.

Wyeth, M.R., Stanley, R.D., Kieser, R., and Cooke, K. 2000. Use and calibration of a quantitative acoustic system on a commercial fishing vessel. Can. Tech. Rep. Fish. Aquat. Sci. 2324: 53pp.

Chapter 1

Using acoustics to evaluate the effect of fishing on school characteristics of walleye pollock[1]

Abstract

Walleye pollock (*Theragra chalcogramma*) is the target of one of the world's largest fisheries and is an important prey species in the eastern Bering Sea (EBS) ecosystem. Little is known about the potential effects of fishing on the school characteristics and spatial distribution of walleye pollock. Few dedicated research surveys have been conducted during pollock fishing seasons so analysis of fishery data is the only feasible approach to study these potential effects. We used acoustic data collected continuously by one fishing vessel from January to February 2003, which operated to the north of Unimak Island in the EBS. Results from comparisons between two fishing periods showed significant changes of pollock distribution at different scales. The schools were smaller and denser during the second period. Furthermore, the spatial distribution of schools became sparser, as evidenced by the lower frequency of schools per elementary distance sampling unit and the increase in average next neighbor distances (NNDs). However, the average NND between schools within a cluster and the average abundance of clusters did not change significantly. Variography was used to investigate the changes at scales larger than 1 nautical mile. The increased range, nugget effect, and sill in the second period indicated changes of pollock spatial distribution; however it is unclear whether these changes are attributable to fishing or ecological processes.

---

[1] Shen, H., Quinn, T.J., II, Wespestad, V., Dorn, M.W., and Kookesh, M. 2008. Using acoustics to evaluate the effect of fishing on school characteristics of walleye pollock. In: Resiliency of gadid stocks to fishing and climate change. Alaska Sea Grant, University of Alaska Fairbanks: 125–140.

1.1 Introduction

Pelagic species usually form dense aggregations, or schools, during daytime and disperse at night. Walleye pollock (*Theragra chalcogramma*), which is semi-pelagic, forms persistent mid-water and near-bottom schools during the spawning season. For schooling species, the pattern of aggregation may have a large effect on fishery catchability (Castillo and Robotham 2004). Harvesters are skilled at finding fish aggregations using search strategies aided by technology (echosounders, oceanographic sensors, satellite imagery, etc). Consequently, strong interactions would be expected between the distribution and behavior of both fish and harvesters (Potier et al. 1997, Wilson et al. 2003, Bertrand et al. 2004). Wilson et al. (2003) studied how fishing activities affect the pollock distribution in Barnabas Trough in 2002, but did not find strong impacts. This paper will focus on changes in pollock schooling during a one-month fishing season in the eastern Bering Sea (EBS) using acoustic data collected aboard a commercial fishing vessel.

The commercial fishery for walleye pollock in the EBS is one of the largest fisheries in the world. This species is also an important component of the EBS ecosystem as a major prey species. Recently there has been great interest in the potential biological interaction between Steller sea lions (*Eumetopias jubatus*) and commercial fishing, following the classification in 1997 of the western population of Steller sea lions as endangered under the Endangered Species Act. It remains unknown whether fishing causes significant decreases in pollock abundance or changes in their spatial distribution that in turn adversely affects the foraging success of sea lions (Zeppelin et al. 2004).

Acoustic survey methods have been widely used for assessment because of their high temporal and spatial resolution (Simmonds and MacLennan 2005). Commercial vessels can be good platforms for collecting scientific acoustic data (Melvin et al. 1998, Wyeth et al. 2000, Melvin et al. 2002, Mackinson and Kooij 2006), and are particularly useful for in-season monitoring of stock trends (Stephenson et al. 1999, Melvin et al. 2001). Pollock is the main sound scatterer at 38 kHz during the winter spawning season

in the EBS (Dorn et al. 2002). Since 1979, acoustics have been used to estimate pollock abundance in mid-water during the echo-integration trawl (EIT) surveys of the EBS (Barbeaux and Dorn 2003). However, these surveys are mainly conducted in the summer, except for several winter surveys conducted in 2001 and 2002 (Honkalehto et al. 2002). The first major fishing season (called the "A" season opening on January 20th) occurs in winter. Consequently, surveys do not provide adequate information about interactions between fishing and pollock aggregations (Barbeaux and Dorn 2003).

Scientists from the Alaska Fisheries Science Center (AFSC) and University of Alaska Fairbanks (UAF) developed a prototype data logger to interface with 38 kHz echosounders onboard fishing vessels and capture the acoustic backscatter returns in 2001 (Dorn et al. 2002). Since 2002, the joint opportunistic acoustic data (OAD) program has been collecting, processing, and storing acoustic data from selected factory trawlers participating in the eastern Bering Sea pollock fishery (Dorn et al. 2002). Seven fishing vessels collected acoustic data during normal fishing operations in the "A" season when the fish form pre-spawning aggregations. These data make it possible to study the relationship between pollock aggregations and fishing activities. However, due to difficult weather conditions and equipment breakdowns, much of the opportunistic data cannot be utilized. Here, only the acoustic data collected by one vessel in 2003, which had fewer missing pings and was generally of higher quality than data from other vessels, were used to examine pollock aggregation patterns in the area north of Unimak Island.

1.2 Materials and methods

1.2.1 Data collection and study area

The vessel is a large factory trawler that mainly operated north of Unimak Island (near 54°46′N, 164°08′W) in the EBS from January to February 2003 (Figure 1.1). The vessel operated in the same area during the early and late periods of the fishing season. Acoustic data were logged with an uncalibrated 38 kHz Simrad ES60 split-beam echosounder with 1 ms nominal pulse length and 7.1° beam width. Uncalibrated acoustic

data are of course not suitable for absolute fish density estimation; however, the purpose of this study was the analysis of school morphology characteristics, spatial patterns, and relative changes in school density, which should be robust to the lack of calibration.

1.2.2 Data analysis

Echoview 3.30 software (SonarData 2005) was used to process raw data and classify the echo trace from 15 m below the surface to 0.5 m above the bottom. Walleye pollock schools were detected and characterized using the school module in Echoview. We used only data collected during daylight hours, when pollock show schooling behavior. Criteria from Wilson et al. (2003) were used to classify the pollock aggregations as follows. The threshold for detecting schools was set to –70 dB at 1 m. The other six input parameters for the school algorithm were minimum school length (40 m), minimum school height (5 m), minimum candidate length, i.e. minimum length allowed for a single school candidate (5 m), minimum candidate height, i.e. minimum height allowed for a single school candidate (2 m), maximum vertical linking distance, i.e. maximum vertical distance allowed between two school candidates being linked to form a school (5 m) and maximum horizontal linking distance (20 m) (SonarData 2005). A representative echogram showing walleye pollock schools is shown in Figure 1.2.

School descriptors were generated by the Echoview software, including morphometric descriptors (length, thickness and area of schools, Figure 1.2), positional descriptors (longitude, latitude, school depth, bottom depth), and energetic descriptors (S_v, volume backscattering strength; *NASC*, nautical area scattering coefficient) (Simmonds and MacLennan 2005). Based on the above descriptors, some relational descriptors were also determined as follows. Fractal dimension of a school is an index of shape complexity and is a function of school perimeter related to school area (Nero and Magnuson 1989). A school with a smooth outline has a fractal dimension close to 1, and a very irregularly shaped school has fractal dimension close to 2. The increase of fractal dimension may be indicative of redistribution of a fish aggregation under disturbance. The line backscattering coefficient, s_L, is a measure of a school's total backscatter and is

calculated by integrating the volume backscattering coefficient (s_v) over the sectional area of aggregation (MacLennan et al. 2002). An abundance index, I_{abun}, was obtained by multiplying *NASC* by school area. The vertical distribution of a school, V_D, is the distance between school depth and bottom depth.

To examine pollock schooling changes during fishing, two separate fishing periods were used to investigate the changes at the school scale and larger scales. Based on the available data and the track of the fishing vessel, the first period was set from January 22 to February 5, and the second period was set from February 14 to February 24. The vessel operated in roughly the same area in both periods, allowing comparisons to be made between periods (Figure 1.1). For hypothesis testing, the detected schools during the two periods were pooled and the statistical significance was determined by Student's *t*-tests (Zar 1999).

It is common for schools of pelagic species to group together in larger scale aggregations, called clusters (Swartzman 1997, Petitgas 2003). To test if there was clustering of schools, the school data for each day were binned into 1 nautical mile (nm) elementary distance sampling units (EDSUs) along the fishing track; this distance is commonly used in acoustic analysis (Reid 2000). Statistical significance was tested by the Pearson χ^2 criterion: $\chi^2 = \sum_{i=1}^{m} (n_i - \overline{n})^2 / \overline{n}$, which has a χ^2 distribution with m–1 degree of freedom (Swartzman 1997), where m is the number of EDSUs, n_i is the number of schools of the ith EDSU, and $\overline{n}$ is the average number of schools in an EDSU.

If there was evidence of clustering, the patterns in school clusters were studied. To define a cluster, the next-neighbor distance (NND) was computed for each school along the fishing track. A 1 km threshold NND was used to group schools into different clusters because it is near the leveling-off point of most NND-cumulative distributions (Figure 1.3) (Petitgas 2003). This point is used as the threshold because the curvature of the distribution curve is related to the repetition rate of the process and hence to the scale of the clustering. Figure 1.4 shows the schematic relationship between a cluster and schools.

After clustering, some additional variables were recorded: the number of clusters (N_{clus}), the length of each cluster (L_{clus}), and the number of solitary schools (N_{soli}) (schools not in clusters), the number of schools per cluster (N_s), and the number of schools per unit cluster length (ρ_{clus}), the average next-neighbor distance among solitary schools (D_{soli}), and the average distance to the next cluster (D_{clus}). The abundance index was also calculated for clusters (I_{clus}) and solitary schools (I_{soli}). To test if the threshold is appropriate, a linear regression was conducted for the number of schools in cluster versus the cluster length (Petitgas 2003).

Variography was used to examine changes in the spatial structure between the two fishing periods. Based on the detected schools, we calculated the arithmetic average of the school volume backscattering coefficient (s_v) within each 1 nm EDSU for constructing one-dimensional variograms. Acoustic survey data are characterized by a few large values with a majority of rather low values. This may cause severe problems in structural analysis based on the semi-variogram and its parameters. Consequently a robust version of the experimental semi-variogram (Cressie and Hawkins 1980) is used:

$$\gamma^*(h) = \frac{1}{2} \frac{\left\{ 1/|N(h)| \sum_{i=1}^{N(h)} |z(s_i) - z(s_i + h)|^{1/2} \right\}^4}{0.457 + 0.494/|N(h)|},$$

where $z(s_i)$ is the value of school descriptor s_v at location s_i, $z(s_i + h)$ is the value of s_v at a distance h from s_i, and $N(h)$ is the number of pairs with a distance h apart.

A spherical model was used to fit semi-variograms (Cressie 1993). The range, sill, and nugget characterize the spatial structure of pollock at a scale larger than 1 nm. The range is the distance where the semi-variogram levels off at the sill (Figure 1.5). The discontinuity at the origin is the nugget effect caused by measurement error and variation at scales smaller than the lag size.

1.3 Results

1.3.1 Echo trace classification

There were 808 schools identified in the first period and 474 schools identified in the second period. Several school characteristics exhibited significant differences between the two periods (Table 1.1). School density was significantly higher in the second period, as evidenced by higher NASC and s_L ($P<0.001$). The density almost doubled but the school size became smaller in the second period, as evidenced by the decrease in all morphometric descriptors (school length, thickness and area in Table 1.1, $P<0.01$). Despite the smaller size in the second period, the abundance index was higher ($P<0.05$). Fractal dimension was significantly different between the two periods ($P<0.001$); the schools became smoother in the second period as indicated by their smaller fractal dimensions. Unlike the differences in morphometric and energetic descriptors, the vertical distribution of schools (approximately 7.5 m above bottom, Table 1.1) was similar for the two periods ($P=0.74$).

1.3.2 NND-clustering

The average number of schools per EDSU for each day, $\overline{n}$, was higher in the first fishing period than in the second period (Table 1.2). A non-parametric test was used to test the difference of the daily $\overline{n}$ in the two periods and the results demonstrated that they are statistically different (Wilcoxon rank test, $P<0.05$). The clustering of schools was apparent for most days (Table 1.2). It is not surprising that the average NND increased in the second period ($P<0.001$, Table 1.3), because the number of schools per EDSU was smaller (Table 1.2).

With a fixed 1 km threshold to identify clusters, 723 schools were grouped into 115 clusters with 85 solitary schools in the first period. In the second period, 349 schools were grouped into 80 clusters with 125 solitary schools. The coefficients of determination (R^2) from the linear regression of the number of schools in a cluster on cluster length are high in the two periods (0.92 and 0.88, respectively).

Although the average NND between schools increased in the second period, the distances between schools within the clusters did not differ in the two periods, because there was similar number of schools per unit cluster length (i.e., ρ_{clus}, Table 1.3). The larger NND is due to the larger distance between clusters (P=0.04) and between solitary schools (P=0.10). In contrast, there are more schools in each cluster in the first period (P<0.05), which resulted in the cluster length being significantly higher in the first period (P<0.05). Also, the number of schools per km significantly decreased and the ratio of solitary schools to total schools significantly increased in the second fishing period (Wilcoxon rank test, P<0.05) (Figure 1.6). However the decrease of the number of clusters per km was not significant (Wilcoxon rank test, P=0.098) (Figure 1.6). The Wilcoxon rank test was used here because these ratios were calculated for each day and sample sizes were small. Cluster abundance was similar for the two periods (P=0.96) although on average clusters were of smaller size with fewer schools in the second period. Similarly, abundance of solitary schools did not differ between the two periods.

1.3.3 Variography

Variograms for the average s_v showed significant structure in the two periods (Figure 1.7). The nugget effect only contributed a small part of the variance (42% for the first period and 25% for the second period). The variograms for the two periods were different, indicating that the spatial structure of walleye pollock changed between the two periods. The estimated nugget, sill, and range (0.12, 0.29, 5.9, respectively) in the first period were smaller than those (0.66, 2.61, 16.8, respectively) in the second period, which indicates an increase in variability of pollock schools at all spatial scales and that the spatial structure of pollock schools was more extended after fishing.

1.4 Discussion

Walleye pollock is the primary prey species of Steller sea lion. The decline in the sea lion abundance has caused concerns about potential competition between commercial

fishing and sea lions. Wilson et al. (2003) described two kinds of fishing effects on pollock. First, fishing removal may cause the decline of the stock abundance in a local area. However, Battaile (2005) found evidence pollock recover from this impact in about one week, so this effect may not be strong. Second, fishing may affect long-term pollock behavior that may cause changes in pollock spatial structure. The fish may dive deeper after fishing or form smaller but denser aggregations. The spatial coverage of fish may decrease after disturbance. Both of these effects may impact the foraging behavior of predators on pollock.

To study the effects of fishing on a fish population, one method is to observe the exploited population over a short period, such as the Wilson et al. (2003) study on the interaction between pollock and fishing in the Gulf of Alaska east of Kodiak Island. The study area was surveyed before, during, and after fishing activities. Pollock spatial distribution, biomass and vertical distribution were compared to investigate the effect of fishing. They were unable to detect significant links between fishing and pollock distribution and biomass.

We used two fishing periods because nearly the same areas were fished in both (Figure 1.1). Although the fishing tracks were not exactly the same in the two periods as in a scientific survey, the fishing tracks were highly overlapped in the study area. Most of the areas traversed in the second period had been traversed during the first period. Therefore, we considered it reasonable to compare the pollock distribution during the two periods.

The study vessel headed northeast after February 6 and returned to the study area on February 14. The other fishing vessels exhibited similar fishing patterns based on our data. This exploitation pattern gave pollock in the study area about one week without fishing impacts. The average abundance was similar in the two fishing periods, suggesting that any local depletion that may have occurred was apparently replenished by pollock moving in from other areas. However, the changed spatial distribution (smaller schools with larger next neighbor distance, Table 1.1 and Table 1.3) may reduce the

encounter rate of Steller sea lions with pollock schools and thus affect the predation process of sea lion.

This paper mainly addressed the question of changes in pollock spatial distribution at different scales over a short time period (about one month). After some days of fishing, the pollock schools seemed to have significant changes at the small scale (school level). The schools became denser (increased *NASC* and s_L), smaller (decreased morphometric descriptors) and smoother (decreased fractal dimension). Since total abundance did not change substantially between the two fishing periods, an increase in school density would be expected to result in a decrease in school frequency and an increase in the distance among schools. Unlike the significant changes in morphometric and energetic descriptors, the vertical distribution did not change significantly, suggesting that the fish did not dive deeper as has been hypothesized. The bottom depth is mostly less than 150 meters on the fishing grounds north of Unimak Island. Since most of the detected schools were just above the bottom, the ability of schools to dive deeper is restricted, so the vertical distribution of disturbed fish in deeper fishing areas cannot be inferred from our study.

Clustering of schools is a common phenomenon for schooling fish (Swartzman 1997, Petitgas 2003). Our study confirmed that there is clustering of EBS pollock schools. To identify the clusters, both fixed distance threshold (Swartzman 1997) and variable threshold (Petitgas 2003) methods have been used. For comparison of clusters in the two fishing periods, we chose the fixed threshold method, because of the short time period and small area covered in this study. The 1 km threshold value was chosen based on the cumulative frequency of NNDs. Our results established that this threshold worked well according to the criteria by Petitgas (2003). There are neither too many clusters nor solitary schools, and there is a high R^2 for the linear regression of the number of schools in a cluster on cluster length.

Similar to the results at the school level, there were also significant changes at the level of clusters of schools and 1 nm EDSU. A decrease of school numbers per EDSU

and the increase in NNDs suggest that fishing may have had a short-term effect. One interesting result is that the NND between schools within clusters did not change. This suggests that there is some attraction/repulsion process that keeps NND within clusters the same while changing the number of schools in a cluster. The increased overall NND was caused by an increase in inter-cluster distance or perhaps distances between solitary schools (Table 1.3). In contrast, the cluster abundance was similar between the two periods despite the changes of school characteristics in clusters. Similarly, average abundance of solitary schools did not differ during the two periods. Pollock may find more places suitable for aggregation in the absence of fishing, but then find fewer areas suitable after encountering fishing impacts. Once these preferred areas are chosen, pollock might form tighter and smaller schools or clusters of schools with high abundances.

Variograms display the spatial distribution pattern of pollock schools at a scale larger than 1 nm. The nuggets for the two periods contributed only a small portion of the variance which suggests the presence of spatial correlation. From the increased sill and nugget, pollock schools became more variable in spatial distribution at all scales greater than 1 nm, which is also found at school level. In the second period, most of the school descriptors had higher variances (Table 1.1). The range in the second period is higher than that of the first period (Figure 1.7), indicating that spatial correlation of pollock extends to greater distances.

In summary, our results suggest the following operative hypothesis of pollock schooling behavior during the A fishing season. Pollock aggregate into schools in the daytime and disperse at night during the spawning season. After about two weeks of fishing, the aggregation pattern changes both at the school scale and scales larger than 1 nm. Pollock aggregate in smaller but denser schools that have a patchier distribution in space. The changed aggregation pattern may be due to commercial fishing or to biological changes in behavior and movement. It is unknown whether the increased patchiness of pollock is a persistent feature of the A fishing season. This study is a first

look at pollock schooling and the affects of fishing on pollock school distribution. The observations are somewhat limited, so it is difficult to draw strong conclusions. However, the results of this study suggest fishing may alter school distribution and density. We recommend further research be undertaken to better understand the relationship between fishing removals and the subsequent reduced spatial extent of the pollock and the possible effect on the foraging ability of Steller sea lions and other predator species dependent on pollock.

1.5 Acknowledgments

This research is funded by a grant from the Pollock Conservation Cooperative Research Center to the University of Alaska Fairbanks. Additional funds for student support were provided by the Alaska Fisheries Science Center. We thank Richard Marasco, Anne Hollowed, James Ianelli, and Steve Barbeaux for their help. Helpful reviews by Christopher Wilson and an anonymous referee are greatly appreciated.

1.6 References

Barbeaux, S.J., and M.W. Dorn. 2003. Spatial and temporal analysis of eastern Bering Sea echo integration-trawl survey and catch data of walleye pollock, *Theragra chalcogramma*, for 2001 and 2002. NOAA Technical Memorandum NMFS, AFSC, No. 136 pp.

Battaile, B.C. 2005. A walleye pollock (*Theragra chalcogramma*) depletion estimator for the eastern Bering Sea. Ph.D. dissertation, University of Alaska, Fairbanks, Alaska. 180 pp.

Bertrand, S., E. Díaz, and M. Ñiquen. 2004. Interaction between fish and fisher's spatial distribution and behaviour: an empirical study of the anchovy (*Engraulis ringens*) fishery of Peru. ICES J. Mar. Sci. 61: 1127–1136.

Castillo, J., and H. Robotham. 2004. Spatial structure and geometry of schools of sardine (*Sardinops sagax*) in relation to abundance, fishing effort, and catch in northern Chile. ICES J. Mar. Sci. 61: 1113–1119.

Cressie, N.A.C. 1993. Statistics for Spatial Data. Wiley, New York. 900 pp.

Cressie, N.A.C., and D.M. Hawkins. 1980. Robust estimation of the variogram. I.J. Int. Assoc. Math. Geol. 12: 115–125.

Dorn, M.W., W.A. Karp, V.G. Wespestad, J. Ianelli, and T.J. Quinn II. 2002. Using fishing vessels to collect acoustic data for scientific purposes: preliminary results from midwater trawlers in the eastern Bering Sea walleye pollock fishery. ICES Symposium on Acoustics in Fisheries and Aquatic Ecology, Montpellier, France, 10–14 June 2002, Contribution 67, 11 pp.

Honkalehto, T., N. Williamson, D. Hanson, D. McKelvey, and S. de Blois. 2002. Results of the echo Integration-trawl survey of walleye pollock (*Theragra chalcogramma*) conducted on the southeastern Bering Sea shelf and in the southeastern Aleutian basin near Bogoslof Island in February and March 2002. AFSC Processed Report 2002-02. 49 pp.

Mackinson, S., and J.V.D. Kooij. 2006. Perceptions of fish distribution, abundance and behaviour: Observations revealed by alternative survey strategies made by scientific and fishing vessels. Fish. Res. 81: 306–315.

MacLennan, D., P.G. Fernandes, and J. Dalen. 2002. A consistent approach to definitions and symbols in fisheries acoustics. ICES J. Mar. Sci. 59: 365–369.

Melvin, G.D., K.J. Clark, F.J. Fife, M.J. Power, S.D. Paul, and R.L. Stephenson. 1998. Quantitative acoustic surveys of 4WX herring in 1997. DFO Canada Stock Assessment Section Research Document, 98/81. 22p.

Melvin, G.D., Y. Li, L.A. Mayer, and A. Clay. 2002. Commercial fishing vessels, automatic acoustic logging systems and 3-D data visualization. ICES J. Mar. Sci. 59: 179–190.

Melvin, G.D., R.L. Stephenson, M.J. Power, F.J. Fife, and K.J. Clark. 2001. Industry acoustic surveys as the basis for in-season decisions in a comanagement regime. In: Funk, F., J. Blackburn, D. Hay, A.J. Paul, R. Stephenson, R. Toresen, and D. Witherell, (Eds.), Herring Expectations for a New Millennium. University of Alaska Sea Grant, AK-SG-01-04, Fairbanks, pp. 675–688.

Nero, R.W., and J.J. Magnuson. 1989. Characterization of patches along transects using high-resolution 70-kHz integrated acoustic data. Can. J. Fish. Aquat. Sci. 46: 2056–2064.

Petitgas, P. 2003. A method for the identification and characterization of clusters of schools along the transect lines of fisheries-acoustic surveys. ICES J. Mar. Sci. 60: 872–884.

Potier M., P. Petitgas, and D. Petit. 1997. Interaction between fish and fishing vessel in the Javanese purse seine fishery. Aquat. Living Res. 10: 149–156.

Reid, D.G. 2000. Report on echo trace classification. ICES Cooperative Research Report 238, 107pp.

Simmonds, J., and D. MacLennan. 2005. Fisheries Acoustics: Theory and Practice. Blackwell Science, Oxford. 437 pp.

SonarData. 2005. Echoview. Version 3.30. <http://www.sonardata.com/webhelp /Echoview.htm>. Tasmania, Australia. (May 2005).

Stephenson, R.L., K. Rodman, D.G. Aldous, and D.E. Lane. 1999. An in-season approach to management under uncertainty: the case of the SW Nova Scotia herring fishery. ICES J. Mar. Sci. 56: 1005–1013.

Swartzman, G. 1997. Analysis of the summer distribution of fish schools in the Pacific Eastern Boundary Current. ICES J. Mar. Sci. 54: 105–116.

Wilson, C.D., A. B. Hollowed, M. Shima, P. Walline, and S. Stienessen. 2003. Interactions between commercial fishing and walleye pollock. Alaska Fish. Res. Bull. 10: 61–77.

Wyeth, M. R., R.D. Stanley, R. Kieser, and K. Cooke. 2000. Use and calibration of a quantitative acoustic system on a commercial fishing vessel. Can. Tech. Rep. Fish. Aquat. Sci. 2324: 53pp.

Zar, J.H. 1999. Biostatistical analysis. Prentice-Hall, New Jersey. 663 pp.

Zeppelin, T.K., J.T. Dominic, A.C. Katherine, J.O. Trevor, and J.G. Carolyn. 2004. Sizes of walleye pollock (*Theragra chalcogramma*) and Atka mackerel (*Pleurogrammus monopterygius*) consumed by the western stock of Steller sea lions (*Eumetopias jubatus*) in Alaska from 1998 to 2000. Fish. Bull. 102: 509–521.

Table 1.1 The school descriptors generated by Echoview and some relational descriptors. Student's *t*-test was used to test for significant differences between the two periods. s_L is the line backscattering coefficient, I_{abun} is the abundance index of school and V_D is the distance between the school depth and bottom depth.

	Period 1		Period 2		*P*-value
	Average	SE	Average	SE	
Length (m)	114.46	7.80	80.75	6.31	0.003
Thickness (m)	15.26	0.26	11.27	0.28	<0.001
Area (m^2)	899.39	73.50	580.77	85.21	0.006
NASC (m^2/nmi^2)	22630	2015	44569	3144	<0.001
Fractal dimension	1.478	0.004	1.429	0.004	<0.001
s_L (m)	0.048	0.004	0.079	0.009	<0.001
I_{abun}	5.80	0.65	8.91	1.46	0.03
V_D (m)	7.42	0.22	7.56	0.40	0.74

Table 1.2. Statistics of schools per elementary distance sampling units (EDSU). $\bar{n}$ is the average number of schools in the EDSU. The asterisk means the chi-square test is statistically significant at a $P<0.05$ level.

Date	$\bar{n}$	$\chi 2$	Date	$\bar{n}$	$\chi 2$
22-Jan	3.18	364*	14-Feb	1.69	107*
23-Jan	3.67	220*	15-Feb	2.14	248*
24-Jan	4.05	168*	16-Feb	1.38	183*
25-Jan	2.21	174*	17-Feb	2.24	169*
26-Jan	0.52	89*	18-Feb	2.48	319*
27-Jan	1.03	258*	19-Feb	0.5	102
28-Jan	1.76	280*	20-Feb	1.17	157*
29-Jan	2.36	402*	21-Feb	1.65	378*
1-Feb	2.71	259*	22-Feb	1.2	185*
2-Feb	0.56	64	23-Feb	0.35	101*
3-Feb	1.78	136*	24-Feb	0.35	131*
4-Feb	1.69	79*			
5-Feb	3.39	412*			

Table 1.3. Parameters estimated by NND-clustering procedure. (NND: average next-neighbor distance among all schools; D_{soli}: average next-neighbor distance among solitary schools; D_{clus}: average distance to the next cluster; L_{clus}: average length of clusters; N_s: average number of schools per cluster; ρ_{clus}: average number of schools per unit cluster length; I_{clus}: average abundance index of clusters; I_{soli}: average abundance index of solitary schools). The Student's *t*-test was used for the statistical significance.

	Period 1		Period 2		
	Average	SE	Average	SE	*P* value
NND (m)	1232.2	104.8	2399.7	251.5	<0.001
D_{soli} (m)	4149.4	368.7	5225.5	538.3	0.10
D_{clus} (m)	6467.3	886.4	10298.7	1832.1	0.04
L_{clus} (m)	1724.7	200.9	1203.0	148.6	0.04
N_s	6.28	0.64	4.36	0.47	0.02
ρ_{clus} (#/km)	5.65	0.42	5.43	0.47	0.74
I_{clus}	34.04	5.81	33.52	9.15	0.96
I_{soli}	8.93	3.27	12.09	3.53	0.53

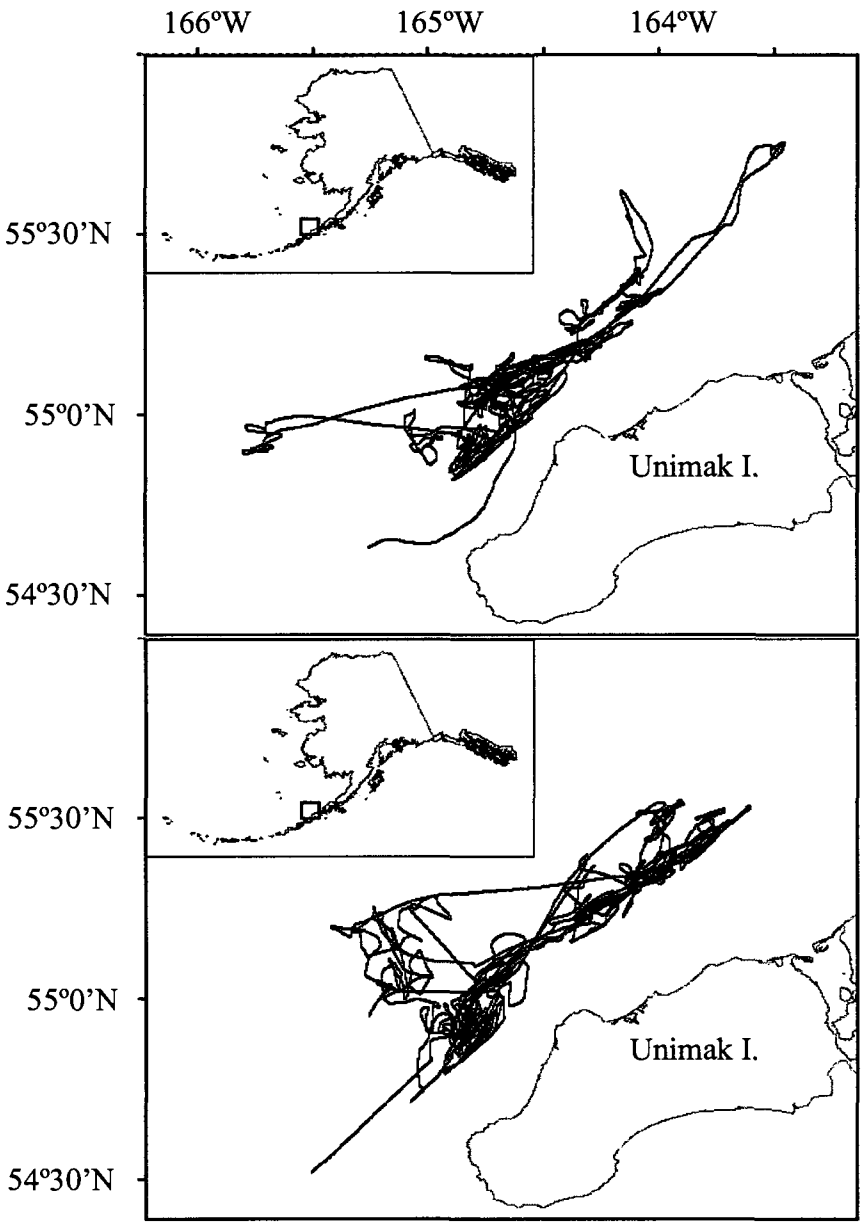

Figure 1.1. Area of operation of the fishing vessel in January-February, 2003. (The upper and lower panels display the fishing tracks from January 22 to February 5, and from February 14 to February 24, respectively.)

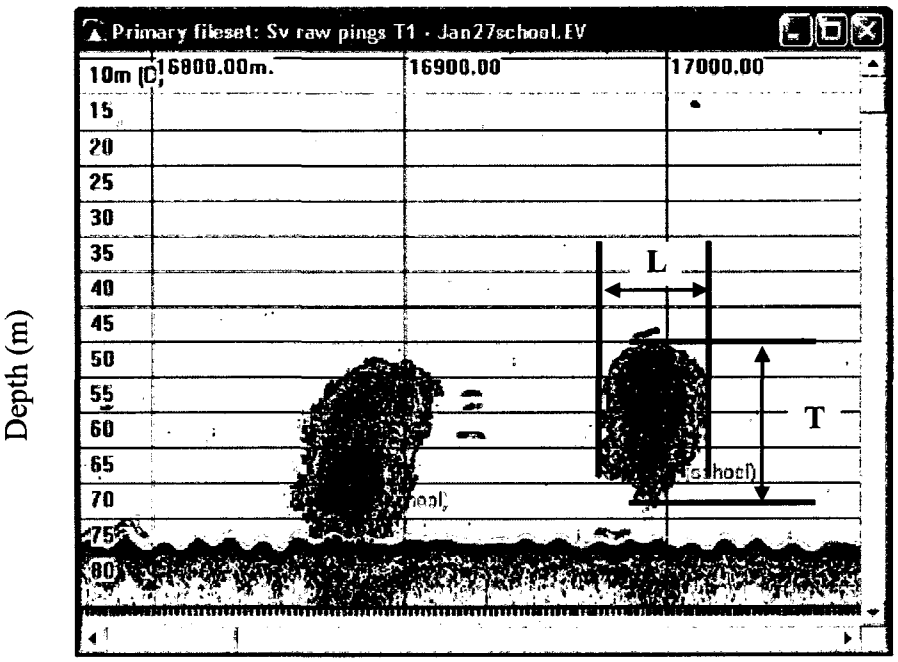

Figure 1.2. Representative echogram of walleye pollock schools. L is the length and T is the thickness of a school.

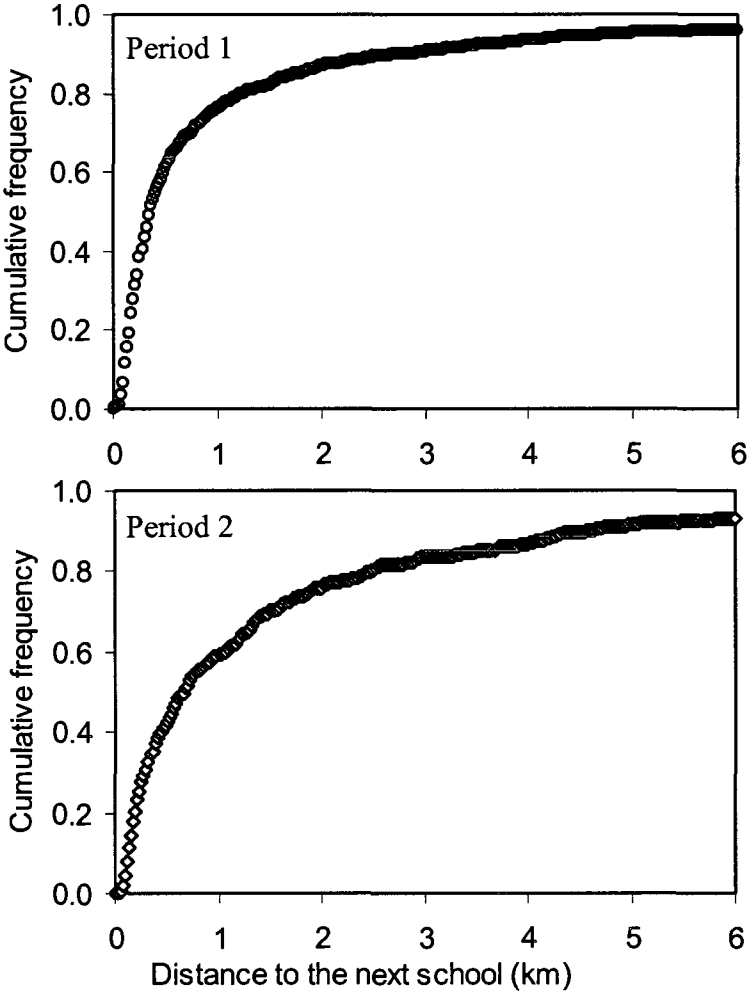

Figure 1.3. The cumulative distribution of the distance to the next school along the fishing track in the two periods.

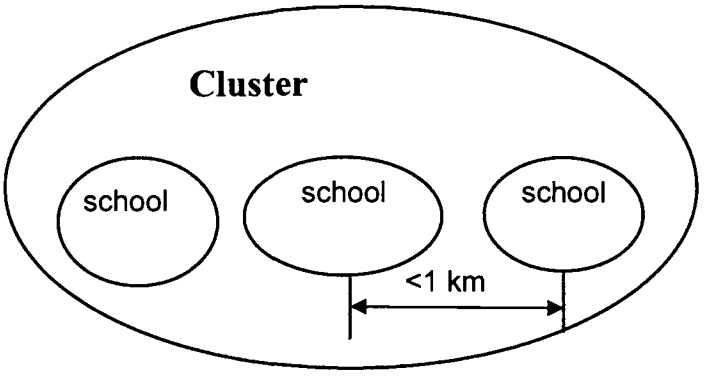

Figure 1.4. Schematic figure showing the relationship between cluster and schools.

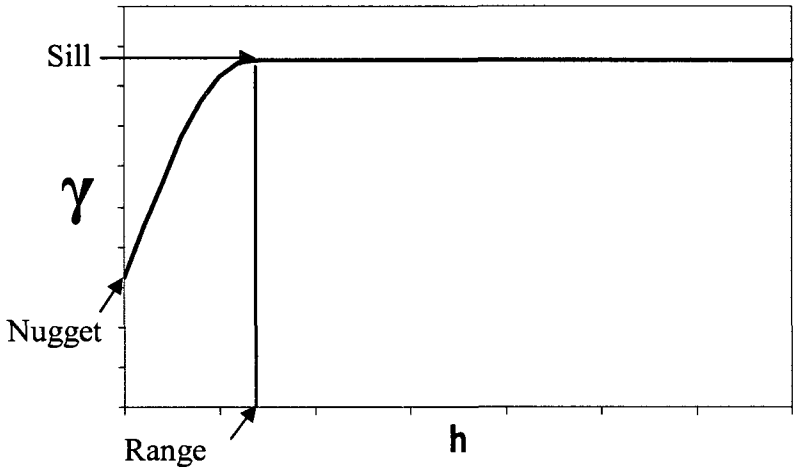

Figure 1.5. Parameters of the model variogram.

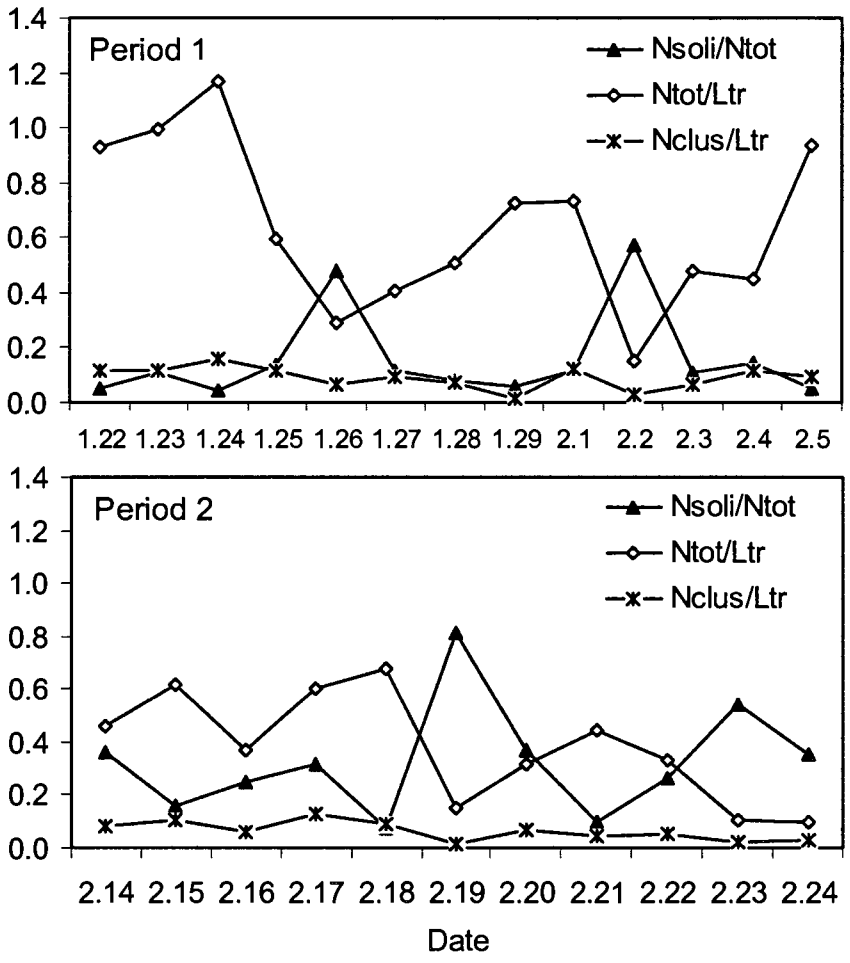

Figure 1.6. Results of the NND-clustering procedure for the two fishing periods: ratio of solitary school (N_{soli}) to total number of schools (N_{tot}), ratio of N_{tot} to track length (L_{tr}), and ratio of N_{soli} to L_{tr}.

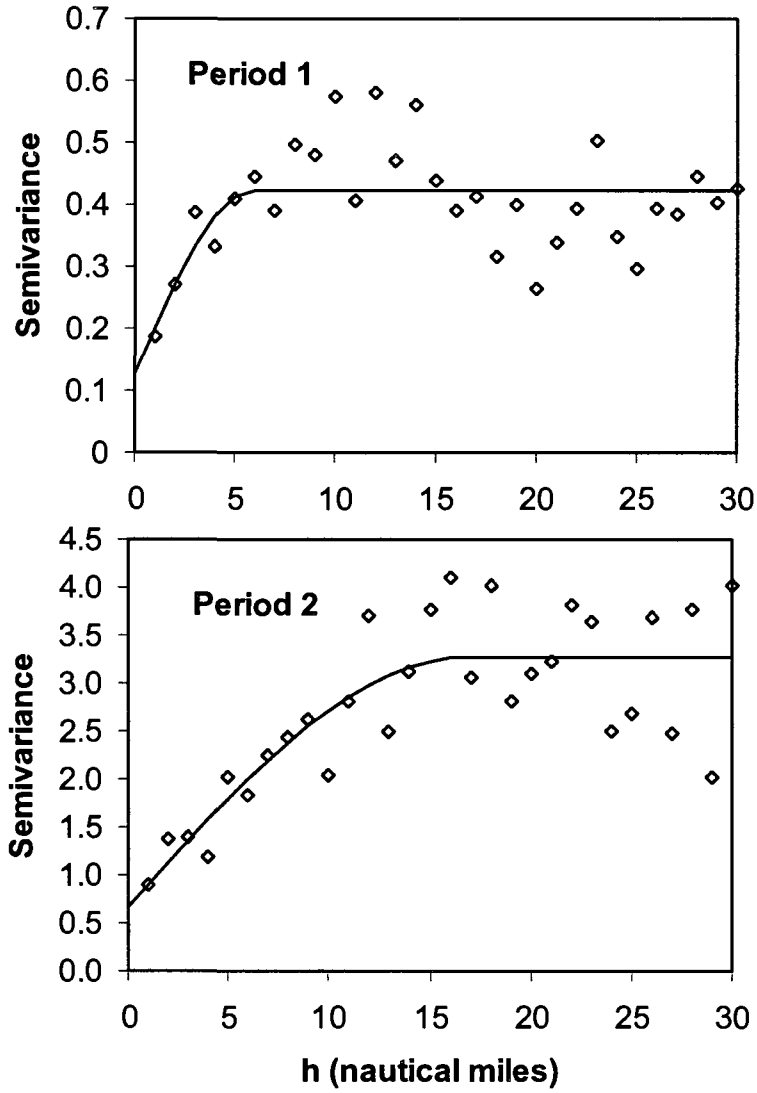

Figure 1.7. Variograms for two fishing periods. Lag interval was 1 nautical mile and a total of 30 lags were used.

Chapter 2

The spatial distribution of walleye pollock in the eastern Bering Sea related to the environmental factors[1]

Abstract

Walleye pollock distribution in the eastern Bering Sea was investigated by examining the relationship between three physical environmental factors and densities of pollock encountered during winter fishing. Temperature and wind appeared to be important factors in pollock distribution, especially pollock distribution around the Pribilof Islands from late February to late March. The dome-shaped relationship between pollock density and temperature indicated that pollock avoided not only cold water but also water with relatively high temperatures. The general spatial distribution of pollock was confined by cold water, especially in cold years, while at smaller temporal and spatial scales, wind was related to pollock distribution. Pollock density decreased as the wind speed increased. The effect of bottom depth was not statistically significant in most data sets, but the range of depths was limited ranging from 65 m to 150 m. Even after accounting for the influence of environmental factors, there was spatial structure in the error component in a spatial model of pollock distribution. Models with spatial autocorrelation fitted the data substantially better than models without spatial structure. Fishery management in the future should include this spatial structure when evaluating the stock status.

---

[1] Shen, H., Quinn, T.J., II, Wespestad, V., and Dorn, M.W. The spatial distribution of walleye pollock in the eastern Bering Sea related to the environmental factors. Prepared for submission to the Fisheries Research.

2.1. Introduction

The eastern Bering Sea (EBS) is a semi-enclosed, high-latitude area and its large continental shelf provides a good habitat for many marine species. Oceanographic variables in the EBS have strong seasonal variability (Stabeno et al., 2005). The sea ice cover in winter has an important effect on the physical and biological ocean environment of the EBS (Schumacher and Stabeno, 1998; Hunt et al., 2002). In the past, there was substantial inter-annual variability in its air-ice-ocean environment. However, the recent decade has been characterized by persistent warm ocean temperatures and lack of sea ice in the southern EBS (Stabeno et al., 2007). Since sea ice plays an important role in determining the timing of the spring phytoplankton bloom, Hunt et al. (2002) found that the warm conditions obviously benefited the pelagic fishery (e.g., 1996, 1998, 2000) because the later spring bloom in warm years matched the growth of zooplankton which provided abundant food for pelagic fish species. Although the ocean temperature was generally higher than temperatures before 2000, the inter-annual variability was still large in the winter season. For example, the temperature in January 2006 was very low and even below the 1961–2000 average, and the coverage of sea ice extended to the south of average locations in January 2006 (Rodionov et al., 2006).

Walleye pollock (*Theragra chalcogramma*) is commercially and ecologically important species in the EBS ecosystem. Walleye pollock support the largest single-species fishery in the world and represent over 40% of the global whitefish production (Ianelli et al., 2008). As an important prey species, pollock represents a major biological component of the EBS ecosystem. Therefore, the abundance and distribution of pollock can influence the abundance and distribution of the predators of pollock, such as Steller sea lions. Some studies found that pollock abundance and distribution are influenced by temperature (Swartzman et al., 1994; Kotwicki et al., 2005) as well as other environmental factors (Mueter et al., 2006). Because of pollock's schooling behavior, the spatial structure of pollock is complex and variable. In this study, model-based geostatistics were used to investigate pollock distribution related to environmental factors as well as spatial autocorrelation.

Sea ice cover can be considered as one of the most important oceanographic features in the EBS affecting pollock distribution. Besides affecting the timing of spring phytoplankton blooms and then the food availability to marine species at higher trophic levels, the sea ice cover and associated ocean environment can also directly influence the spatial distribution of marine species because each species has their preferred physical conditions (e.g., temperature, current, and salinity) (Swartzman et al., 1994; Castillo et al., 1996; Agostini et al., 2008). In particular, walleye pollock is a semi-pelagic schooling fish and its distribution is influenced by abiotic, biotic, and anthropogenic factors. The influence of temperature on pollock distribution has been well studied (Swartzman et al., 1994; Kotwicki et al., 2005). Pollock avoid cold temperature and prefer environmental conditions that are linked to food availability related to temperature (Swartzman et al., 1995). This characteristic determines the spatial distribution of pollock in the southern EBS during winter and spring seasons.

Wind stress is another important feature in the EBS. Wind strongly influences the flux of heat from Gulf of Alaska and nutrient availability to the surface water, and then biological production in the EBS because wind mixing determines the timing of spring phytoplankton blooms when there is no ice cover (Stabeno et al., 2005). Wind mixing also influences the food distribution in the upper water and consequently the vertical and horizontal distribution of fish by a bottom-up mechanism because many fish species form aggregations with thousands of individuals at a spatial location with preferred abiotic and biotic conditions. The EBS is well known by its strong storms in winter season due to the presence of the Aleutian Low (Stabeno et al., 1999). Mueter et al. (2006) investigated the relationship between pollock recruitment and the wind mixing. They found that feeding success decreased at high levels of wind mixing. The wind blowing over the surface can result in disturbance which may affect the fish distribution in the upper layer, and even deep water when a strong storm presents. Therefore our model includes wind as one of the environmental factors.

In the winter spawning season, pollock tend to form persistent mid-water or near-bottom schools in the daytime in the EBS. Many studies have investigated the summer spatial distribution and abundance of pollock related to the bottom temperature using summer survey data (Swartzman et al., 1994; Swartzman et al., 1995; Kotwicki et al., 2005). Due to harsh weather conditions, there were few surveys in the winter season, except for some conducted in 2001 and 2002 (Honkalehto et al., 2002). Data from the winter commercial fishery could help to uncover the mechanism of pollock distribution in the winter season. Knowledge about the relationship between pollock distribution in the fishery and environmental factors may provide some information for better fishery management. Because of the stormy weather, there were few winter scientific surveys in the EBS. But environmental data are available from satellites with a large spatiotemporal coverage. In this study, we used sea surface temperature (SST) and sea wind data. Stabeno et al. (2007) illustrated the vertical profile of temperature from M2 (56.9°N, 164.1°W) and M4 (57.9°N, 168.9°W) on the Bering Sea shelf. Their figures indicated that the water was well mixed in the EBS during the winter until stratification developed in April. So the SST can be considered as the indicator of the mid-water or near-bottom temperature on the southeastern Bering Sea shelf where pollock are mainly distributed during the spawning season.

Fish form aggregations at different times and locations. However, their distribution is not random, either in space or time. Generally, individual fish will locate in response to a combination of marine environmental factors (Maravelias et al., 1996) and in relation to other fish. In this study, we investigate the spatial structure of pollock in relation to environmental factors by using geostatistics, a branch of applied statistics that focuses on detecting, modeling and estimating spatial patterns (Rossi et al., 1992). The spatial dependence among neighbors is considered in this type of modeling approach, which is difficult to take into account in traditional statistics. Spatial dependence is very important in ecology because of the similarity of the environmental conditions and the related animals in the neighboring areas. Geostatistics have been successfully applied to terrestrial problems (Cressie, 1993) and marine problems (Rivoirard et al., 2000; Petitgas,

2001). Geostatistics can provide the measure of uncertainty of sampling process, mapping the spatial distribution of the stock (Rivoirard et al., 2000), estimating abundance from survey data (Barange et al., 2005), and quantifying the relationship between environmental variables and fish distributions (Maravelias et al., 1996; Agostini et al., 2008).

Fisheries acoustic data from commercial fishing vessels provided the information of pollock distribution during winter fishing season in the EBS. Previous studies (Swartzman et al., 1994; Kotwicki et al., 2005) have demonstrated the influence of physical condition on pollock distribution in the Bering Sea. In this study, spatial autocorrelation was also included into our models to quantify the relationships between pollock distribution and environmental factors as well as the spatial dependence among fish over a wide geographical area.

2.2. Materials and methods

2.2.1. Acoustic data

The acoustic data were collected with the uncalibrated Simrad ES60/38-kHz echo sounder onboard several pollock factory trawlers during 2002–2006. To avoid variability caused by using different acoustic systems and vessels, we only used the acoustic data from one factory trawler which had successfully collected data from 2002 to 2006. The acoustic data were standardized to account for the variation among years using a generalized linear model (Xiao et al., 2004). In the winter fishing season, the vessels mainly operated north of Unimak Island and in waters around the Pribilof Islands (Figure 2.1). All echograms were integrated in 1 km elementary sampling distance units (EDSU) using Echoview 3.30 software (SonarData, 2005), and the energetic parameter (nautical-area-scattering coefficient: NASC; Simmonds and MacLennan, 2005) was extracted as the index of pollock density from 15 m below the surface to 0.5 m above the seabed. For the main statistical analysis, NASC was normalized using the natural logarithm

transformation. Pollock form dense schools in the daytime and loose layers at nighttime (Barbeaux et al., 2005; Shen et al., 2008). To investigate the relation between pollock and environmental data, we only used the daytime data because of its clear signal.

2.2.2. Environmental data

Pollock avoid cold temperature so that temperature plays an important role in pollock distribution (Swartzman et al, 1995). On the other hand, pollock form mid-water or near-bottom schools during the winter spawning season. The Bering Sea is very stormy during winter due to the presence of the Aleutian Low (Stabeno et al., 1999). The turbulence caused by storms may affect pollock schooling on the southeastern Bering Sea shelf. Other environmental factors may potentially influence pollock distribution but the data are barely available in winter. Therefore, two environmental variables were included to examine the pollock distribution in the winter fishing season (January 20th –late March): sea surface temperature (SST) and sea wind vector. Daytime data were used to be consistent with the acoustic data. Both satellite data sets were obtained from the NASA Jet Propulsion Laboratory (http://podaac.jpl.nasa.gov/). Terra/Moderate Resolution Imaging Spectroradiometer (MODIS) provides daily SST (°C) data to a spatial resolution of 4.63 km. SeaWinds on QuikSCAT provides daily a sea wind speed (m/s) on an approximately 0.25 x 0.25 degree. We used the daytime data from the ascending pass (6AM LST equator crossing). Wind blows over the surface of the water and generates waves. Because of the Coriolis force and the friction of the water, the direction of the water movement is not the same as that of the wind, which is known as Ekman layer (Mann and Lazier, 2005). The speed of the water get progressively less with depth and the depth of Ekman layer is related to the wind speed and the latitude as $D_E \approx 4.3W/(\sin\varphi)^{1/2}$, where D_E is the depth of Ekman layer, W is the wind speed, and φ is the latitude (Pond and Pickard, 1983).

Due to the harsh weather in the winter, some environmental data were missing to match to the daily vessel trajectories. To address this, a simple kriging model was used to extrapolate the environmental data (Issaks and Srivastava, 1989). We used the

exponential omni-directional semivariogram model with 40 nearest neighbors for kriging extrapolation. The details about spatial process will be discussed in section 2.2.3.

Besides the satellite data, the acoustic data also provided the bottom depth at the location of the vessel which may influence pollock distribution. Thus, there were a total of 3 explanatory variables (two dynamic variables: SST and wind speed; one static variable: bottom depth) for exploring the relationship between pollock and physical environment. For each EDSU of the vessel trajectory, the corresponding environmental data were extracted based on the position of the center of the EDSU.

2.2.3. Model formulation

2.2.3.1. Structural analysis

The goal of structural analysis was to describe and model the relationship between pollock distribution and environmental data, as well as to incorporate spatial correlations among pollock. The model was constructed with the following two components.

Assume y_i is the measured pollock density at location x_i, which is the function of a combination of environmental variables C_{ki}, and influenced by the y_j ($i \neq j$) in surrounding locations (Diggle et al., 1998):

$$y_i = y(x_i) = \mu(x_i) + S(x_i) + \varepsilon_i \ ,$$

where $\mu(x_i)$ is the mean effect including the environmental variables, $S(x_i)$ is a stationary Gaussian process with expected value $E[S(x)] = 0$ and covariance $\text{cov}[S(x_i), S(x_j)] = \sigma^2\rho(x_i - x_j)$ (σ^2 is variance; ρ is correlation coefficient), and the ε_i are mutually independent random variables with a mean of zero and variance of τ^2.

2.2.3.2. Mean effect

This mean effect is modeled as a function of environmental variables as

$$\mu(x_i) = \beta_0 + \sum \beta_m C_{ki} + \sum \beta_n C_{ki}^2 \ ,$$

where the C_{ki} is the k^{th} environmental variables measured at location x_i, and the β's are the regression coefficients. Both linear and quadratic terms were used as environmental factors for flexibility if exploratory data analysis suggested a quadratic effect.

2.2.3.3. The spatial process

In a stationary Gaussian process, $S(x_i)$, the covariance depends only the vector difference between two locations. Here, we did not consider the directional trend among data, so only the Euclidean distance between locations mattered. This suggests that the measures of fish density are more similar at short distance than those far away. In a stationary process, the variance is constant, $\sigma^2 = \gamma(0)$. And the correlation function $\rho(h) = \gamma(h) / \sigma^2$, where the $\gamma(h)$ is the variogram defined as below.

There are two steps involved in spatial structural analysis: calculating the variogram and variogram model fitting. The variogram, as a tool for exploratory data analysis, can be used to visualize the spatial correlations against the corresponding distances among spatial locations. The variogram provides the semi-variance between data points as a function of the spatial distance between them. The omni-directional variogram is computed based on the assumption of stationarity (Cressie, 1993):

$$\hat{\gamma}(h) = \frac{1}{2|N(h)|} \sum_{i=1}^{N(h)} \left\{ [y(x_i) - \mu(x_i)] - [y(x_i + h) - \mu(x_i + h)] \right\}^2 ,$$

where $\hat{\gamma}(h)$ denotes the empirical variogram for distance h, $N(h)$ denotes the number of all pairs of observations at distance h, $|N(h)|$ denotes the number of distinct pairs in $N(h)$.

The resulting empirical variogram can be modeled with a semi-variance function for estimating stability, which is common in geostatistics (Cressie, 1993). There are three different theoretical variogram models. They are linear, spherical and exponential models (Cressie, 1993; Mello and Rose, 2005). After several preliminary tries, we chose to use exponential variogram model, because its shape provided better fit to the observations. The exponential variogram can be described by

$$\gamma(h) = \tau^2 + \sigma^2\left[1 - \exp\left(-\frac{|h|}{\phi}\right)\right]$$

(Cressie, 1993), where $|h|$ denotes the absolute distance between two data points, τ^2 denotes the nugget effect caused by measurement error or microscale variation, σ^2 denotes the sill which is the maximum level of variability in the data, and ϕ is the range represents the maximum distance of correlation among data.

Due to the large sample size and high overlap, a sample of 1000 points was randomly chosen to estimate the parameters if the sample size was larger than 1000. The parameters of the linear regression and variogram model were simultaneously estimated using the 'geoR' package (Ribiero and Diggle, 2001) and 'sp' package (Pebesma and Bivan, 2005) in the R software. ArcGIS was also used to create and display some results.

2.2.3.4. Model selection and validation

Different terms were added into the models and the Akaike Information Criterion (AIC) was used to find the most parsimonious models with the lowest AIC values (Chambers and Hasties, 1992). In geostatistics, the goal of modeling is to predict the dependent variable at locations other than where the data are located. To evaluate the prediction ability of the models, we used the cross-validation method, in which the data set is split into two subsets: a modeling subset and a validation subset. The modeling set is used for variogram modeling and kriging on the locations of the validation subset, and the validation measurements can be compared to their predictions.

2.3. Results

2.3.1. Monthly sea surface temperature

The pollock fishery occurred in north Unimak Island from January 20th to mid- or late February, and waters around the Pribilof Islands from late February to late March in the

EBS. Thus we used the SST in January and February for north Unimak Island, and in March around the Pribilof Islands (Figure 2.2). Because the fishery mainly occurred off of north Unimak Island during March 2002, March SST was used in areas around Unimak Island (Figure 2.2). Generally speaking, the water temperature was higher in January than February. Inter-annual variation was large during 2002–2006 (Figure 2.2). The water temperature was highest in all three months of 2003. The SST in 2002 and 2006 was relatively lower than the other three years. Although SST was generally lower than 2°C in February 2002, there were some patchy areas with temperature higher than 2°C which was not obvious in February 2006 (Figure 2.2). And SST's in March 2002 and March 2006 were also pretty low with large areas of very low temperature (<0°C, the waters displayed as white) north of the Pribilof Islands (Figure 2.2). The SST was generally higher than 2°C in north Unimak Island March 2002 (Figure 2.2) when the fishery occurred in this area (Figure 2.3).

2.3.2. Pollock distribution associated with SST

Because pollock avoid cold temperature, the spatial distribution of pollock was influenced by the water temperature. In January and February of all years, there was a water mass with relatively low temperature in northeast Unimak Island compared to the surrounding area (Figure 2.2). Pollock obviously avoided this cool water so pollock density was relatively lower and there was less observed fishing effort in this area (Figure 2.3). The temperature in March played a very important role in pollock distribution. In the warmest year 2003, pollock distributed northwest of the Pribilof Islands and extended to 59.2°N (Figure 2.3). In 2004 and 2005, pollock mostly distributed around the Pribilof Islands and northern extension was about 57.5°N (Figure 2.3). In cold years (2002 and 2006), pollock distributed further to the south compared to other years. In 2002, there were fewer fishing days around the Pribilof Islands, and more effort north of Unimak Island (Figure 2.3). In 2006, most pollock distributed south of St. George Island in deep water (Figure 2.1). Due to the depth, acoustic data collected were of poor quality, and fish density could not be extracted for this period. Overall, the above information

suggested that temperature governed the general spatial distribution of pollock during winter.

2.3.3. Spatial process

Geostatistical regression models with explicit spatial correlation fitted the data set substantially better than traditional models without spatial correlation as indicated by the decreases in AIC values (Table 2.1). If the difference in AIC values is 7 or more, the model with a lower AIC is strongly suggested (Burnham and Anderson, 2002). The decrease of AIC in models with autocorrelation was much larger than 7. The results from cross-validation (r^2 values) also demonstrated that geostatistical models were superior to standard statistical regression models in prediction ability (Table 2.1). Although the coefficient of determination, r^2, was generally low, there was large improvement when the spatial autocorrelation was included in regression models.

In geostatistical models, there is a spatial process error component $S(x)$ which describes the spatial dependence among data. Here we used an exponential variogram to model $S(x)$ with parameters (nugget, sill, and range). If there was no autocorrelation, $\gamma(h)$ was constant regardless of h, i.e., the variogram was a flat line which means the random spatial process. If there was autocorrelation among data, the values of gamma were supposed to be small at short distances h and then increase with h. If this increase continued, the variogram was said to be unbounded, which was characterized by the linear model. Another type of variogram was bounded because the value of gamma leveled off where correlation with distance approached zero. One example was displayed using data in January 2003 (Figure 2.4). This bounded variogram was typical when fish were patchy. The fitted variogram demonstrated that there was a substantial spatial component to the pollock density even after accounting for the effects of some environmental factors. The range (2207) denoted the maximum distance beyond which samples were no longer spatially autocorrelated. The nugget (2.29) represented variation at scales smaller than lag size or variability due to measurement error. The sill (3.88) was the maximum level of variability among points or the variability that occurred at large

distances. The existing spatial autocorrelation suggested that pollock density was a function of where other pollock were located (schooling or aggregating). Including spatial correlation in models obviously improved the fit to the data and the prediction ability of the geostatistical models (Table 2.1).

The parameters of variogram (range, sill and nugget) can be used as the quantitative indicators to investigate the distribution and aggregation patterns of fish. Generally, the fishing vessel revisited the same areas in February except 2002 (Figure 2.3). After accounting for the influence of environmental factors, we expected similar spatial structures in January and February. However, the range increased and the partial sill decreased in February of 2003–2006 (Table 2.2). The nugget effect was relatively large and contributed 39%–75% of the variances (Table 2.2).

2.3.4. Model inferences

From an exploratory analysis of the data (Figure 2.5), pollock density seemed linearly related to wind speed and quadratically related to SST and bottom depth. In winter, the wind speed was very high (>15m/s), especially in February (Figure 2.6). Based on the function given by Pond and Pickard (1983), the depth of Ekman layer could have been deeper than 60 m (Figure 2.7). There was an obvious negative effect of wind speed on pollock density (Figure 2.5, Table 2.1). The pollock density decreased as wind speed increased which can be deduced from the negative regression coefficients (Table 2.1).

There appeared to be a dome-shaped relationship between pollock density and SST for three year-month combinations (January 2004, January 2005 and March 2005) (Table2.1). When the temperature was lower, pollock density increased as temperature increased. For instance, the temperature at most observation locations was relatively low in January 2002, March 2003, and January 2006 (<4°C) (Figure 2.8). There was a positive relationship between SST and pollock density in these data sets (Table 2.1). In contrast, when the temperature was higher than 4°C, pollock density decreased as temperature increased. For instance, in January and February 2003, the temperature at

most observation locations was higher than 4°C (Figure 2.8). There was a negative correlation between SST and pollock density in this data set (Table 2.1). The effect of bottom depth was relatively small which was mainly important to the pollock distribution in January and March 2002, and February 2004 (Table 2.1)

2.4. Discussion

Pollock perform seasonal migrations: feeding migration in spring and summer and spawning migration in winter. The pollock fishery targets pre-spawning pollock for roe in the winter, primarily in the southeastern portion of the Bering Sea. Pollock generally distribute to the north of Unimak Island in January to mid- or late February, and to waters around the Pribilof Islands. Some studies demonstrated that temperature plays an important role in pollock distribution in the EBS (Swartzman et al., 1994; Kotwicki et al., 2005). Our analyses also indicated the pollock spatial distribution associated with temperature. In warm years, pollock distributed northwest of Unimak Island in January and February (2003–2005 in Figure 2.3). In cold years, pollock tended to spread out to find preferred temperatures (>2°C) (2002 and 2006 in Figure 2.3). The patch of high fish density in 2002 spatially matched the water with temperature >2°C well (Figure 2.2 and Figure 2.3). The significantly different pollock March distributions among years may be due to the inter-annual differences in water temperature. The warmer the temperature, the further north the pollock extended. In cold years, pollock stayed south of St. George Island in 2006 (Figure 2.1) and in 2002 even stayed in north Unimak Island (Figure 2.3).

Pollock form schools during the winter spawning season and Figure 2.9 shows the density distribution of depth of the uppermost layer of schools. In winter, the wind speed in the EBS is large during a storm, even larger than 15m/s (Figure 2.6). The disturbance caused by wind can reach waters deeper than 60 m (Figure 2.7). Therefore, it is reasonable that the turbulence by wind can affect pollock schooling behavior in mid-water or near-bottom. This can be inferred from the negative correlation between pollock

density and wind speed in Table 2.1. Although bottom depth did not show an important effect on pollock density in most of data sets, it is still important and cannot be overlooked. Pollock distributed in areas with bottom depth ranging from 65 m to 150 m, except in March 2006 (Figure 2.10). It is interesting to note the dome-shaped relationship between pollock density and temperature which has not been mentioned in previous studies.

The geostatistical approach was used here to examine the potential relationship between pollock and physical environment. This approach allowed us to account for the spatial dependence between data points, a process we considered important in our analysis. Traditional statistics have developed many methods based on independent data; however independence is an unrealistic assumption in many situations (Legendre, 1993). This independence rarely holds in ecology. The presence of an organism at a specific location is influenced by a combination of physical environment, such as ocean current, winds, substrate, and climate. It is also influenced by autocorrelation which accounts for some of these unmeasured factors affecting distribution. Analysis based on independence could lead to wrong identification of existing relationships.

The spatial methods used here allowed us to effectively explore mechanisms that may explain the distribution of fish populations. This kind of mechanism cannot be explored by simple generalized linear models. Understanding the spatial process is very important to evaluate the status of fish stocks. Some collapsed fisheries were accompanied by significant changes in spatial pattern of the fish stock, such as northern cod stock (Atkinson et al., 1997). Thus far, the focus of fisheries science is to evaluate management performance with indicators based on non-spatial population dynamics models, ignoring the spatial variability of a stock's distribution. For stocks such as pollock with spatial structure in distribution, some efforts should be made to incorporate a spatial component in models.

Here the relationship between pollock and some environmental factors were examined using model-based geostatistics. The removal by the fishery is also important

but was not considered in this analysis. Some recent studies focused on whether the fishery has an adverse impact on pollock distribution and consequent effects on the Steller sea lion predation process especially in the Steller sea lion conservation area (SCA). The fishery mainly occurs in the SCA in January and February. The density in February in north Unimak Island was generally lower than that in January (Figure 2.3). Besides the decrease of fish density, the spatial structure in the error component differed in January and February after accounting for the environmental effects by regression models (Table 2.2). The changes of parameters (sill, range and nugget) can be considered as the indicators of changed spatial pattern. Generally a large range and small sill and nugget are expected for the low-density and large aggregations. However, if fish aggregate in a small portion of the study area, the variogram will be characterized by small range and high sill and nugget (Mello and Rose, 2005). The increased range and decreased partial sill (Table 2.2) suggest that fishing activities may smooth out the clumpy distribution of pollock and make spatial correlation of pollock extend to greater distances. In 2003, the nugget effect accounted for a larger part of the variation in January and February (Table 2.1). This means that there may be large portions of variation at smaller scales (<1 km) than examined in our data and analysis.

Although this and other studies are increasing information about pollock distribution, the driving mechanism is still poorly understood, making prediction a difficult task. The ability of the model to predict pollock distribution was poor. The results of cross-validation indicated that our models only predicted a small part of the variation in data (low r^2 values in Table 2.1), although geostatistical models with a spatial autocorrelation component improved the fit over models without a spatial component. Including some other factors may improve our models because there are some other factors which may play important roles on pollock distribution, such as ocean current and biological factors. However, these kinds of data are difficult to get especially in winter in the EBS with few scientific surveys. And satellite data can be of poor quality at times due to heavy cloud cover. Fox example, the SeaWiFS ocean color data hardly provided any data for this

study area in winter. Increased cooperation with fishing vessels may help get more information about winter pollock distribution during winter fishing season.

The primary objective of this study was to examine the relationship between pollock and the physical environment to find what and how the physical environment affects pollock spatiotemporal distribution during winter. During the daytime, pollock form schools in winter spawning season (Shen et al., 2008). In this study, the integrated NASC at 1 km EDSU was used as the index of pollock density from 15 m below the surface to 0.5 m above the seabed. High pollock density means the presence of dense and large schools, and low pollock density means the presence of small and less dense schools, and even the absence of pollock schools. Temperature can be considered as the most important factor influencing pollock spatial extent at the large scale as well as density at the small scale. The pollock distribution was confined by the cold water, especially the distribution in March (Figure 2.1). The results from the geostatistical model suggested there was sometimes a dome-shaped relationship between pollock density and water temperature and often there was a negative correlation between pollock density and wind speed (Table 2.1). These results suggested that pollock prefer schooling in areas with warm temperature and weak wind, rather than areas with cold or hot temperature and strong wind. Although the prediction ability of our models was not good, including spatial correlation in models improved the fit to the data and the prediction ability. Therefore, spatial correlation among fish should be included in stock assessment.

2.5 Acknowledgments

This research was funded by a grant from the Pollock Conservation Cooperative Research Center to the University of Alaska Fairbanks (UAF). A major portion of student support was provided by the Alaska Fisheries Science Center, through the Cooperative Institute for Arctic Research (NA17RJ1224) at UAF.

2.6 References

Agostini, V.N., Hendrix, A.N., Hollowed, A.B., Wilson, C.D., Pierce, S.D., Francis, R.C., 2008. Climate-ocean variability and Pacific hake: A geostatistical modeling approach. J. Mar. Sys. 71, 237–248.

Atkinson, D.B., Rose, G.A., Murphy, E.F., Bishop, C.A., 1997. Distribution changes and abundance of northern cod (*Gadus morhua*), 1981–1993. Can. J. Fish. Aquat. Sci. 54, 132–138.

Barange, M., Coetzee, J.C., Twatwa, N.M., 2005. Strategies of space occupation by anchovy and sardine in the southern Bengulea: the role of stock size and intra-species competition. ICES J. Mar. Sci. 62, 645–654.

Barbeaux, S.J., Dorn, M., Ianelli, J., Horne, J., 2005. Visualizing Alaska pollock (*Theragra chalcogramma*) aggregation dynamics. ICES Document CM 2005/U, 01. 12 pp.

Burnham, K.P., Anderson, D.R., 2002. Model selection and multi-model inference: A practical information – Theoretic approach, 2nd Edition. Springer-Verlag, New York, USA.

Castillo, J., Barbieri, M.A., and Gonzalez, A. 1996. Relationships between sea surface temperature, salinity, and pelagic fish distribution off northern Chile. ICES J. Mar. Sci. 53: 139–146.

Chambers, J.M., Hasties, T.J., 1992. Statistical Models in S. Wadsowrth and Brooks Cole Advanced Books, Pacific Grove, California.

Cressie, N.A.C., 1993. Statistics for spatial data, John Wiley and Sons, Inc., New York, New York, USA.

Diggle, P.J., Tawn, J.A., Moyeed, R.A., 1998. Model-based geostatistics. Appl. Stat. 47, 299–350.

Honkalehto, T., Williamson, N., Hanson, D., McKelvey, D., de Blois, S., 2002. Results of the echo Integration-trawl survey of walleye pollock (*Theragra chalcogramma*) conducted on the southeastern Bering Sea shelf and in the southeastern Aleutian basin near Bogoslof Island in February and March 2002. AFSC Processed Report 2002–02. 49 pp.

Hunt, Jr., G.L., Stabeno, P., Walters, G., Sinclair, E., Brodeur, R., Napp, J.M., Bond, N., 2002. Climate change and control of the southeastern Bering Sea pelagic ecosystem. Deep-Sea Res. II, Topical Studies in Oceanography. 49, 5821–5853.

Ianelli, J.N., Barbeaux, S., Honkalehto, T., Kotwicki, S., Aydin, K., Williamson, N., 2008. Assessment of walleye pollock stock in the eastern Bering Sea. In: Stock assessment and fishery evaluation report for the groundfish resources of the Bering Sea/Aleutian Islands regions. North Pac. Fish. Mgmt. Council, Anchorage, AK, section 1, 47–136.

Issaks, E.H., Srivastava, R.M., 1989. An introduction to applied geostatistics. Oxford University Press, New York.

Kotwicki, S., Buckley T.W., Honkalehto, T., Walters, G., 2005. Variation in the distribution of walleys pollock (*Theragra chalcogramma*) with temperature and implications for seasonal migration. Fish. Bull. 103, 574–587.

Legendre, P., 1993. Spatial autocorrelation: trouble or new paradigm? Ecol. 74, 1659–1673.

Mann, K.H., Lazier, J.R.N., 2005. Dynamics of Marine Ecosystems: Biological-Physical Interactions in the Oceans. Blackwell Science, Oxford.

Maravelias, C.D., Reid, D.G., Simmonds, E.J., Haralabous, J., 1996. Spatial analysis and mapping of acoustic survey data in the presence of high local variability: geostatistical application to North Sea herring (*Clupea harenus*). Can. J. Fish. Aquat. Sci. 53, 1497–1505.

Mello, L.G.S., Rose, G.A., 2005. Using geostatistics to quantify seasonal distribution and aggregation patterns of fishes: an example of Atlantic cod (*Gadus morhua*). Can. J. Fish. Aquat. Sci. 62, 659–370.

Mueter, F.J., Ladd, C., Palmer, M.C., Norcross, B.L., 2006. Bottom-up and top-down controls of walleye pollock (*Theragra chalcogramma*) on the eastern Bering Sea shelf. Prog. Oceanogr. 62, 152–183.

Pebesma, E.J., Bivand, R.S., 2005. Classes and methods for spatial data in R. R News 5 (2), http://cran.r-project.org/doc/Rnews/.

Petitgas, P., 2001. Geostatistics in fishery survey design and stock assessment: models, variances and applications. Fish Fish. 2, 231–249.

Pond, S., Pickard, G.L., 1983. Introductory Dynamical Oceanography (2nd edition). Pergamon, Oxford.

Ribeiro Jr., P.J., Diggle, P.J., 2001. A package for geostatistical analysis. R-NEWS 1(2), 15–18 ISSN 1609–3631. WWW Page, http://cran.r-project.org/doc/Rnews.

Rivoirard, J., Simmonds, J., Foote, K.G., Fernandes, P., Bez, N., 2000. Geostatistics for estimating fish abundance. Blackwell Science, Oxford.

Rodionov, S., Stabeno, P., Overland, J., Bond, N., Salo, S. (Editors), 2006. Temperature and ice cover – FOCI, WWW page, http://www.beringclimate.noaa.gov.

Rossi, R.E., Mulla, D.J., Journel, A.G., Franz, E.H., 1992. Geostatistical tools for modeling and interpreting ecological spatial dependence. Ecol. Monogr. 62, 277–314.

Schumacher, J.D., Stabeno, P.J., 1998. Continental shelf of the Bering Sea. *In*: The Sea: Vol. 11–The Global Coastal Ocean: Regional Studies and Synthesis, John Wiley & Sons, Inc., New York, NY: 789–822.

Shen, H., Quinn, T.J., II, Wespestad, V., Dorn, M.W., Kookesh, M., 2008. Using acoustics to evaluate the effect of fishing on school characteristics of walleye pollock. In: Resiliency of gadid stocks to fishing and climate change. Alaska Sea Grant, University of Alaska Fairbanks: 125–140.

Simmonds, E. J., and MacLennan, D. N. 2005. Fisheries Acoustics: Theory and Practice, 2nd edn. Blackwell Science, Oxford. 437 pp.

SonarData, 2005. Echoview. Version 3.30. <http://www.sonardata.com/webhelp /Echoview.htm>. Tasmania, Australia. (May 2005).

Stabeno, P.J., Bond, N.A., Salo, S.A., 2007. On the recent warming of the southeastern Bering Sea shelf. Deep-Sea Res. II 54, 2599–2618.

Stabeno, P.J., Hunt, G.L., Napp, Jr., J.M., Schumacher, J.D., 2005. Physical forcing of ecosystem dynamics on the Bering Sea Shelf, *in* The Sea, Vol. 14, The Global Coastal Ocean: Interdisciplinary Regional Studies and Syntheses, A.R. Robinson and K.H. Brink (eds.), John Wiley & Sons, 1175–1209.

Stabeno, P.J., Schumacher, J.D., Ohtani, K., 1999. The physical oceanography of the Bering Sea. In: *Dynamics of the Bering Sea: A summary of physical, chemical, and biological characteristics, and a synopsis of research on the Bering Sea*, T.R. Loughlin and K. Ohtani (eds.), North Pacific Marine Science Organization (PICES), Univ. of Alaska Sea Grant, AK-SG-99-03, 1–28.

Swartzman, G., Stuetzle, W., Kulman, K., Powojowski, M., 1994. Relating the distribution of pollock school in the Bering Sea to environmental factors. ICES J. Mar. Sci. 51, 481–492.

Swartzman, G., Silverman, E., Williamson, N., 1995. Relating trends in walleye pollock (*Theragra chalcogramma*) abundance in the Bering Sea to environmental factors. Can. J. Fish. Aquat. Sci. 52, 369–380.

Xiao, Y.S., Punt, A.E., Miller, R.B., and Quinn, T.J., II. (Editors), 2004. Models in fisheries research: GLMs, GAMs and GLMMs. Fish. Res. 70: 137–428.

Table 2.1. Model parameter estimates for the model structure with the lowest Akaike Information Criterion (AIC) value (nac denotes model without autocorrelation component, ac denotes model with autocorrelation component). T denotes sea surface temperature. v denotes wind speed. D denotes bottom depth. r^2 is coefficient of determination from the cross-validation results.

	2002			2003			2004		
	Jan	Feb	Mar	Jan	Feb	Mar	Jan	Feb	Mar
Intercept	7.81	9.62	10.29	6.31	12.65	4.08	−5.33	6.86	5.70
T	1.18			−0.30	−1.63	0.34	6.69		
T^2							−0.95		
v	−0.20	−0.12	−0.12		−0.06		−0.12		−0.13
D	0.01		−0.04					−0.03	
AIC_nac	2055	2185	2216	2656	2130	2372	1944	1639	2229
AIC_ac	2006	1989	2139	2564	2115	2214	1862	1507	2117
r^2_nac	0.08	0.09	0.05	0.08	0.02	0.02	0.11	0.15	0.02
r^2_ac	0.21	0.24	0.28	0.25	0.17	0.31	0.43	0.31	0.25

	2005			2006	
	Jan	Feb	Mar	Jan	Feb
Intercept	−26.79	5.84	−0.11	3.04	6.32
T	17.66		2.90	0.72	
T^2	−2.30		−0.33		
v	−0.08	−0.13	−0.11		−0.24
D					
AIC_nac	1957	1536	2014	2038	1766
AIC_ac	1844	1371	1921	1933	1681
r^2_nac	0.09	0.02	0.05	0.02	0.15
r^2_ac	0.34	0.24	0.42	0.25	0.38

Table 2.2. The estimated parameters by fitting exponential variogram to model the spatial autocorrelation in monthly pollock distribution.

		nugget	partial sill	sill	range
2002	January	2.60	1.88	4.48	1669.7
	February	1.69	1.95	3.64	2185.5
	March	2.27	2.61	4.88	2625.3
2003	January	2.29	1.59	3.88	2207.7
	February	2.72	1.33	4.05	3474.4
	March	2.68	1.85	4.53	4533.2
2004	January	0.97	1.51	2.48	1167.6
	February	1.51	1.23	2.74	3561.2
	March	3.05	1.71	4.76	5429.3
2005	January	1.41	0.92	2.33	2337.4
	February	1.74	0.83	2.57	3227.9
	March	2.20	0.72	2.92	4766.5
2006	January	2.01	1.47	3.48	1670.8
	February	1.39	0.58	1.97	3647.2

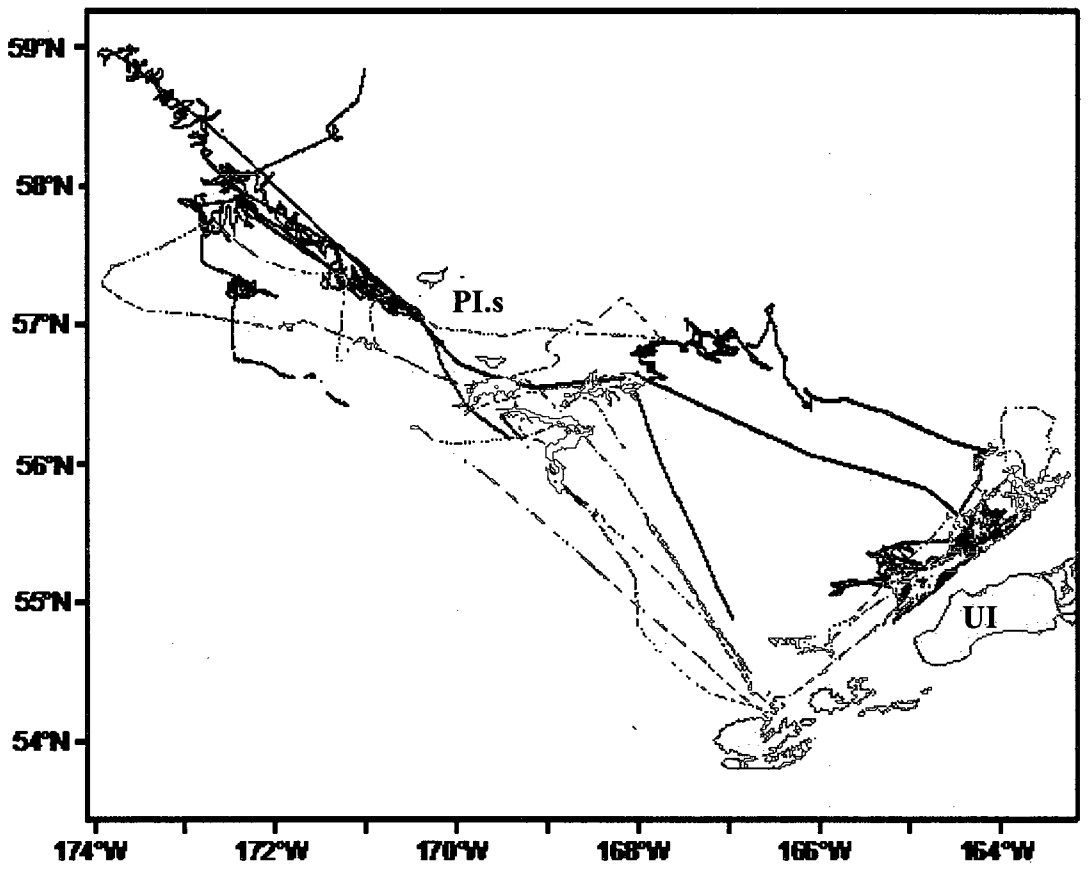

Figure 2.1. The fishing track in 2003(black) and 2006 (dark red) from late January to late March. UI= Unimak Island. PI.s= Pribilof Islands.

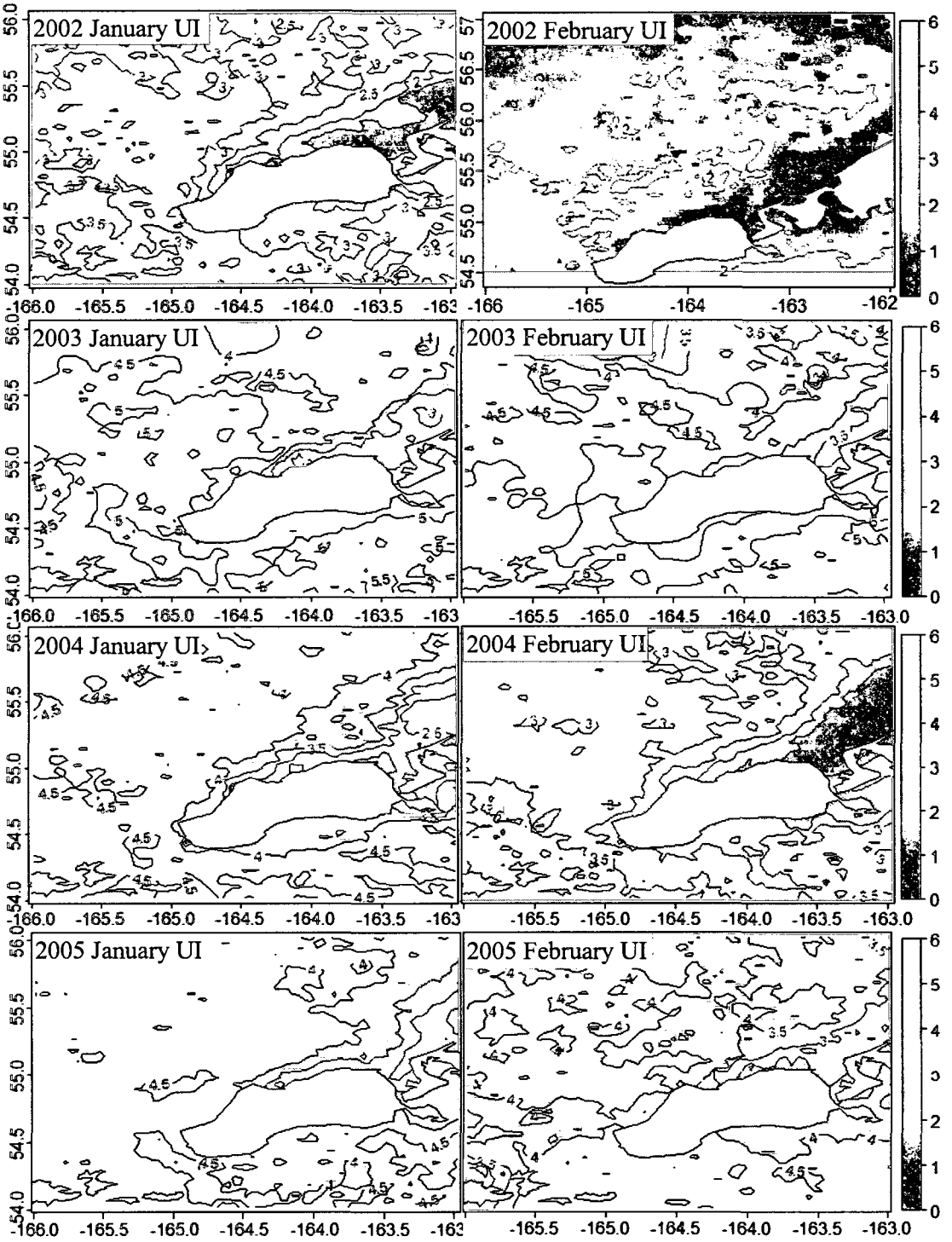

Figure 2.2. The monthly sea surface temperature north Unimak Island and waters around the Pribilof Islands in January-March during 2002–2006. Cold water (<0°C) is displayed as white. UI=Unimak Island. PI=Pribilof Islands.

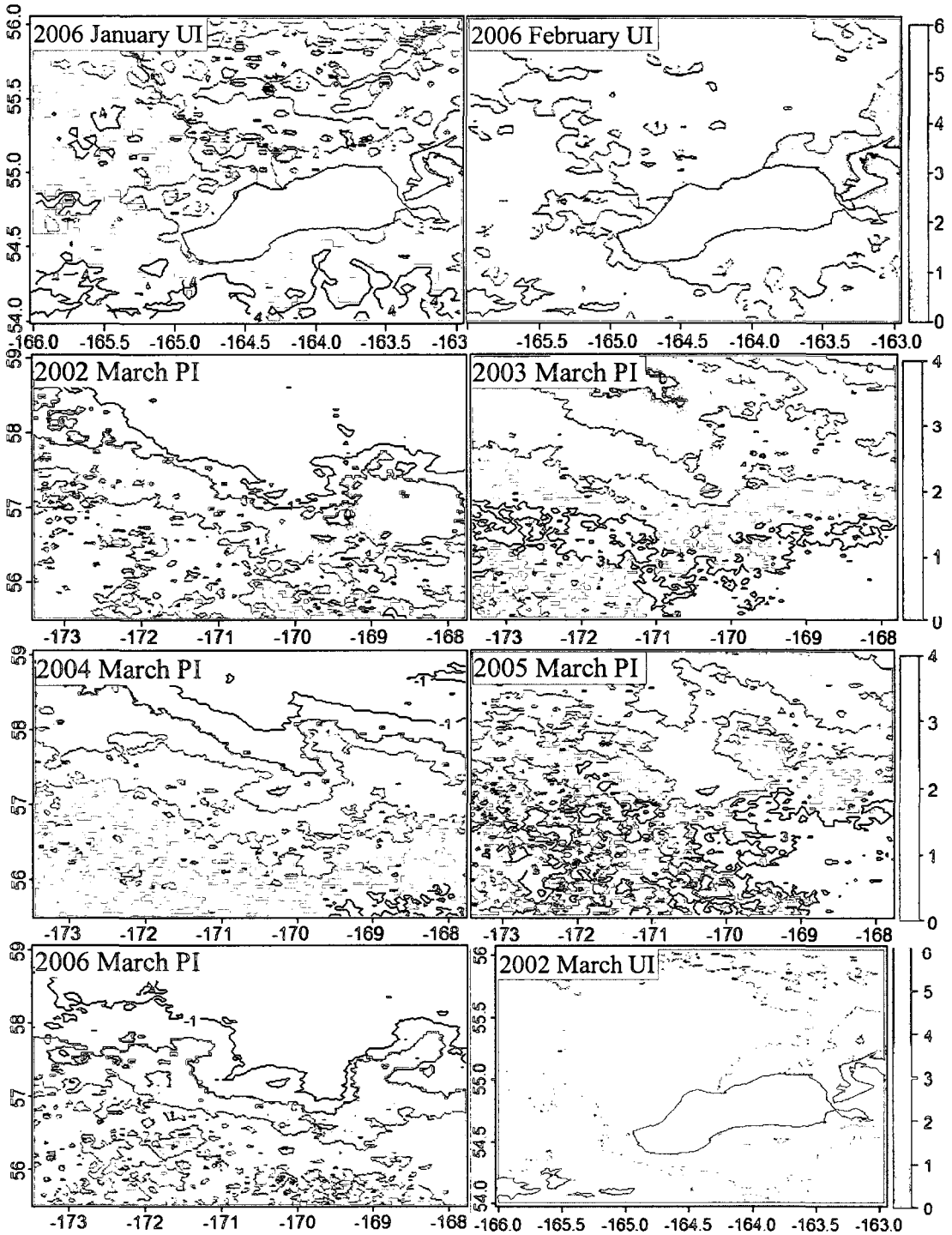

Figure 2.2 (Continued)

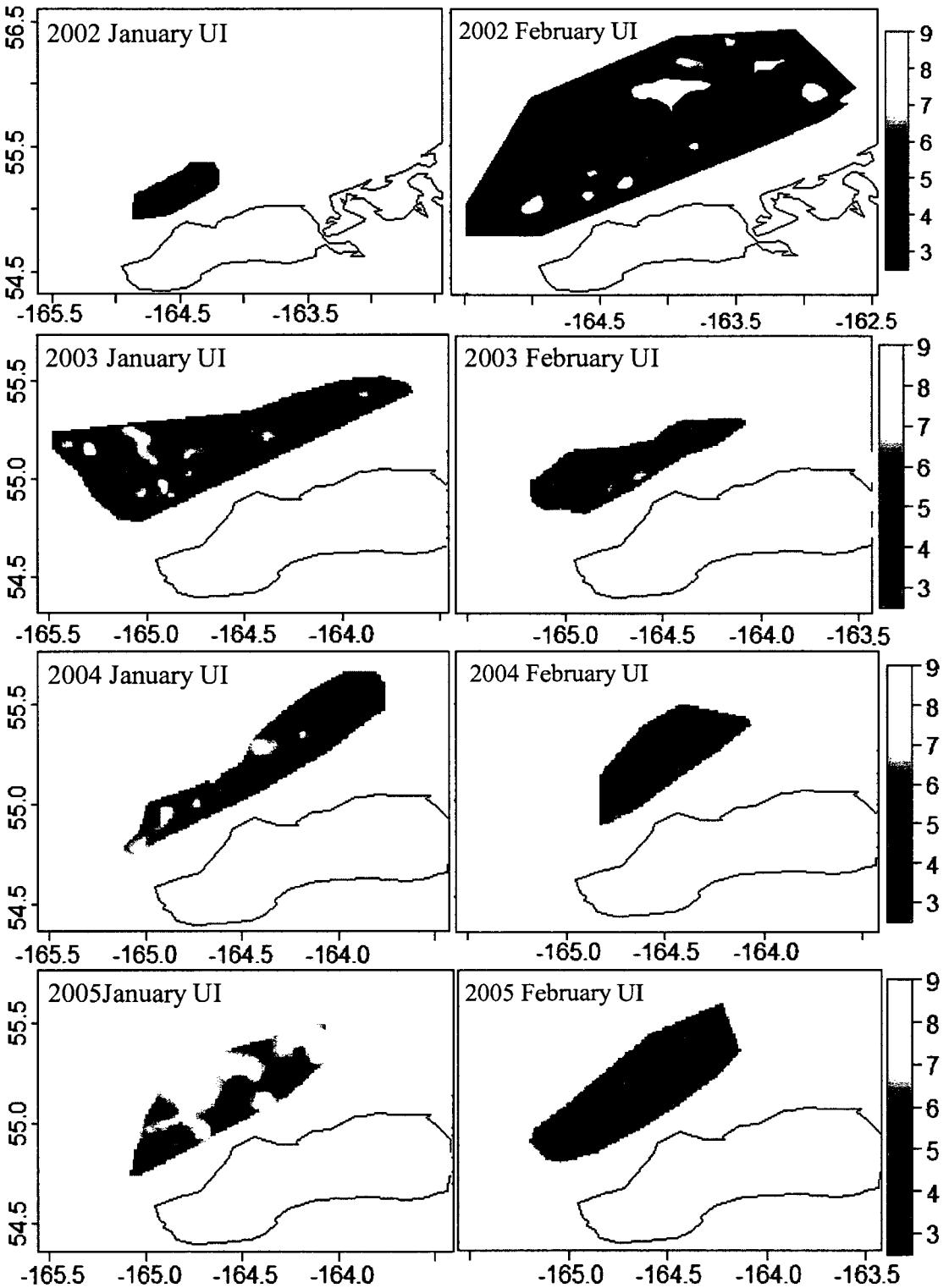

Figure 2.3. The interpolated monthly ln(NASC) in January, February and March during 2002–2006. UI= Unimak Island. PI= Pribilof Islands.

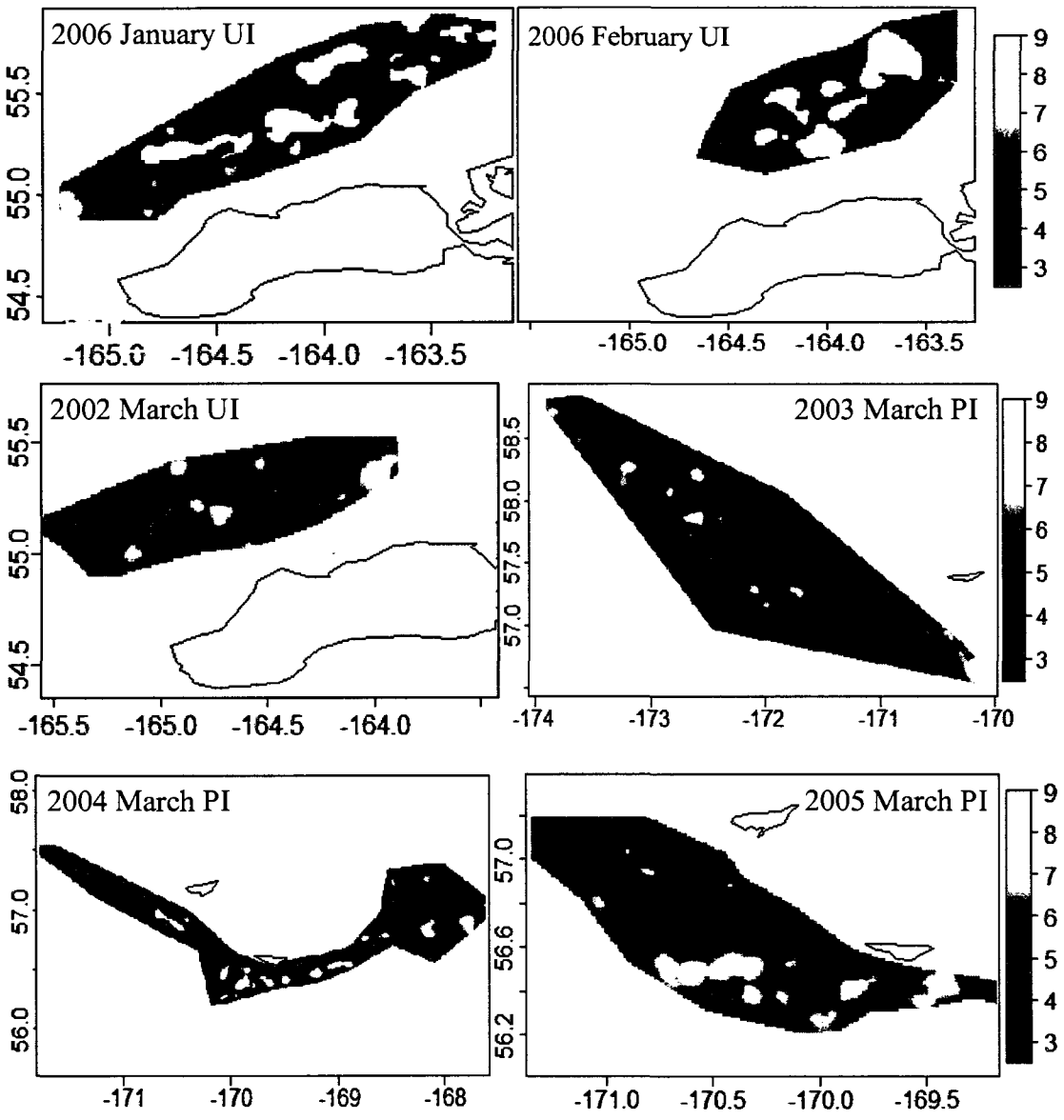

Figure 2.3 (Continued)

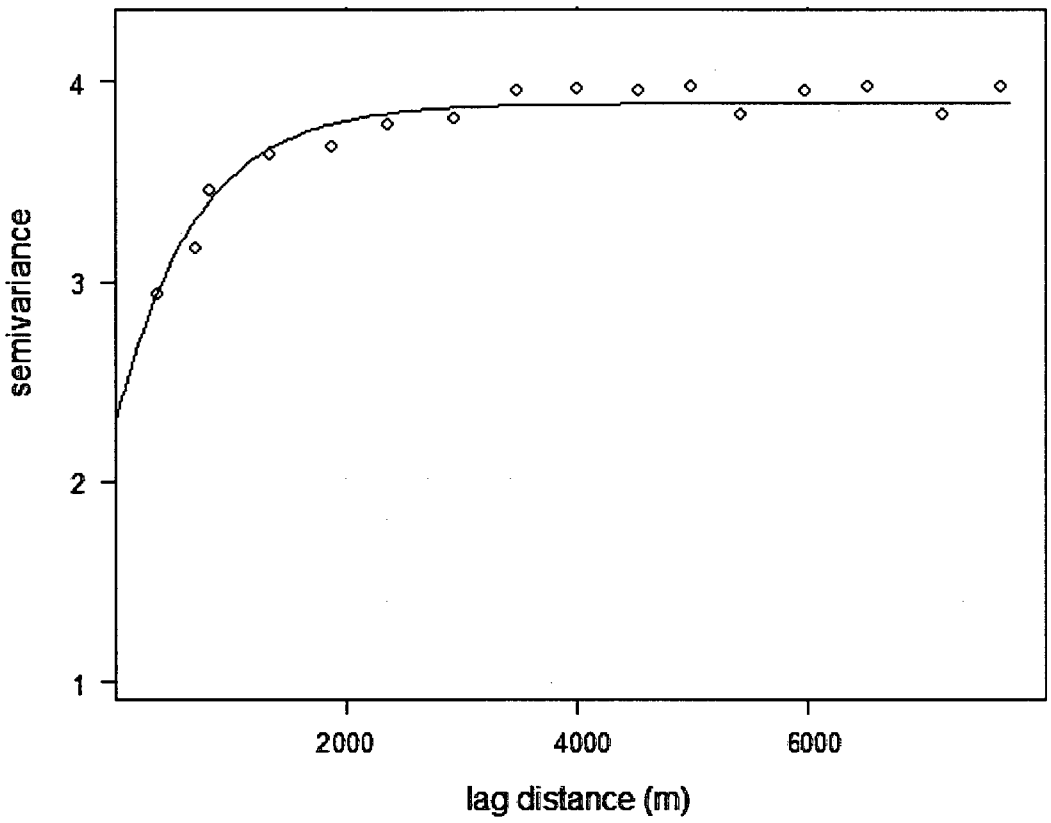

Figure 2.4. Example of fitting an exponential function (solid line) to experimental variogram (semi-variance between data points as a function of distance).

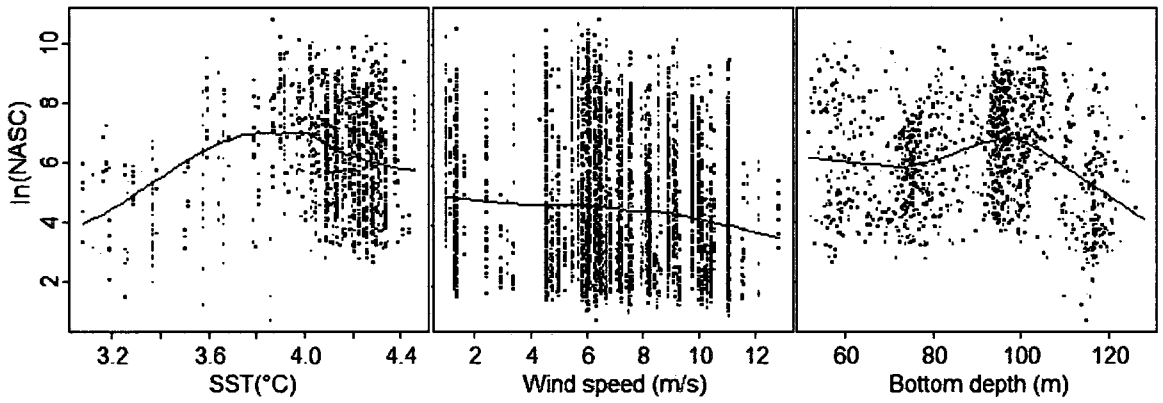

Figure 2.5. The relationship between ln(NASC) and the physical variables (SST, wind speed and bottom depth)

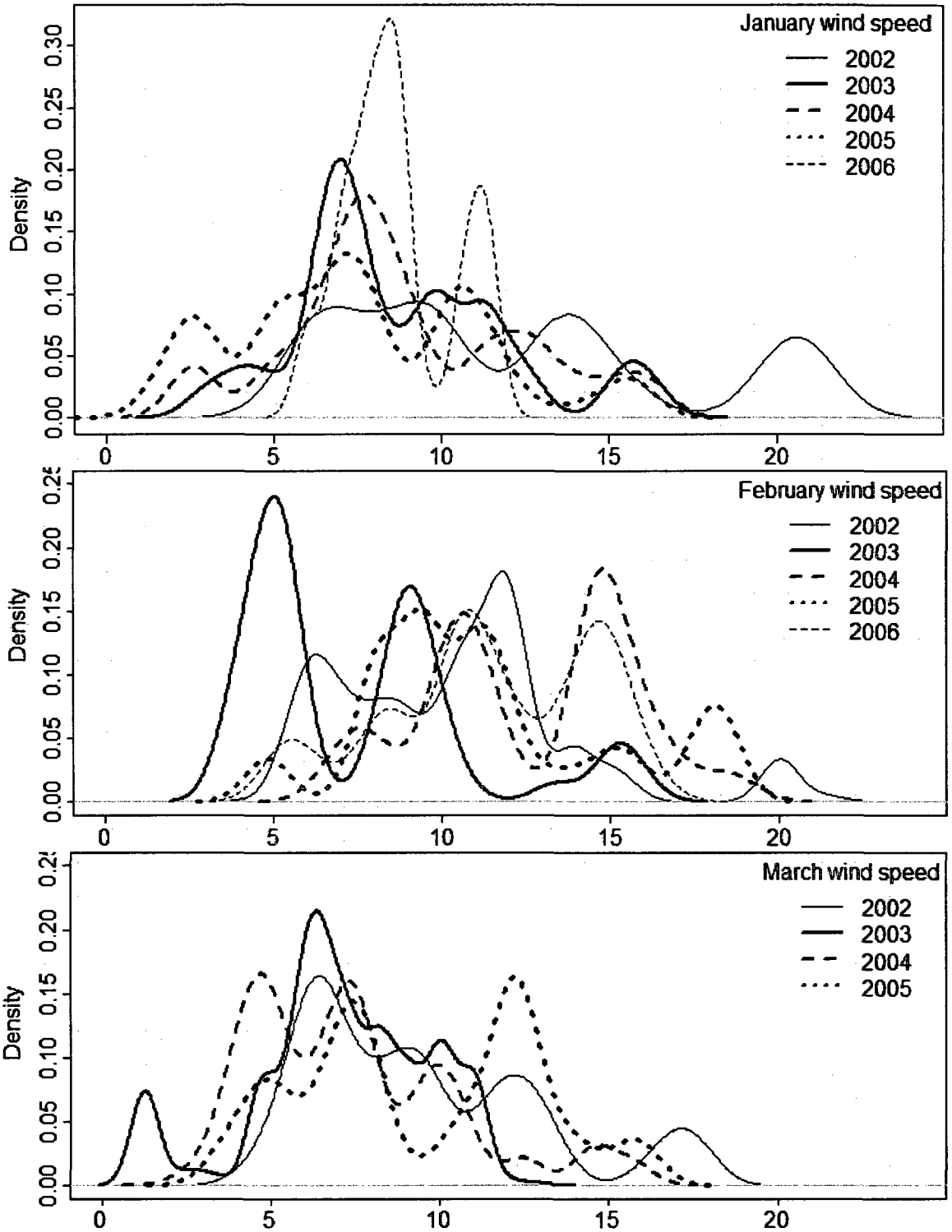

Figure 2.6. The density distribution of the wind speed (m/s) along the pollock fishing track in different months during 2002–2006

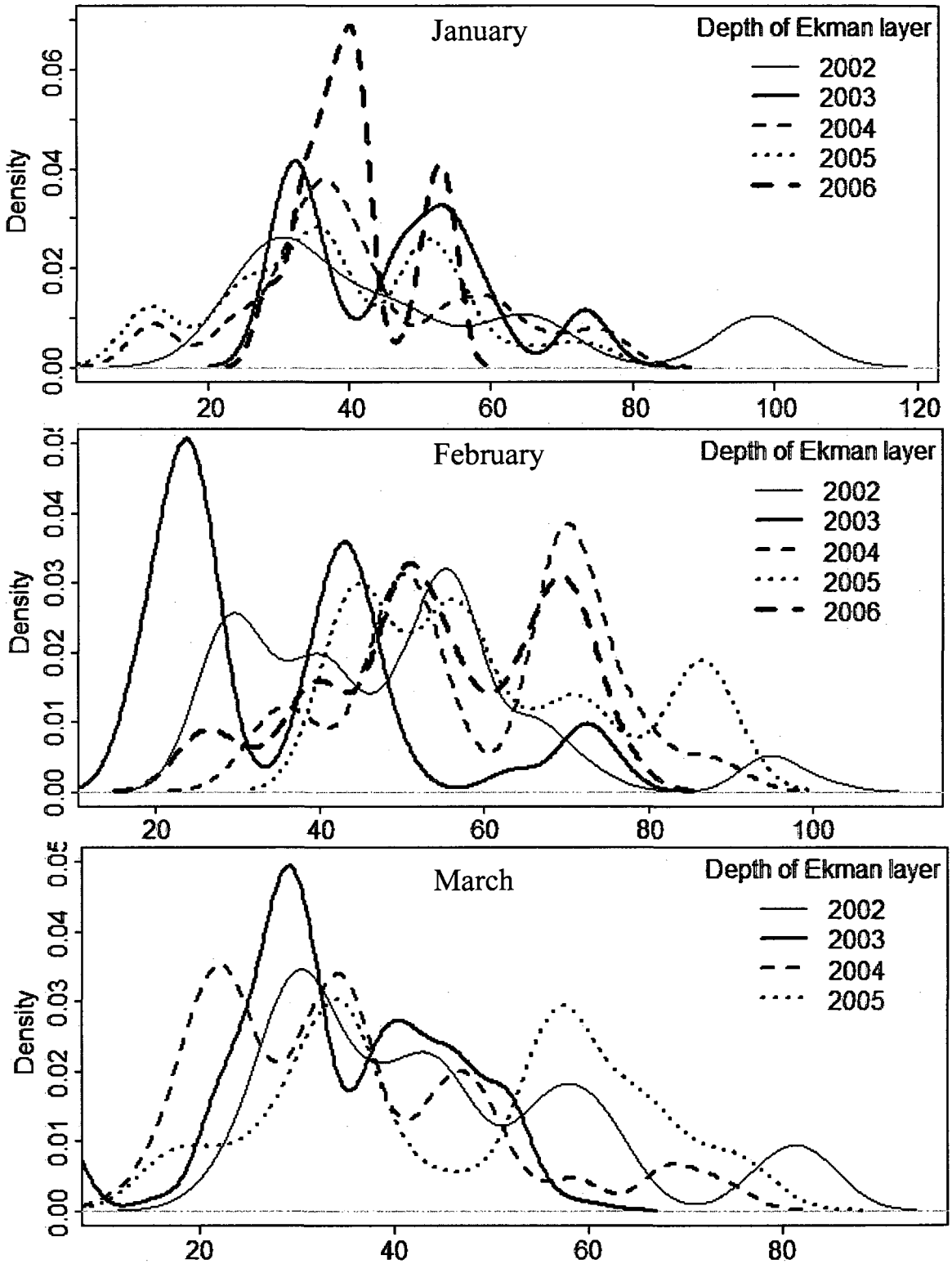

Figure 2.7. The density distribution of the depth (m) of Ekman layer in different months during 2002–2006

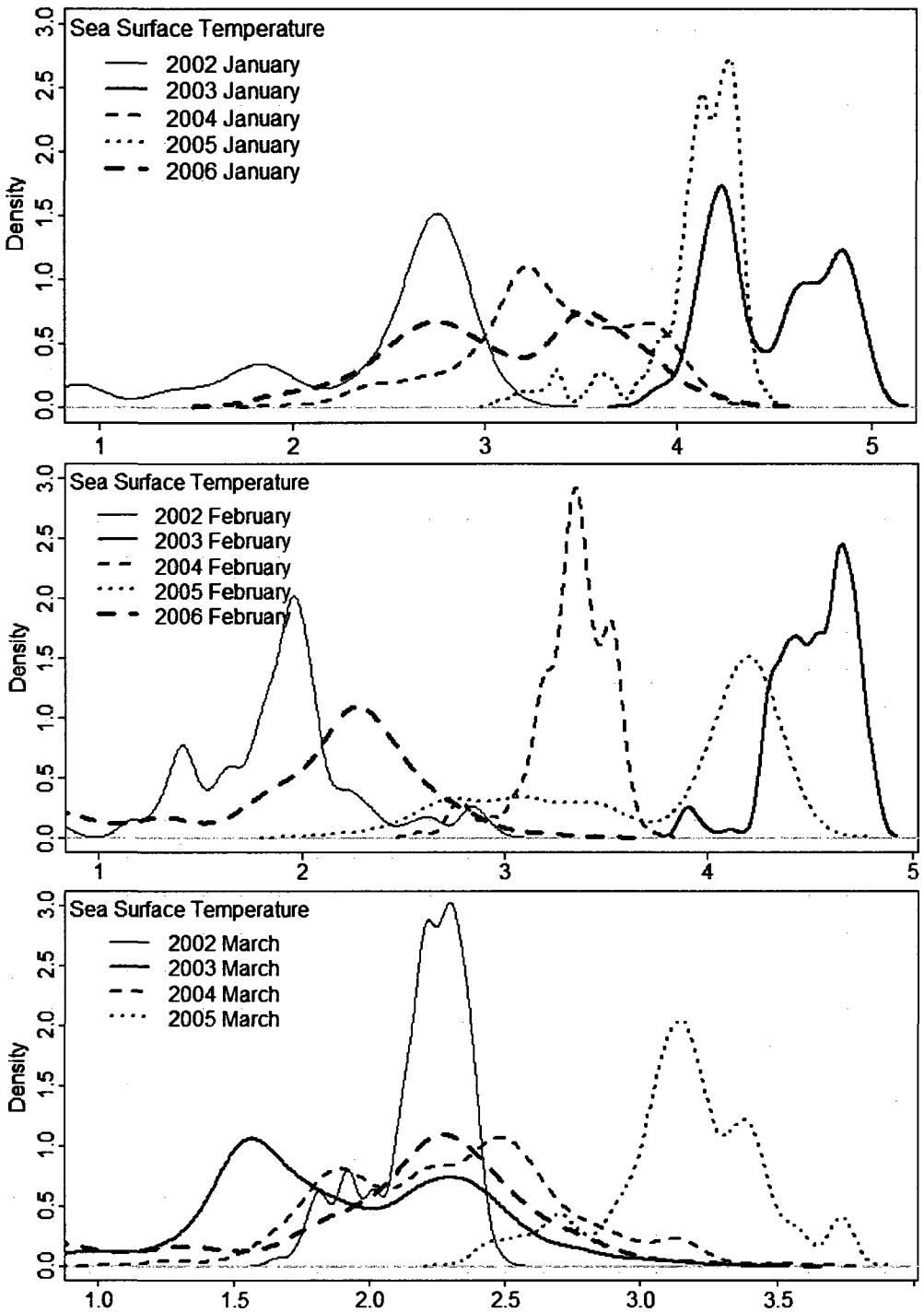

Figure 2.8. The density distribution of the sea surface temperature (°C) along the pollock fishing track in different months during 2002–2006.

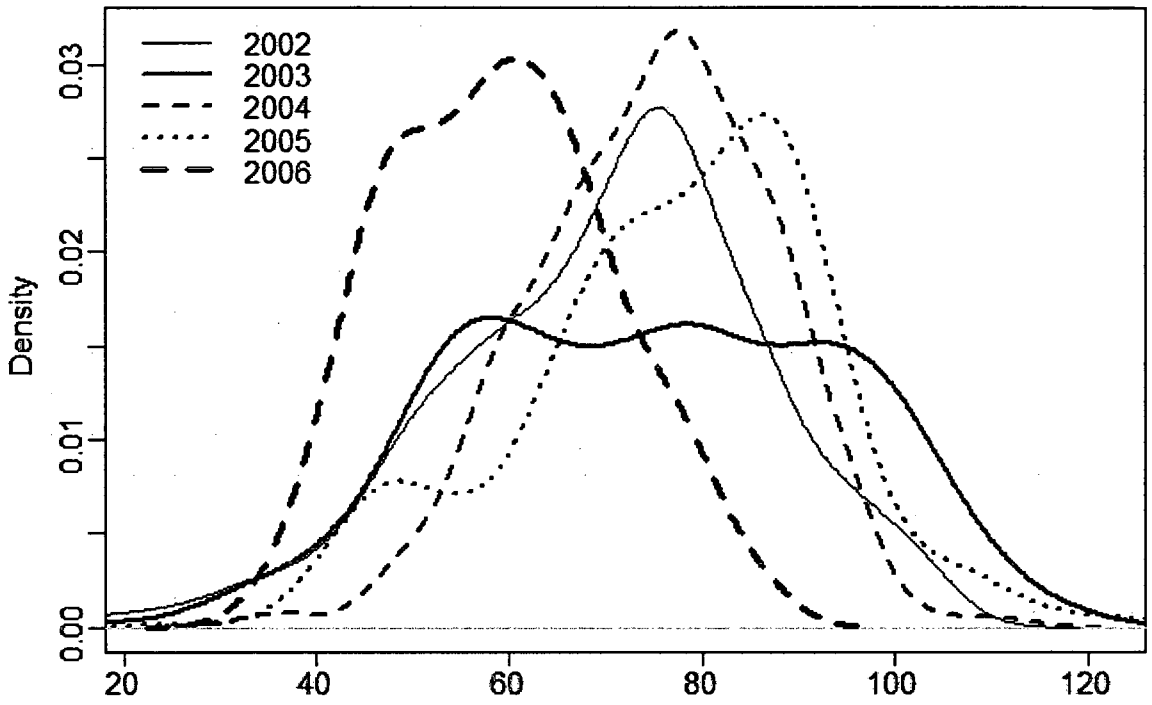

Figure 2.9. The density distribution of the depth (m) of the uppermost layer of schools during 2002–2006.

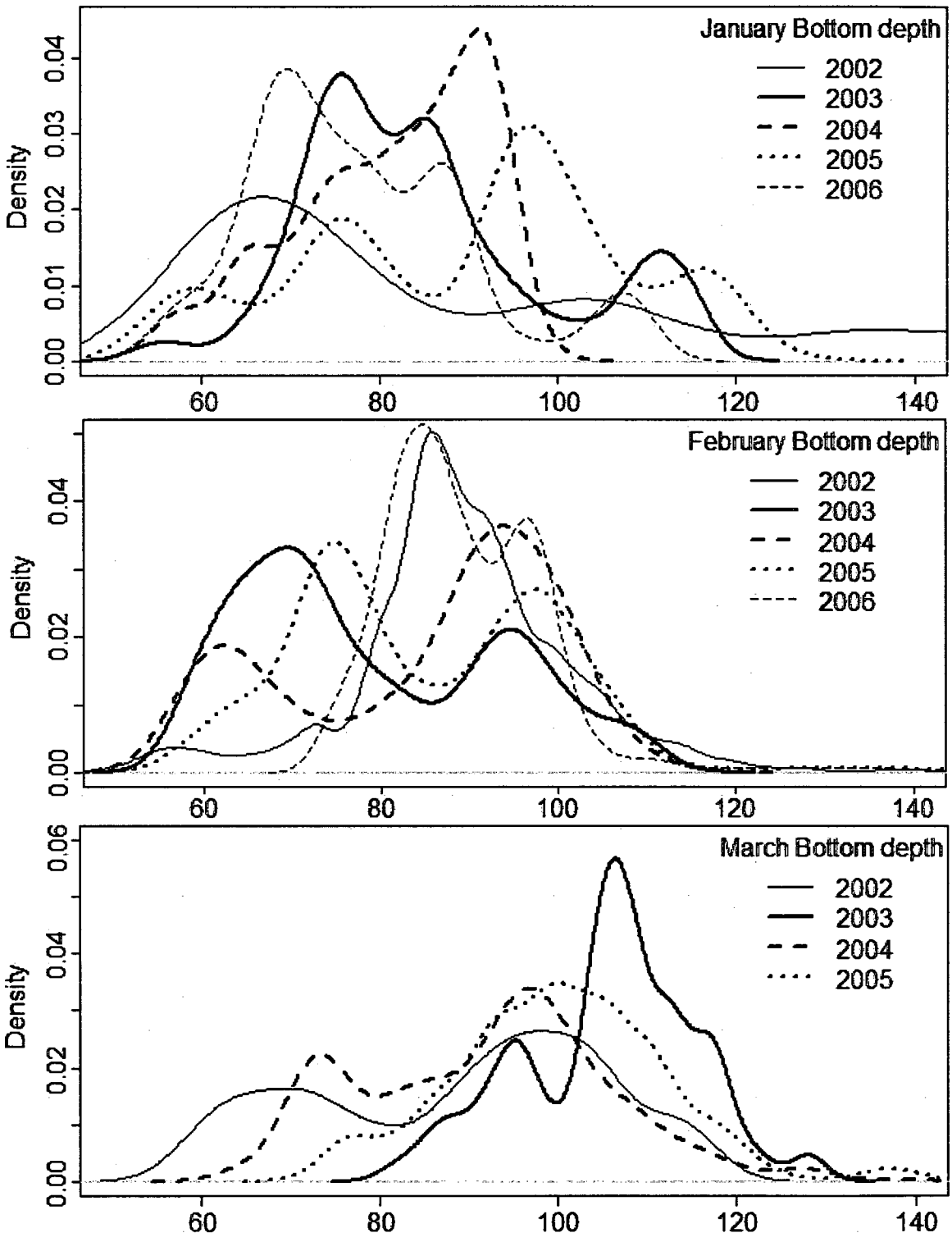

Figure 2.10. The density distribution of the bottom depth (m) along the pollock fishing track in different months during 2002–2006.

Chapter 3

Searching behavior of harvesters and its relation to fish distribution in the eastern Bering Sea pollock fishery[1]

Abstract

The Global Positioning System data, coupled with acoustic observations of walleye pollock, were collected from commercial fishing vessels in the eastern Bering Sea from 2002 to 2006. These data provided precise geographic locations of fishing vessels and of fish over time, which made it possible to study the temporal and spatial harvesting patterns and fish aggregation patterns at both small and large scales. Vessel trajectories were analyzed in terms of the distribution of the lengths of movement of vessels (the move length). Fish spatial distribution was characterized by spatial concentration and by fractal dimension. The harvesters' search pattern was reasonably described by a Levy flight process, one kind of random walk model with an exponential movement parameter μ. The movement parameter, μ, was significantly correlated ($p<0.01$) with fractal dimension of fish distribution, but not with spatial concentration. Therefore, μ can be considered as a good indicator of fish spatial distribution, and it might contribute to real-time monitoring of the eastern Bering Sea pollock fishery.

[1] Shen, H., Quinn, T.J., II, Dorn, M.W., and Wespestad, V. Searching behavior of harvesters and its relation to fish distribution in the eastern Bering Sea pollock fishery. Prepared for submission to the Fisheries Research.

3.1. Introduction

Harvesters, analogous to other predators, search for patchy resources and catch them using search strategies aided by technology. The removal of fish by fisheries may result in the variations in fish abundance which can be reflected by the changes of fish density and/or of fish spatial distribution. Historically, fishery catch and effort data were used to obtain abundance indices (e.g. catch per unit effort, CPUE) to track variation in fish abundance. However, when fishing effort is concentrated on fish aggregations, the catch rate may be an inappropriate indicator of population trend because of hyperstability of CPUE (Quinn and Deriso, 1999). The spatial extent rather than catch rate may be the better indicator of population size for some species which change their spatial distribution rather than the density under disturbance. Peruvian anchovy and Atlantic cod (Atkinson et al., 1997) are two examples of fish stock collapse, in which the spatial distribution reorganized when stock abundance decreased rather than there being strong reduction in fish density in their distribution areas.

In spite of the recent increase in scientific surveys, the data for harvested species are often insufficient to study the temporal and spatial distribution at different scales due to limited coverage of survey data in space and time. In contrast to survey data, commercial fishery data provided detailed information about vessel distribution and often have broad spatial coverage and temporal continuity with less cost. Because harvesters chase fish and catch them, the vessel distribution can provide information about underlying fish distribution on different temporal and spatial scales that is not available through other means. Therefore, if the relation between spatial distribution of fish and vessels are well defined, studying harvester behavior can provide enough information about fish temporal and spatial distribution. The ideal free distribution (Fretwell and Lucas, 1970), which has become a cornerstone of behavioral ecology, was indirectly used to investigate the relation between fish and vessels (Gillis, 2003). There are also some studies focused directly on the behaviors of both fish and harvesters with simultaneous and independent sources of information (Hancock et al., 1995; Potier et al., 1997; Bertrand et al., 2004;

Bertrand et al., 2005). Here we use simultaneous fish and vessel information to investigate the relation between fish and harvesters in the walleye pollock (*Theragra chalcogramma*) fishery in the eastern Bering Sea (EBS).

The pollock fishery is one the largest fisheries in the world. As a major prey species, pollock is also an important component of the EBS ecosystem. Thus, study of population trend and spatial distribution of pollock is important not only for fishery management but also for understanding ecosystem functioning. Historical catch data and survey data are used for stock assessment. However, the surveys are mainly conducted in the summer, except for several surveys conducted in 2001 and 2002 (Honkalehto et al., 2002). It is impossible to get information about pollock distribution and abundance in other seasons from these surveys, which is when the fisheries occur. But the fishery data can supplement the information of fish distribution. Since 2002, the joint opportunistic acoustic data program has been collecting, processing, and storing acoustic data from selected factory trawlers participating in the EBS pollock fishery (Barbeaux et al., 2005). The acoustics data not only provides pollock spatiotemporal distribution, but Global Positioning System (GPS) data also provide precise geographic locations of vessel trajectories. In this paper, data from 2002 to 2006 were used first to characterize the harvester behavior and pollock spatial distribution and second to investigate the relation between the spatial behaviors of fish and harvesters.

3.2. Materials and methods

3.2.1. Data

The EBS pollock fishery starts on January 20th in every year. Large factory trawlers mainly operated north of Unimak Island in the EBS from January 20th to February and waters around the Pribilof Islands from late February to late March (Figure 3.1). From 2002 to 2006, acoustic data were logged with uncalibrated 38 kHz Simrad ES60 split-beam echosounders with 1 ms nominal pulse length and 7.1° beam width. Uncalibrated

acoustic data are of course not suitable for absolute fish density estimation; however, the purpose of this study was to examine the fishing behaviors and fish spatial patterns, which should be robust to the lack of calibration. Echoview 3.30 software (SonarData, 2005) was used to process raw data and classify the echo trace from 15 m below the surface to 0.5 m above the bottom. Global Positioning System (GPS) data and observer data were used to separate searching trajectories from hauling trajectories for further analysis.

3.2.2. Levy process

Every 1km point along the searching trajectories was picked to determine if there was a change in vessel's move direction. The searching trajectories were split into "elementary moves", which are the consecutive positions of a vessel moving in a single direction. Due to high variability in the direction of search, we defined a change of 15 degrees between two consecutive points as a changed direction. Move lengths, move durations, move directions, and turning angles were then obtained. In a random walk process, the most important factor is the independence between statistical events. Move length and move duration are linear variables, whose correlation coefficients between successive moves were computed using the Kendall rank-based test. Higher-order autocorrelations were investigated by estimating the autocorrelation function (ACF). For the angular variables, move direction and turning angle, we used a generic function in **R** (http://cran.r-project.org) to test for the circular correlation.

The analysis of move length was based on Levy flight theory (Viswanathan et al., 1996). Levy flight is a kind of random walk, which is characterized by a probability density function with a power law tail for move length l : $p(l) \sim l^{-\mu}$ with $1<\mu<3$. Other μ values are related to different random walk families: $\mu \geq 3$ corresponds to a Gaussian distribution or Brownian motion, and $\mu \leq 1$ corresponds to a probability distribution that cannot be normalized. Compared to Brownian motion, the Levy flights generate trajectories with many short moves and a few long moves so that Levy motion is more diffusive than Brownian motion.

To identify the power-law behavior, the searching trajectories from one vessel during January-February 2003 (operated north Unimak Island) were used to construct the histogram for the move-length frequency distribution (Figure 3.2) on normal and logarithmic scales which is an common method used in quantifying searching pattern (Viswanathan et al., 1996; Bertrand et al., 2005; Newman, 2005). The linear relation on the logarithmic scale suggests the power-law distribution with the exponent μ. The estimate of μ can be obtained simply by fitting a linear regression in the logarithmic plot. Unfortunately, this method will introduce systematic biases (Newman, 2005). Thus, here we used an alternative, the maximum likelihood method to estimate μ as follows.

The power-law behavior has the probability density function: $p(l) = Cl^{-\mu}$, $l \geq l_{\min}$ because the power law distribution diverges as $l \rightarrow 0$. Here μ is the exponent of the power law, $l_{\min}$ is the minimum value of l at which the power-law behavior holds and we consider only the statistics of l above this value, where the C is the normalization constant, $C = (\mu - 1) l_{\min}^{\mu-1}$ (Newman, 2005). In this study, 2 km was chosen as the minimum value of l based on the data.

The log-likelihood function is given by

$$\log[\{l_i\}] = n\log(\mu - 1) + n(\mu - 1)\log l_{\min} - \mu \sum_{i=1}^{n} \log(l_i).$$

The maximum likelihood estimator of μ was obtained analytically by

$$\hat{\mu} = 1 + n/(n\log l_{\min} - \textstyle\sum_{i=1}^{n} \log l_i) .$$

Because of some very long moves, Levy motion should be more diffusive than Brownian motion. To characterize the diffusive process, we examined the relationship between the number of moves and the expected net squared displacement, $E(R_n^2)$, from a starting reference point. $E(R_n^2)$ was calculated by

$$E(R_n^2) = \frac{1}{N-n+1}\sum_{M=n}^{N}[(x_M - x_{M-n})^2 + (y_M - y_{M-n})^2],$$

where N is the number of total moves, and the starting position of fishing is (x_0, y_0). The scaling behavior of $E(R_n^2)$ with n ($E(R_n^2) \sim n^{\alpha}$) characterizes the diffusive process. For Brownian motion, $E(R_n^2)$ increases linearly with n ($\alpha = 1$) (Turchin, 1998). If $\alpha>1$, we have super-diffusive motion. One reason for this super-diffusion is the probability density function of move lengths with a heavy tail, such as Levy motion.

3.2.3. Resource characteristics

Using the collected acoustic data, pollock density was represented by the s_A (nautical area scattering coefficient) in each elementary sampling distance unit (EDSU) of 1 km. To investigate the spatial distribution of pollock, we calculated the space concentration index (Ss; Petitgas, 1998) using s_A. The non-zero s_A values were ranked by decreasing value. Then the cumulative empirical distribution of the fraction of EDSU (y) was plotted against the corresponding cumulative fraction of s_A (x). An exponential function was used to fit the empirical data:

$$y = ae^{bx} .$$

The spatial concentration index was computed by integrating the difference between the identity function (theoretically the homogeneous spatial distribution) and the fitted exponential function. The regression was strongly affected by the large number of EDSUs contributing little to the overall s_A. As suggested by Bertrand et al. (2004), the exponential function was only fitted to the first 90% of cumulative s_A,

$$Ss = \int_0^{0.9}\int\left[x - ae^{bx}\right]dx = 0.405 + \frac{a}{b}(1 - e^{0.9b}) .$$

Pollock form schools, clusters of schools, and clusters of clusters in winter pre-spawning season (Shen et al., 2008), which suggests the fractal structure of pollock spatial distribution (Fréon et al., 2005). Thus fractal dimension was the other variable

used to characterize pollock spatial distribution in EBS. Unlike dedicated survey data, the acoustic data from fishing vessels were irregularly scattered across the fish distribution. According to Halley et al. (2004), the semivariogram method was particularly appropriate to estimate the fractal dimension for this kind of dataset. For each year, we computed the log-log semivariogram on s_A. For a fractal pattern on a two dimensional landscape, the fractal dimension (D) was linearly related to the slope at the origin (m) of the log-transformed semivariogram (Figure 3.3):

$$D = 2 - \frac{m}{2} .$$

The number of points included in the linear regression was chosen so as to maximize r^2.

3.3. Results

The raw data included 17 data sets from 6 different vessels in two fishing grounds during 2002 and 2006. The searching trajectories were extracted from these 17 data sets for further analysis. The Kendall test and ACF showed that over 90% of searching trajectories of each data set did not have significant first-order and higher-order autocorrelations for move lengths or for move durations. The circular correlation test showed that over 90% of the searching trajectories of each data set did not have significant correlation between move directions or between turning angles. So the searching behavior was considered as a kind of random walk.

One example of log-log regression between frequencies and move length given in Figure 3.2 shows the linear relationship usually seen. All slopes of the log-log regressions were significantly different from zero ($p<0.01$). The mean estimated μ values among vessels by years and areas ranged between 1.880 and 2.189 which is located in the range between 1 and 3 (Table 3.1). About 79% of the vessels had α higher than 1 which suggested that most of fishing vessels performed a super-diffusive motion for searching. The range of estimated μ and super-diffusive behavior of most vessels suggested that the

searching behavior is reasonably considered as a Levy flight motion. In 2002, the vessel trajectories were too limited to estimate the μ in waters around the Pribilof Islands because the vessels returned to fish north Unimak Island in some days of March. Generally speaking, there were higher μ values north of Unimak Island than in waters around the Pribilof Islands, except for 2006 (Figure 3.4). The higher μ value may be the result of larger coverage of vessel trajectories in waters around the Pribilof Islands. The highest value of μ was in waters around the Pribilof Islands in 2006. In this year, the fishing area in March was located in the Pribilof Canyon area which was not the case in other years. Because of the interaction of bathymetry and pollock vertical distribution, pollock were concentrated in a very small area close to the 200 m isobath.

The exponential function fit that was for the relation between cumulative fraction of EDSU and cumulative fraction of s_A was statistically significant (Kolmogorov-Smirnov test, $p<0.05$) for all datasets; one example is given in Figure 3.5. Table 3.1 gives the estimated a, b and Ss values. The estimated Ss values ranged between 0.294 and 0.370 (Table 3.1). When the distribution of pollock became more unequal, i.e., more concentrated, the fitted curve bended downwards with a higher Ss value, which implies a higher deviation from a theoretical homogeneous distribution. Figure 3.5 displays an example of the fitted exponential curves of one vessel in 2003. It shows that fish were more concentrated in waters around the Pribilof Islands with a higher Ss value. There were similar results for other vessels in different years.

The fractal dimension measures the object's ability to occupy the Euclidean space E in which it is embedded (Mandelbrot, 1983). So fractal dimension can be used to summarize the messy complexity of shapes in nature. In two-dimensional space, the fractal dimension ranges between 0 and 2. In ecology, fractal dimension can be used to describe the degree of patchiness or aggregation. The estimated fractal dimension (D) ranged between 1.26 and 1.67 (Table 3.1). To examine which characteristics of pollock distribution played an important role in searching pattern, we estimated the correlation among μ and D or Ss in each year in the two fishing grounds. The correlation between D

and μ of 0.76 was significant ($p<0.05$), which provides evidence that there is a relationship between the spatial distributions of fish and harvesters. There was no significant correlation between μ and Ss.

3.4. Discussion

Compared to research survey data, fishery data stands out for its large coverage and low cost. In our program, inexpensive acoustic data loggers were installed onboard commercial fishing vessels since 2002. This allowed the simultaneous observations of fish abundance and vessel fishing pattern during the winter pollock fishing season when there were no research surveys. When collecting acoustic data, the equipment also provided precise GPS positions of vessel trajectories, which made it possible to study fishing behavior in conjunction with fish spatial distribution. Harvesters, similar to other top predators, search for and catch the fish aggregations and catch them. Therefore, the vessel distribution may reflect the spatiotemporal distribution of targeted fish species to some extent. Compared with less information about the targeted fish species, there is much more information about vessel distribution, such as observer data and VMS (vessel monitoring system) data which are available to investigate harvester behavior. If some links exist between fish and vessel distribution, harvesters as samplers of the ecosystem can be used to provide an indicator of fish spatial distribution.

Movement is crucial to spatial population dynamics for animals with strong migration capability and tendency. For example, pollock undergo seasonal migrations for spawning, feeding and wintering. Pollock also make diurnal movements which form denser aggregations (i.e., schools) in daytime and sparser aggregations (i.e., layers or clouds) in nighttime. There are two approaches, Lagrangian and Eulerian approaches, used to study movements (Turchin, 1998). The Lagranian approach centers on the individual's movement which corresponds to individual level of organization. On the other hand, the Eulerian approach centers on a point in space which corresponds to

population level of organization. The Lagrangian approach has been successfully used to study harvester behaviors of Peruvian anchovy fishery (Betrand et al., 2005) and North Sea fisheries (Marchal et al., 2007). The individual vessel trajectories were analyzed using the Lagrangian approach in this study. The analysis of vessel trajectories showed that fishing behavior can be characterized by Levy flight with a heavy tail when they are searching for fish. Bertrand et al. (2005) also demonstrated the success of using Levy theory to describe harvester behavior and interpreted the Levy parameter as ecosystem indicator in Peruvian anchovy fishery. The independence between move length, move duration and move heading also confirmed the random walk searching strategy. The super-diffusive feature of Levy motions was also evidenced by the relationship between the net squared displacement and number of moves. Thus, it is reasonable to use Levy random walk to characterize harvester searching behavior in the EBS pollock fishery.

In a Levy random walk, the μ value characterizes the sinuosity of the trajectories. A decrease of sinuosity results in the decrease of μ, which means longer long moves and shorter short moves in the trajectories. And then the power-law distribution has a heavier tail. From an Eulerian point of view, the decrease of μ suggests the increase of diffusion of individuals, such that the area exploited increases.

Pollock are fractally structured in their spatial distribution. The Levy flight was inferred to be an efficient foraging strategy for food which is fractally distributed (Viswanathan et al., 1996) because of the higher encounter rate (the number of encounters per unit volume swept) compared to Brownian motion. Thus the Levy searching behavior can let harvesters have high searching efficiency. Viswanathan et al. (1999) indicated that the Levy motion has optimal searching efficiency with μ=2 for non-destructive foraging. The pollock fishery can be considered non-destructive because pollock can recover from fishing removal in about one week (Battaile and Quinn, 2006). Our estimated μ's are very close to this value with some variation in different years among different vessels.

Harvesters search for fish aggregations and catch them. Thus the vessel distribution should reflect the underlying fish spatial distribution to some extent. The spatial distribution of pollock was characterized by the spatial concentration index (Ss) and fractal dimension (D) in this paper. The relationship between the Levy parameter μ and the above two metrics may provide information about the relation between fish and harvester spatial distributions. Although weak correlation occurred between μ and Ss, the correlation between D and μ was significant which confirms the relationship between the harvester's spatial behavior and fish spatial distribution. The weak relation between Ss and μ suggested that the harvester's spatial searching behavior is mainly determined by the degree of clustering of fish. Our results are comparable to studies by Bertrand et al. (2005). They used total surface occupied by anchovy, spatial concentration index and fractal dimension to characterize Peruvian anchovy distribution. They also found that μ was significantly correlated to the fractal dimension (D) of fish distribution rather than other two characteristics.

Pollock in the EBS avoided water colder than –2°C which restricts the distribution of pollock, especially in winter season. In January to February, pollock spread south to north Unimak Island when the water temperature was relatively low. Thus there was less spatial coverage of pollock distribution and less variation of spatial coverage. But in March, pollock concentrated in waters around the Pribilof Islands when the temperature increased. Pollock had a broader distribution in this area, especially in warm years. However, there was higher variation of spatial coverage depending on the ocean conditions in different years. In some years, a high portion of pollock was still distributed in north Unimak Island in March, such as in 2002 which resulted in inadequate vessel trajectories for estimating the Levy parameter in waters around the Pribilof Islands. Pollock spread to 58°50'N in 2003 and 56°30'N in 2006 which was the only year with many vessel trajectories in Pribilof Canyon.

Generally speaking, there were smaller Ss and larger μ and D values for north Unimak Island than for the Pribilof Islands, which could be considered as the result of

smaller spatial coverage of pollock. The estimated μ values in north Unimak Island were not as variable as those in waters around the Pribilof Islands. Fish distribution was confined in relatively small areas by the cold water in north Unimak Island which caused less variation of spatial coverage of pollock distribution and then less variation of μ values in this area. However, the fish distribution changed dramatically in waters around the Pribilof Islands depending on the biomass and ocean conditions. The estimated μ values changed a lot, as did the estimated D values. The estimated μ and D values increased from 2003 to 2006 in waters around the Pribilof Islands, while the estimated biomass decreased from 2003 to 2006 (Ianelli et al., 2008). In colder years, pollock may distribute in smaller areas, so there are less long moves from the vessel trajectories which resulted in a less heavy tail in the power law distribution and then the higher μ value. In warmer years, pollock have higher abundance and sparser distribution which result in increased long moves of vessel trajectories. So the μ value in waters around the Pribilof Islands may provide some information about the fish abundance besides the clustering degree of fish aggregations.

2006 was an unusual year, in which there were very high values of μ in both north Unimak Island and waters around the Pribilof Islands. As mentioned above, the increase of μ was the result of less long moves in vessel trajectories. The distribution of trajectories had smaller spatial coverage north Unimak Island in 2006 than other years which suggested that fish distribution had smaller coverage in that year. In 2006, the estimated biomass for EBS pollock was quite low compared to other years (Ianelli et al., 2008). Can the high μ value be considered as the indicator of low abundance? If so, we can take the estimated μ value as an indicator of lower than expected abundance for in-season management at the end of February.

This was a preliminary study of harvester behavior using Levy theory. Although we do not have many years in the dataset, the available data suggested that the fishing behavior in the pollock fishery could be characterized by a Levy random walk. The μ statistic was a good candidate as an ecosystem indicator. The μ value was easily

calculated and intuitively used to describe the spatial behavior of harvesters. The property of scale-invariance also made Levy flight appropriate to describe multi-scale processes. Although acoustic data are expensive, VMS data are available for the US pollock fishery. A long time-series of VMS data may improve the power and cost effectiveness of this research. If long time-series analysis also confirms the correlation between D and μ, μ may be a promising indicator of the degree of clustering of fish aggregations that could contribute to real-time monitoring of ecosystems.

3.5. Acknowledgments

This research was funded by a grant from the Pollock Conservation Cooperative Research Center to the University of Alaska Fairbanks (UAF). Additional funds for student support were provided by the Alaska Fisheries Science Center, through the Cooperative Institute for Arctic Research (NA17RJ1224) at UAF.

3.6. References

Atkinson, D.B., Rose, G.A., Murphy, E.F., Bishop, C.A., 1997. Distribution changes and abundance of northern cod (*Gadus morhua*), 1981–1993. Can. J. Fish. Aquat. Sci. 54, 132–138.

Barbeaux, S.J., Dorn, M., Ianelli, J., Horne, J., 2005. Visualizing Alaska pollock (*Theragra chalcogra*mma) aggregation dynamics. ICES Document CM 2005/U: 01. 12 pp.

Battaile, B.C., Quinn, T.J., II, 2006. A DeLury depletion estimator for walleye pollock (*Theragra chalcogramma*) in the eastern Bering Sea. Nat. Resour. Model. 19, 655–674.

Bertrand, S., Burgos, J.M., Gerlotto, F., Atiquipa, J., 2005. Lévy trajectories of Peruvian purse-seiners as an indicator of the spatial distribution of anchovy (*Engraulis ringens*). ICES J. Mar. Sci. 62, 477–482.

Bertrand, S., Díaz, E., and Ñiquen, M., 2004. Interactions between fish and fisher's spatial distribution and behaviour: an empirical study of the anchovy (*Engraulis ringens*) fishery of Peru. ICES J. Mar. Sci. 61: 1127–1136.

Fréon, P., Cury, P., Shannon, L.J., Roy, C., 2005. Sustainable exploitation of small pelagic fish stocks challenged by environmental and ecosystem changes: a review. Bull. Mar. Sci. 76, 385–462.

Fretwell, S.D., Lucas, H.L., 1970. On territorial behaviour and other factors influencing habitat distribution in birds. I. Theoretical development. Acta Biotheoretica 19, 16–36.

Gillis, D.M., 2003. Ideal free distributions in fleet dynamics: a behavioral perspective on vessel movement in fisheries analysis. Can. J. Zool. 81, 177–187.

Halley, J.M., Hartley, S., Kallimanis, A.S., Kunin, W.E., Lennon, J.J., Sgardelis, S.P., 2004. Uses and abuse of fractal methodology in ecology. Ecol. Letters 7, 254–271.

Hancock, J., Hart, P.J.B., Antezana, T., 1995. Searching behaviour and catch of horse mackerel (*Trachurus murphyi*) by industrial purse-seiners off south-central Chile. ICES J. Mar. Sci. 52, 991–1004.

Honkalehto, T., Williamson, N., Hanson, D., McKelvey, D., de Blois., S., 2002. Results of the echo Integration-trawl survey of walleye pollock (*Theragra chalcogramma*) conducted on the southeastern Bering Sea shelf and in the southeastern Aleutian basin near Bogoslof Island in February and March 2002. AFSC Processed Report 2002–02. 49 pp.

Ianelli, J.N., Barbeaux, S., Honkalehto, T., Kotwicki, S., Aydin, K., Williamson, N., 2008. Assessment of the Walleye Pollock stock in the Eastern Bering Sea. North Pacific Fishery Management Council, Bering Sea and Aleutian Islands Stock assessment and Fishery Evaluation Report, 47–136.

Mandelbrot, B.B., 1983. The Fractal Geometry of Nature. Freeman, New York.

Marchal P., Poos, J., Quirijns, F., 2007. Linkage between fisher's foraging, market and fish stock density: examples from some North Sea fisheries. Fish. Res. 83, 33–43.

Newman, M.E.J., 2005. Power laws, Pareto distributions and Zipf's law. Contemp. Phys. 46, 323–351.

Petitgas, P., 1998. Biomass-dependent dynamics of fish spatial distributions characterized by geostatistical aggregation curves. ICES J. Mar. Sci. 55, 443–453.

Potier, M., Petitgas, P., Petit, D., 1997. Interactions between fish and fishing vessels in the Javanese purse seine fishery. Aquat. Living Resour. 10, 149–156.

Quinn, T.J., II, Deriso, R.B., 1999. Quantitative Fish Dynamics, Oxford Univ. Press, New York.

Shen, H., Quinn, T.J., II, Wespestad, V., Dorn, M.W., Kookesh, M., 2008. Using acoustics to evaluate the effect of fishing on school characteristics of walleye pollock. In: Resiliency of gadid stocks to fishing and climate change. Alaska Sea Grant, University of Alaska Fairbanks: 125–140.

SonarData. 2005. Echoview. Version 3.30. <http://www.sonardata.com/webhelp /Echoview.htm>. Tasmania, Australia. (May 2005).

Turchin, P., 1998. Quantitative analysis of movement: measuring and modeling population redistribution in animals and plants. Sinauer Associates, Inc., Sunderland, Mass.

Viswanathan, G.M., Afasynev, V., Buldyrev, S.V., Murphy, E.J., Prince, P.A., Stanley, H.E., 1996. Levy flight search patterns of wandering albatrosses. Nature 381, 413–415.

Viswanathan, G.M., Buldyrev, S.V., Havlin, S., DaLuz, M.G.E., Raposo, E.P., Stanley, H.E., 1999. Optimizing the success of random searches. Nature 401, 911–914.

Table 3.1. The average estimated parameters (movement parameter, μ; fractal dimension, D; spatial concentration index, Ss; parameters of exponential function, a and b) from different fishing vessels in the two fishing areas during 2002 and 2006. (UI=Unimak Island, PI=Pribilof Islands)

Year	Fishing area	μ	D	Ss	a	b
2002	UI	2.121	1.670	0.335	4.25×10^{-3}	4.892
2003	UI	2.044	1.580	0.320	5.01×10^{-3}	4.928
2004	UI	2.119	1.640	0.294	11.31×10^{-3}	4.143
2005	UI	2.054	1.485	0.305	6.98×10^{-3}	4.691
2006	UI	2.189	1.612	0.310	7.08×10^{-3}	4.612
2003	PI	1.880	1.260	0.340	4.36×10^{-3}	4.746
2004	PI	1.949	1.555	0.337	5.13×10^{-3}	4.578
2005	PI	1.981	1.585	0.352	2.11×10^{-3}	5.475
2006	PI	2.216	1.650	0.370	2.47×10^{-3}	4.676

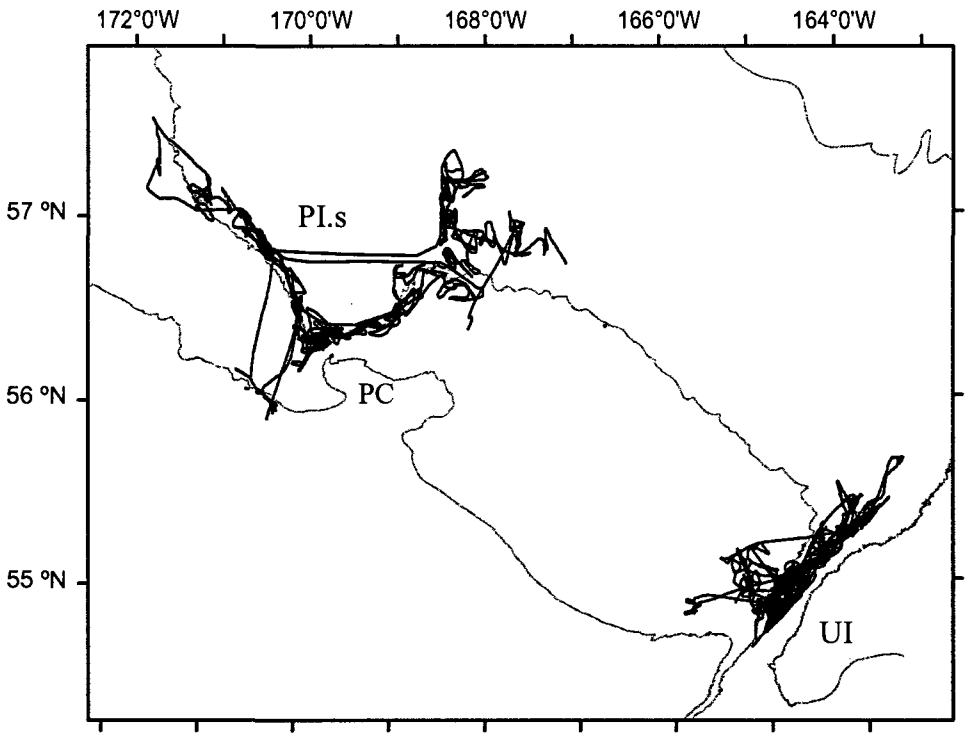

Figure 3.1. The vessel trajectories of one vessel in 2004. UI = Unimak Island. PI.s = Pribilof Islands. PC = Pribilof Canyon.

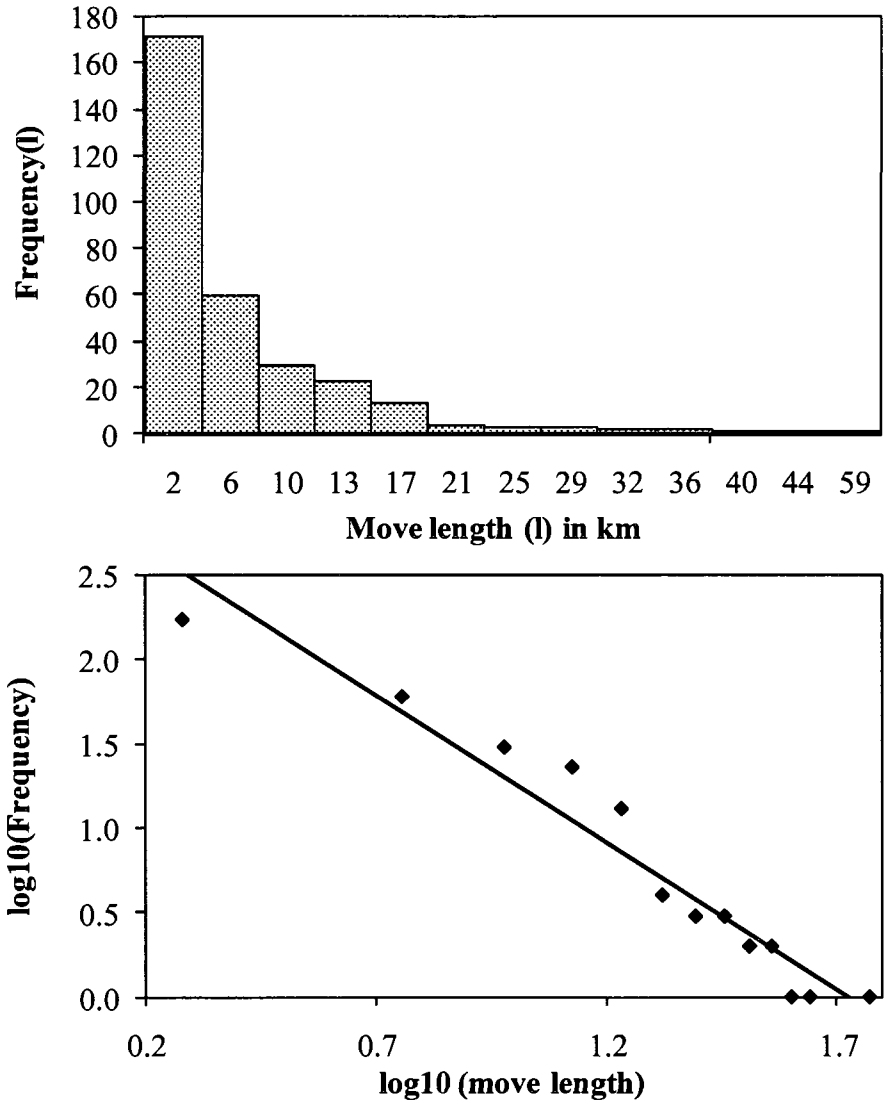

Figure 3.2. The top panel is the move-length frequency distribution. The bottom panel is the corresponding log-log scale plot with a fitted regression line.

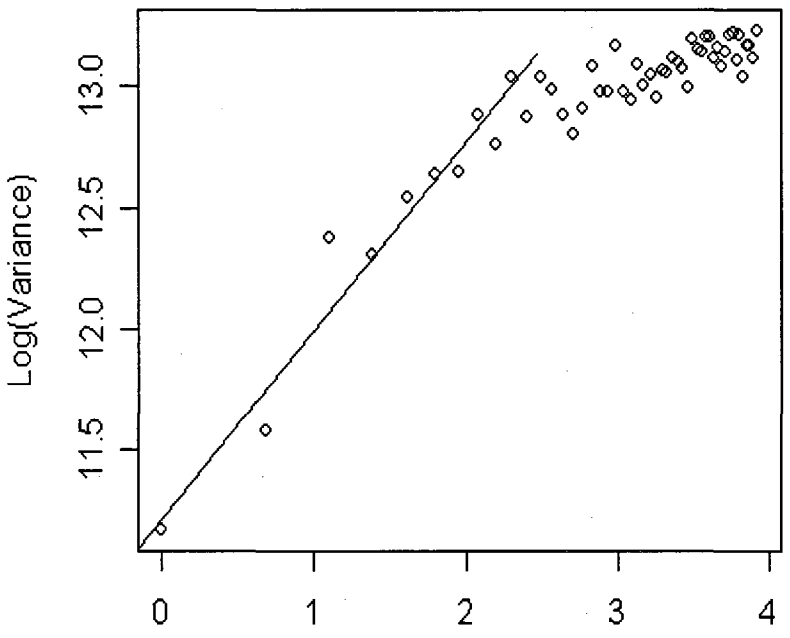

Figure 3.3. The log-log transformation of the semi-variogram of the pollock distribution from one vessel.

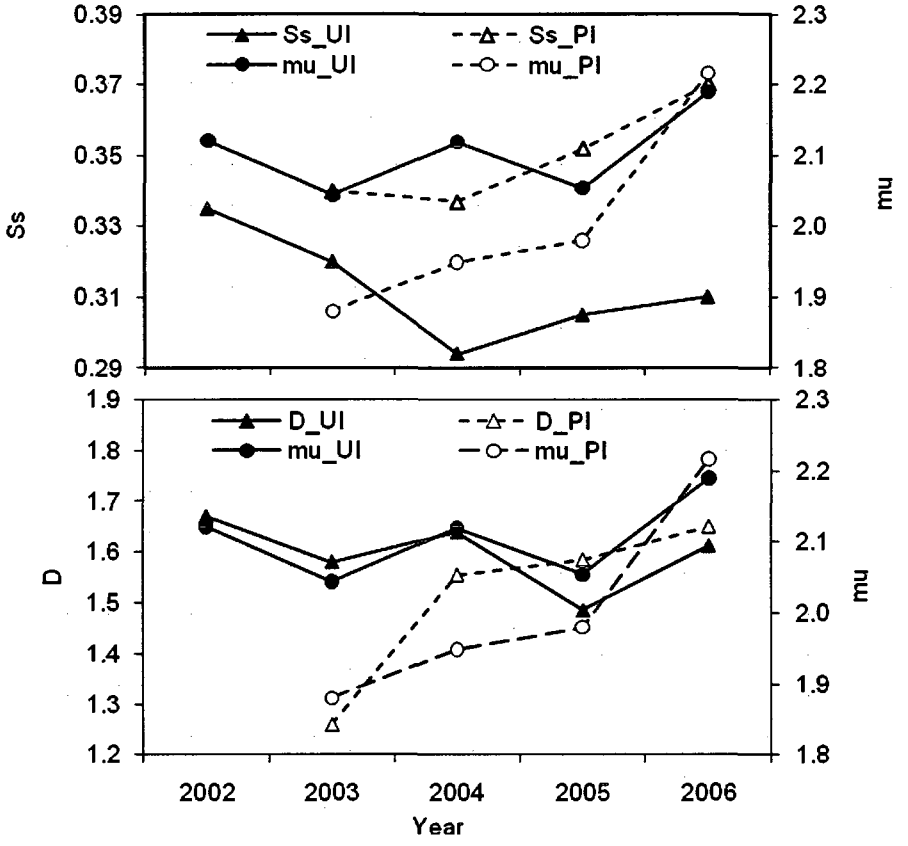

Figure 3.4. Time-series comparisons between the power law parameter of vessel trajectories (μ) and (upper panel) spatial concentration (Ss), and (bottom panel) fractal dimension (D). UI = Unimak Island, PI = Pribilof Islands.

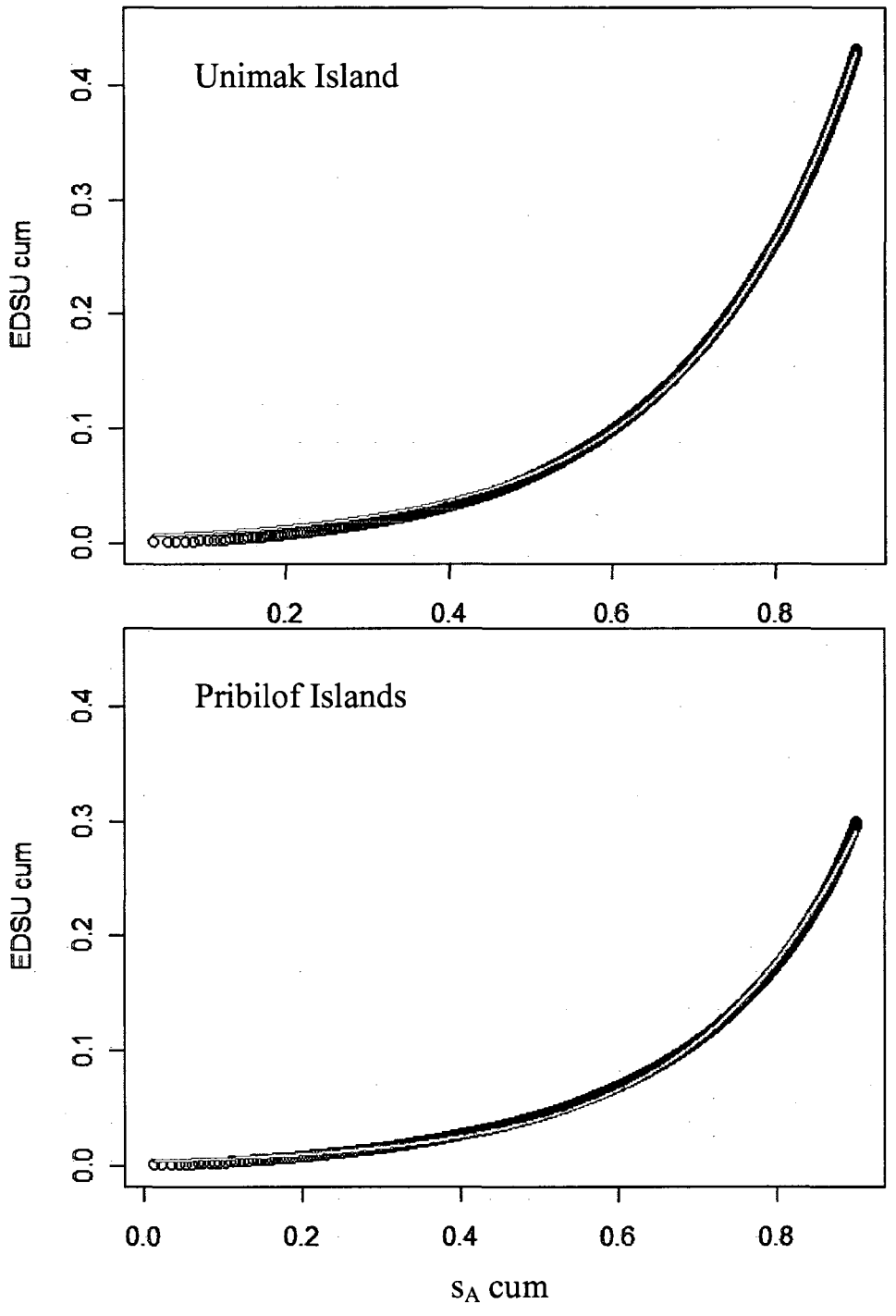

Figure 3.5. Example of exponential relations (red line) fitted to the empirical distribution of cumulative percentage of EDSU against cumulative percentage of s_A (black circle) for one vessel in 2003 and in the two fishing areas.

Chapter 4

Schooling pattern of eastern Bering Sea walleye pollock and its effect on fishing behavior[1]

Abstract

Walleye pollock (*Theragra chalcogramma*) form persistent midwater and near-bottom schools in the daytime during the winter spawning season in the eastern Bering Sea (EBS). Two spawning areas in the EBS, north of Unimak Island and near the Pribilof Islands, are the main fishing grounds. To study the schooling pattern of pollock and its effect on fishing behavior on these two fishing grounds, a principal component analysis with instrumental variables was carried out using acoustic and observer data from 2003 and 2005. Significant differences between the school descriptors distinguished the schooling patterns among areas and years. The harvester, that is to say, the fishing vessel and its crew taken together, searched for fish aggregations, which were caught in a different manner when the schooling pattern changed. School density had a greater effect than school size on fishing behavior. Aggregations were less dense in 2003 than in 2005, and the harvester tended to fish with longer tows, at higher speeds, when it encountered less dense aggregations.

[1] Shen, H., Dorn, M.W., Wespestad, V., and Quinn, T.J., II. 2009. Schooling pattern of eastern Bering Sea walleye pollock and its effect on fishing behaviour. ICES Journal of Marine Science, 66: 1284–1288.

4.1 Introduction

Pelagic fish usually form different kinds of aggregations, such as schools, clusters of schools, clouds, and layers (Reid, 2000). As a semi-pelagic species, walleye pollock (*Theragra chalcogramma*) form persistent midwater and near-bottom schools during the spawning season. Knowledge of pollock schooling pattern provides information about fish behavior essential to the management of the fishery (Marchal and Petitgas, 1993). In addition to being the main target of a fishery, walleye pollock is also an important component of the eastern Bering Sea (EBS) ecosystem as a major prey species (NRC, 1996). Its schooling pattern may affect the predation success of species in higher trophic levels, such as Steller sea lions (Wilson *et al.*, 2003) and, therefore, it is important for ecological studies.

Acoustic methods have been used commonly in pelagic fisheries to explore the schooling behavior of fish (Simmonds and MacLennan, 2005). Since 1979, such methods have been used to estimate the pollock abundance in midwater during the echo-integration and trawl surveys of the EBS, using research vessels (Ianelli *et al.*, 2007). However, these surveys were usually conducted in summer, except for a few winter surveys in 2001 and 2002 (Honkalehto *et al.*, 2002). Although their results may be less precise than those of dedicated scientific surveys, commercial vessels can be suitable platforms for collecting acoustic data for scientific purposes (Melvin *et al.*, 2002; Mackinson and van der Kooij, 2006) and are particularly useful for in-season monitoring of stock trends (Melvin *et al.*, 2001). Since 2002, a joint, opportunistic, acoustic-data program has been collecting, processing, and storing acoustic data from selected factory trawlers participating in the EBS pollock fishery (Barbeaux *et al.*, 2005).

Fish schools are formed when a number of fish aggregate. Many parameters are required to describe a fish school, *inter alia* morphometric, positional, and energetic descriptors; univariate analysis alone cannot adequately describe this complex entity. In this paper, the schooling pattern of pollock is examined by comparing observations in two fishing grounds (north of Unimak Island and around the Pribilof Islands) during two

years (2003 and 2005), using a principal component analysis with instrumental variables (PCAIV) of the school descriptors. The concurrent fishing behavior was also analyzed using the PCAIV to study its relationship with the schooling pattern.

4.2 Material and methods

Acoustic data were collected using a large factory trawler that usually operated north of Unimak Island in the EBS from January to late February and around the Pribilof Islands from late February to March (Figure 4.1). There were no differences in the way data were collected and logged in both areas and years. An uncalibrated, 38-kHz, Simrad ES60 split-beam echosounder with a 1 ms nominal pulse length and a 7.1° beam width was used. The data were corrected for the triangle-wave problem using the algorithm of Ryan and Kloser (2004). Although uncalibrated acoustic data are unsuitable for absolute fish-density estimation, the purpose of this study was to compare schooling patterns in different years and on different fishing grounds, but detected by the same vessel, so this should therefore not be affected by the lack of calibration.

Echoview 3.30 software (SonarData, 2005) was used to process the raw data and classify the echotrace from 15 m below the surface to 0.5 m above the seabed. Pollock within the near-bottom zone were not included in this analysis. This problem was unimportant in the study, because all the schools were compared using the same methods. Schools of walleye pollock were detected and characterized using the school module in Echoview. The data were collected only during daylight, when pollock displayed schooling behavior. To detect the schools, a volume-scattering strength (S_v) threshold of -70 dB re 1 m^{-1} was applied, with the other criteria for the school algorithm being the minima of school length (40 m), school height (5 m), candidate length (5 m), and candidate height (2 m), and the maxima of vertical (5 m) and horizontal (20 m) linking distances (Wilson *et al.*, 2003; SonarData, 2005).

The school descriptors generated by the Echoview software included morphometric (length, L; thickness, T; perimeter, P; and area of schools, A), positional (longitude, latitude, school depth D), and energetic descriptors (S_v and s_A, the nautical-area-scattering coefficient; Simmonds and MacLennan, 2005). Based on these descriptors, two others, namely school fractal dimension and school elongation, were determined. The fractal dimension (F) of a school is an index of shape complexity, which depends on the relationship between the school perimeter and area (Nero and Magnuson, 1989). The elongation (E) is the ratio of the school length to the school thickness (Weill *et al.*, 1993). A Kolmogorov–Smirnov test (K–S test; Zar, 1999) was done to test for significant differences at the confidence level α=0.05 between the two years in the two fishing grounds. The confidence level was not adjusted for the multiple tests, because there were few descriptors, and the aim was not to specify the significance level for the entire testing procedure, as might be done in a multiple-comparisons procedure.

To evaluate the effects of area and year, a PCAIV of the fish school descriptors was done using the statistical software "R" (http://cran.r-project.org). The PCA was based on eight nonredundant variables as defined above: L, T, P, A, D, S_v, F, and E. The schools were divided into four classes: U3 (Unimak Island; 2003), P3 (Pribilof Islands; 2003), U5 (Unimak Island; 2005), and P5 (Pribilof Islands; 2005). Before the PCA, outliers were identified by the multivariate method in "R" (Filzmoser *et al.*, 2008), which computes the Mahalanobis distances based on robust principal components. The Mahalanobis distances were transformed so that a critical value from a Chi-squared distribution could be used to remove the outliers. To examine differences in the schooling pattern between classes, a between-class PCA was done; this is a particular case of the PCAIV with one qualitative instrumental variable (Dolédec and Chessel, 1994; Pélissier *et al.*, 2003). In this case, class was used as the instrumental variable, so the analysis focused on the differences that best distinguished the classes. This was done by minimizing the between-class inertia, which is the variance of the class determinations (Akhisar and Bener, 2002). A Monte Carlo test was done to examine the significance of differences between the classes (Romesburg, 1985).

Data collected simultaneously by a fishery observer on the vessel were used to investigate how fishing behavior changed in response to the schooling pattern. The vessel track was separated into search and fishing paths, by combining the observer-recorded deployment and retrieval times of the net with the acoustic data. In winter, the backscatter emanated mainly from pollock aggregations on both fishing grounds. Therefore, the school density could also be indexed by the s_A for the whole water column, averaged over 1 km, as the elementary sampling distance unit for both search and fishing time. Similarly, the observer data were divided into four classes: U3, P3, U5, and P5. Seven variables were chosen for the PCA: fishing depth (fd), fish density during search (ss_A), fish density during fishing (fs_A), searching duration (sD), fishing duration (fD), searching speed (sS), and fishing speed (fS). The PCAIV and Monte Carlo tests were also done to examine the differences in fishing behavior between the school classes.

4.3 Results

In all, 2405 schools were identified after removing 216 outliers among the four classes, namely U3 (936), P3 (470), U5 (433), and P5 (566). The acoustic data were generally of higher quality with less missing pings in north Unimak in 2003; therefore, there were a larger number of schools in the U3 class. Univariate analysis of school descriptors revealed significant differences between the two years in the two fishing grounds usually (Table 4.1). The main Unimak Island school descriptors were significantly different always, except for school length and perimeter. The Pribilof Islands schools were significantly different between years, except for school length. There was no clear difference in the observed schools between fishing and searching periods for both areas and years (K–S test, $p > 0.05$). Therefore, all schools were used to test for differences among the four classes using the PCAIV.

Figure 4.2 shows the results of the PCAIV in the factorial planes (1, 2) and (1, 3). The eigenvalue histograms in Figure 4.2 illustrate the percentage of the between-class

inertia explained by different axes. The first accounted for 64% of the inertia, which was mainly defined by school depth and school area (on the left) and school elongation (on the right). The second axis contributed 20%, mainly defined by the school fractal dimension, with little contribution from other descriptors. The third was positively related to school elongation and negatively related to school thickness. School length and school perimeter were unimportant variables as regards distinguishing between schools.

From the Monte Carlo test, the inertia percentage was significant ($p < 0.001$), indicating important differences in the schools between classes. From the factorial planes in Figure 4.2, the four school classes were distinguished by different descriptors. P3 and P5 (Pribilof Islands; 2003 and 2005) were both on the negative side of the first axis; in these years, the Pribilof Islands schools were deeper and larger in area than the Unimak Island schools (Figure 4.3). Pollock form schools near the bottom. Therefore, the greater depth near the Pribilof Islands probably explains the deeper schools. The schools were distinguished between years by the fractal dimension and S_v on the second axis (Figure 4.2). In 2005, the schools were denser and had a higher fractal dimension for both fishing grounds (Figure 4.3), and U3 and U5 were situated on the positive side of the first axis, which corresponds to shallower schools with smaller area. The Unimak Island schools were distinguished between years by elongation and thickness on the third axis. The schools in 2005 were thinner, which resulted in a larger elongation for the same school length (Figure 4.3).

Most fishing-behavior variables differed significantly between the two years for both fishing grounds (Table 4.2). The results from the PCAIV for fishing behavior are displayed in Figure 4.4. The first axis accounted for 49% of the between-class inertia and was mainly a function of fishing depth and ss_A (on the left) and searching speed (on the right). An inverse relationship between ss_A and each of the descriptors fishing duration, searching, and fishing speed was observed with both principal components (Figure 4.4), because the harvester tended to decrease the searching and fishing speeds and hauling time when denser fish aggregations were encountered. Search duration had a weaker

relationship with searching speed and fishing duration. The second axis accounted for 43% of the between-class inertia and was mainly defined by fishing duration and searching speed. The third axis accounted for only a small percentage of the between-class inertia and can be ignored.

The Monte Carlo test also confirmed a significant difference in fishing behavior between classes ($p < 0.001$). Fishing behavior in 2003 was distinguished from that in 2005 by longer fishing duration and higher searching speed (Figures 4.4 and 4.5). In 2003, the fishing behavior in the two areas differed in fishing speed and search duration (Figure 4.4). The Pribilof tracks in 2003 exhibited the highest fishing speed and fishing duration, and the shortest search duration, among the four classes (Figure 4.5). There was no significant difference between areas as regards fishing behavior in 2005, although the fishing and searching speeds were slightly higher at Unimak Island (Table 4.2).

4.4 Discussion

The aim of this study was to examine the schooling pattern of pollock and to evaluate the relationship between fishing behavior and pollock-schooling patterns in the EBS. Acoustic data from a single factory trawler were used to avoid variability caused by using different acoustic systems and vessels. The skipper and fishing mate had been on this vessel for the past 10 years. There were no important changes in the acoustic equipment or the vessel machinery during the study period. Therefore, the observations describe real differences in schooling patterns and fishing behaviors. Further, the application of a volume-scattering strength threshold and exclusion of bad acoustic data ensured reliable results. The school descriptors are mostly relative indicators that should be robust to calibration changes. That is not the case for the energetic descriptors, and this means that apparent changes in fish density could be caused by calibration variability. Further, the presence or proximity of other fishing vessels may induce fish avoidance and thus result in a lower density of observed fish. Given the similar and

consistent practices of the pollock fleet, however, this problem is not expected to have had any large effect on the present study. The results should be applicable to other fishing vessels operating in a similar manner in the EBS. Nevertheless, it would be wise to study different vessels in the same area to substantiate this conclusion.

The schools displayed different structures between years in both fishing grounds. This may have been because of changes in the physical environment, especially water temperature. There was a larger biomass in 2003 than in 2005 (Ianelli *et al.*, 2007), which could have affected schooling patterns. Although the winter temperature at the seabed in the study area was not recorded directly, other sources could inform the winter conditions in 2003 and 2005. The mean sea surface temperature (SST) for January through April at 56°52'N 164°3'W, where a moored data buoy was maintained by the NOAA, was 2.44 and 1.95°C in 2003 and 2005, respectively (http://www.beringclimate.noaa.gov). The winter SSTs at the Pribilof Islands were 2.46 and 1.78°C, respectively, in the same years. Both datasets indicated a warmer winter in 2003 than in 2005.

A larger biomass of fish could result in larger and denser schools or an expanded range of the stock itself (Aukland and Reid, 1998). In the present study, a larger biomass resulted in either larger schools or a greater area occupied by the stock, but no increase in school density was observed (Table 4.1). The schools at Unimak Island were larger in 2003, with no increase in the occupied area, because the stock was constrained by ice cover. In the Pribilof Islands area, however, the stock occupied a larger area in 2003 (Figure 4.1), but the schools were smaller and of lower density. The lower density in that year was probably a consequence of the warmer winter. Although both the size and density of schools may affect fishing behavior, the latter is primarily motivated by density changes. For both fishing grounds, the fish densities were lower in 2003, which resulted in longer fishing durations and higher fishing speeds. School density also affected fishing speed and fishing duration (Figure 4.4).

The PCAIV revealed that three morphometric descriptors, school fractal dimension, school thickness, and school elongation, were useful for identifying schools among the

four classes distinguished. School fractal dimension is a smoothness measure of school boundary; a higher value indicates a school with a more complex shape. In 2005, the schools had higher fractal dimensions on both fishing grounds, suggesting that cool conditions resulted in more complex school shapes, especially for the large schools in the Pribilof Islands. There was an inverse relationship between school thickness and school elongation (Figure 4.2). Because school length was similar in the two years, we conclude that pollock evidently form schools with different thickness, rather than length, in response to varying conditions. The water column is well mixed during winter in the EBS, and the homogeneous vertical conditions might have allowed fish to spread in depth more easily than they could have done in stratified water.

Data from a single vessel were used to compare schooling patterns, and their effect on fishing behavior. Further studies are needed to examine the effect of different fishing practices among vessels and any interaction that might occur, dependent on the spatial-activity pattern of the fleet.

4.5 Acknowledgments

This research was funded by a grant from the Pollock Conservation Cooperative Research Center to the University of Alaska Fairbanks (UAF). Additional funds for student support were provided by the Alaska Fisheries Science Center, through the Cooperative Institute for Arctic Research (NA17RJ1224) at UAF.

4.6 References

Akhisar, İ., and Bener, A. 2002. Hierarchy analysis of three-way tables. Hacettepe Journal of Mathematics and Statistics, 31: 37–43.

Aukland, R., and Reid, D. 1998. The impact of changing stock size on the aggregative behaviour of North Sea herring. ICES Document CM 1998/J: 2. 19 pp.

Barbeaux, S. J., Dorn, M., Ianelli, J., and Horne, J. 2005. Visualizing Alaska pollock (*Theragra chalcogramma*) aggregation dynamics. ICES Document CM 2005/U: 01. 12 pp.

Dolédec, S., and Chessel, D. 1994. Co-inertia analysis: an alternative method for studying species–environment relationship. Freshwater Biology, 31: 277–294.

Filzmoser, P., Maronna, R., and Werner, M. 2008. Outlier identification in high dimensions. Computational Statistics Data Analysis, 52: 1694–1711.

Honkalehto, T., Williamson, N., Hanson, D., McKelvey, D., and De Blois, S. 2002. Results of the echo integration-trawl survey of walleye pollock (*Theragra chalcogramma*) conducted on the southeastern Bering Sea shelf and in the southeastern Aleutian basin near Bogoslof Island in February and March 2002. Alaska Fisheries Science Center Processed Report, 2002–02. 47 pp.

Ianelli, J. N., Barbeaux, S., Honkalehto, T., Kotwicki, S., Aydin, K., and Williamson, N. 2007. Eastern Bering Sea walleye pollock. North Pacific Fishery Management Council, Bering Sea and Aleutian Islands Stock Assessment and Fishery Evaluation Report, pp. 41–138.

Mackinson, S., and van der Kooij, J. 2006. Perceptions of fish distribution, abundance and behaviour: observations revealed by alternative survey strategies made by scientific and fishing vessels. Fisheries Research, 81: 306–315.

Marchal, E., and Petitgas, P. 1993. Precision of acoustic fish abundance estimates: separating the number of schools from the biomass in schools. Aquatic Living Resources, 6: 211–219.

Melvin, G., Li, Y., Mayer, L., and Clay, A. 2002. Commercial fishing vessels, automatic acoustic logging systems and 3D data visualization. ICES Journal of Marine Science, 59: 179–190.

Melvin, G. D., Stephenson, R. L., Power, M. J., Fife, F. J., and Clark, K. J. 2001. Industry acoustic surveys as the basis for in-season decisions in a comanagement regime. *In* Herring Expectations for a New Millennium, pp. 675–688. Ed. by F. Funk, J. Blackburn, D. Hay, A. J. Paul, R. Stephenson, R. Toresen, and D. Witherell. University of Alaska Sea Grant, AK-SG-01-04, Fairbanks.

NRC (National Research Council). 1996. The Bering Sea Ecosystem. National academies Press, Washington, DC. 307 pp.

Nero, R.W., and Magnuson, J. J. 1989. Characterization of patches along transects using high-resolution 70-kHz integrated acoustic data. Canadian Journal of Fisheries and Aquatic Sciences, 46: 2056–2064.

Pélissier, R., Couteron, P., Dray, S., and Sabatier, D. 2003. Consistency between ordination techniques and diversity measurements: two strategies for species occurrence data. Ecology, 84: 242–251.

Reid, D. G. (Ed.) 2000. Report on echo trace classification. ICES Cooperative Research Report, 238. 107 pp.

Romesburg, H. C. 1985. Exploring, confirming and randomization tests. Computers and Geosciences, 11: 19–37.

Ryan, T. E., and Kloser, R. J. 2004. Quantification and correction of a systematic error in Simrad ES60 Echosounders. Paper presented at the ICES-FAST Working Group, Gdańsk. 9 pp.

Simmonds, E. J., and MacLennan, D. N. 2005. Fisheries Acoustics: Theory and Practice, 2nd edn. Blackwell Science, Oxford. 437 pp.

SonarData. 2005. Echoview. Version 3.30. <http://www.sonardata.com/webhelp /Echoview.htm>. Tasmania, Australia. (May 2005).

Weill, A. C., Scalabrin, C., and Diner, N. 1993. MOVIES-B: an acoustic detection description software. Application to shoal species classification. Aquatic Living Resources, 6: 255–267.

Wilson, C. D., Hollowed, A. B., Shima, M., Walline, P., and Stienessen, S. 2003. Interactions between commercial fishing and walleye pollock. Alaska Fishery Resources Bulletin, 10: 61–77.

Zar, J.H. 1999. Biostatistical Analysis. Prentice-Hall, New Jersey. 663 pp.

Table 4.1. Average school descriptors in two areas (U: Unimak Island, P: Pribilof Islands) in two years (3: 2003, 5: 2005). The schools were compared using the K–S test; *p* is the significance level of differences between the two years.

	U3	U5	*p*	P3	P5	*p*
L	61.5	64.1	0.08	63.2	68.9	0.06
T	11.9	10.3	0.00	11.5	13.9	0.00
P	276.5	279.2	0.46	273.9	361.9	0.00
A	332.2	284.9	0.00	359.7	391.9	0.02
D	86.2	87.4	0.23	102.2	101.0	0.01
S_v	–44.2	–43.2	0.00	–44.1	–43.6	0.02
F	1.47	1.51	0.00	1.45	1.52	0.00
E	5.4	7.1	0.00	6.2	5.4	0.00

Table 4.2. Average variables for fishing behavior in two areas (U and P) in two years (3: 2003, 5: 2005). The variables were compared using the K–S test; *p* is the significance level of differences between the two years.

	U3	U5	*p*	P3	P5	*p*
fd	84.8	91.5	0.00	105.4	105.2	0.51
ss_A	1 178.0	1 461.6	0.07	840.2	2 020.6	0.01
fs_A	1 612.7	1 331.3	0.26	1 454.1	1 824.4	0.43
sD	219.2	1 66.5	0.03	167.5	182.5	0.00
fD	135.1	106.2	0.04	187.3	82.2	0.00
sS	6.3	5.6	0.00	6.7	5.2	0.00
fS	5.3	5.0	0.00	5.7	4.8	0.00

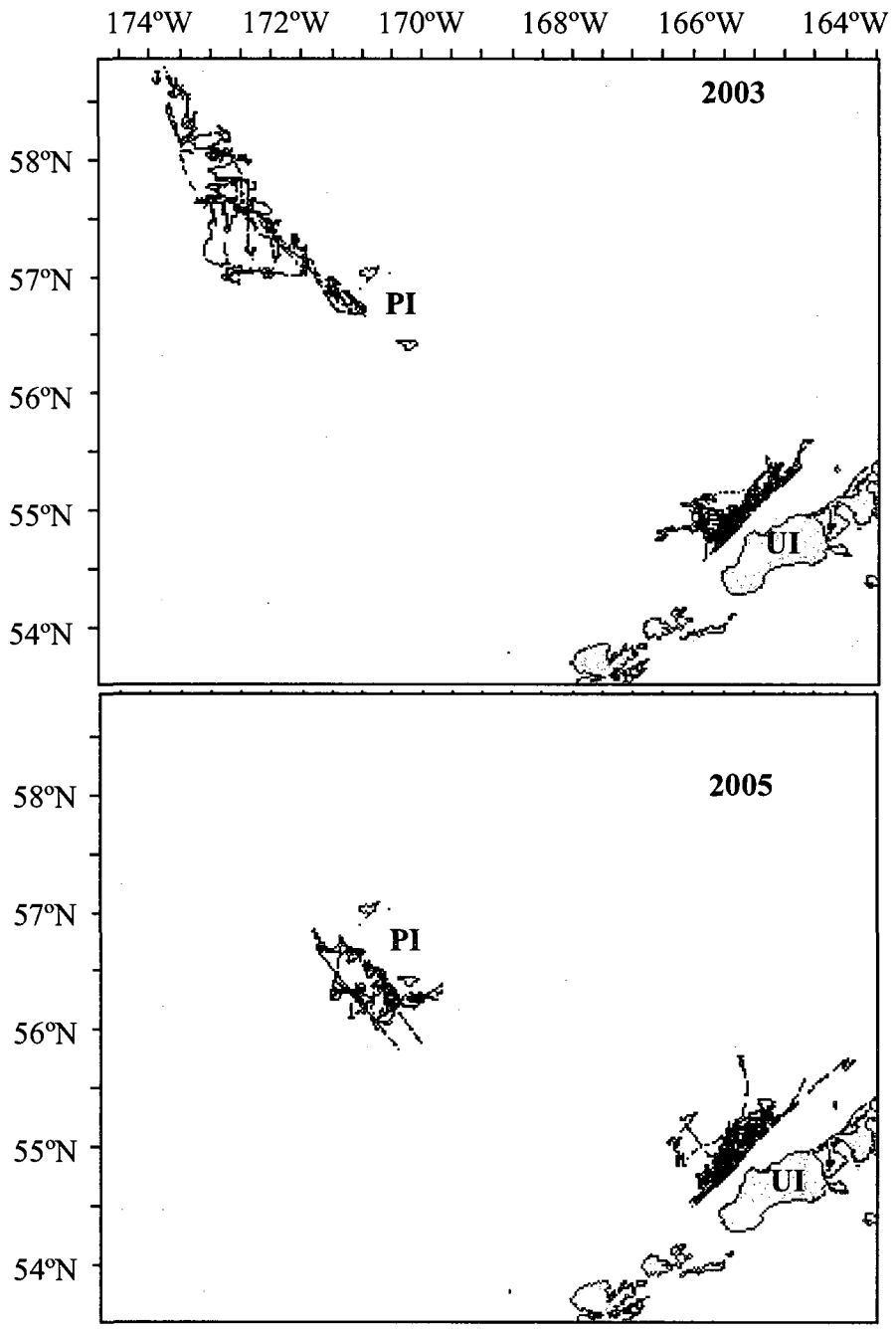

Figure 4.1. Tracks of the fishing vessel in January-March in 2003 and 2005. UI=Unimak Island; PI=Pribilof Islands

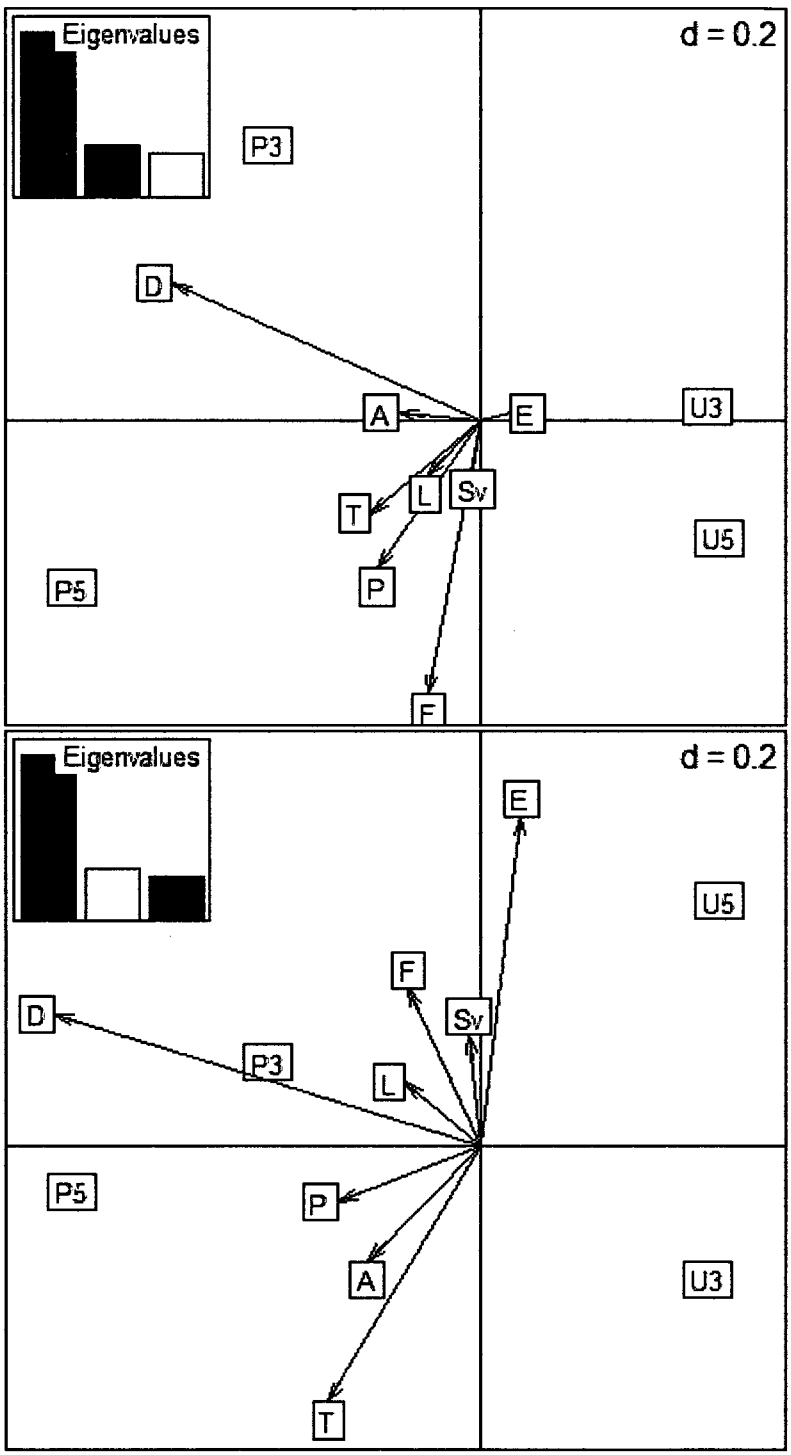

Figure 4.2. Bi-plots of principal components 1 and 2 and 1 and 3 from the between-class PCAIV using acoustic data. The two black bars in the eigenvalue chart (upper left corner) correspond to the axes used to draw the bi-plot. The scale of the graph is given by the grid size d in the upper right corner.

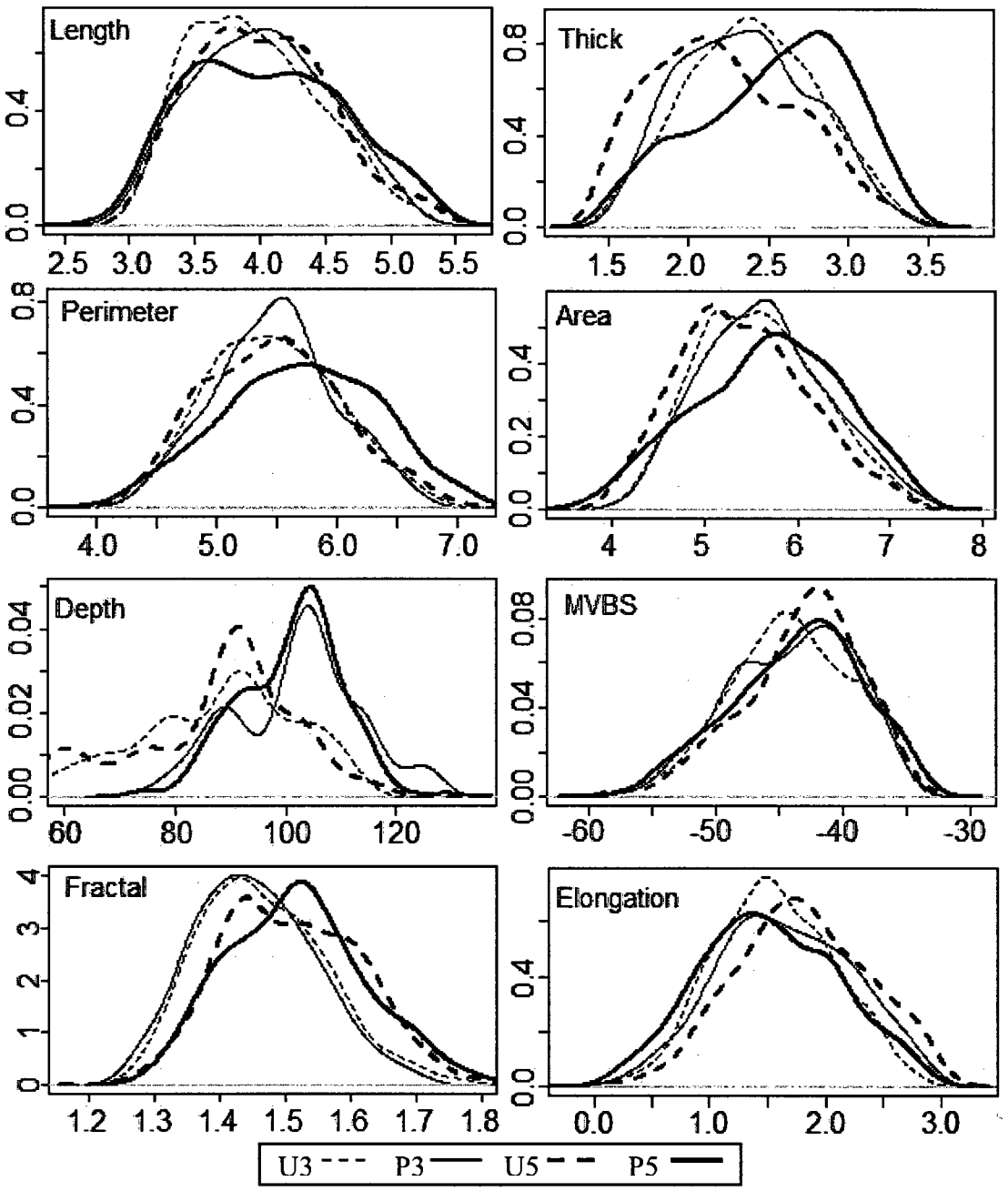

Figure 4.3. Frequency distributions of fish-school descriptors (length, thickness, perimeter, area, fractal dimension, elongation, depth, and mean volume-backscattering strength) obtained in two areas (U, P) in 2003 and 2005 (3, 5). Thickness, perimeter, area and elongation were log-transformed.

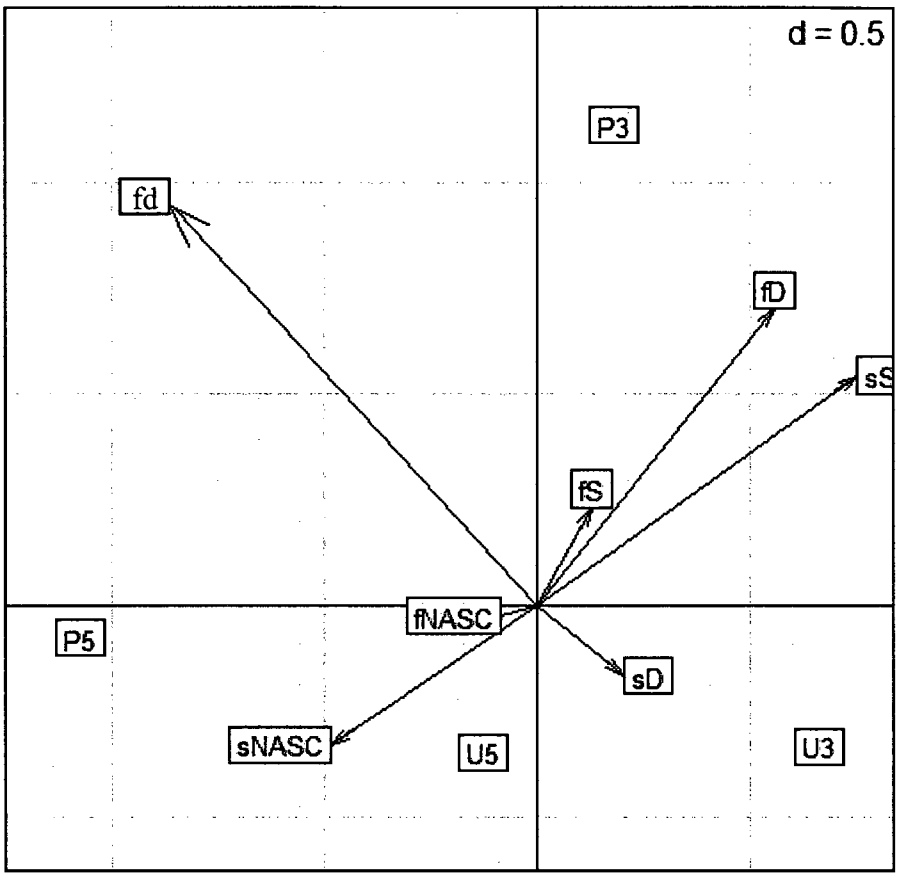

Figure 4.4. Bi-plot of principal components 1 and 2 from the between-class PCAIV using observer data.

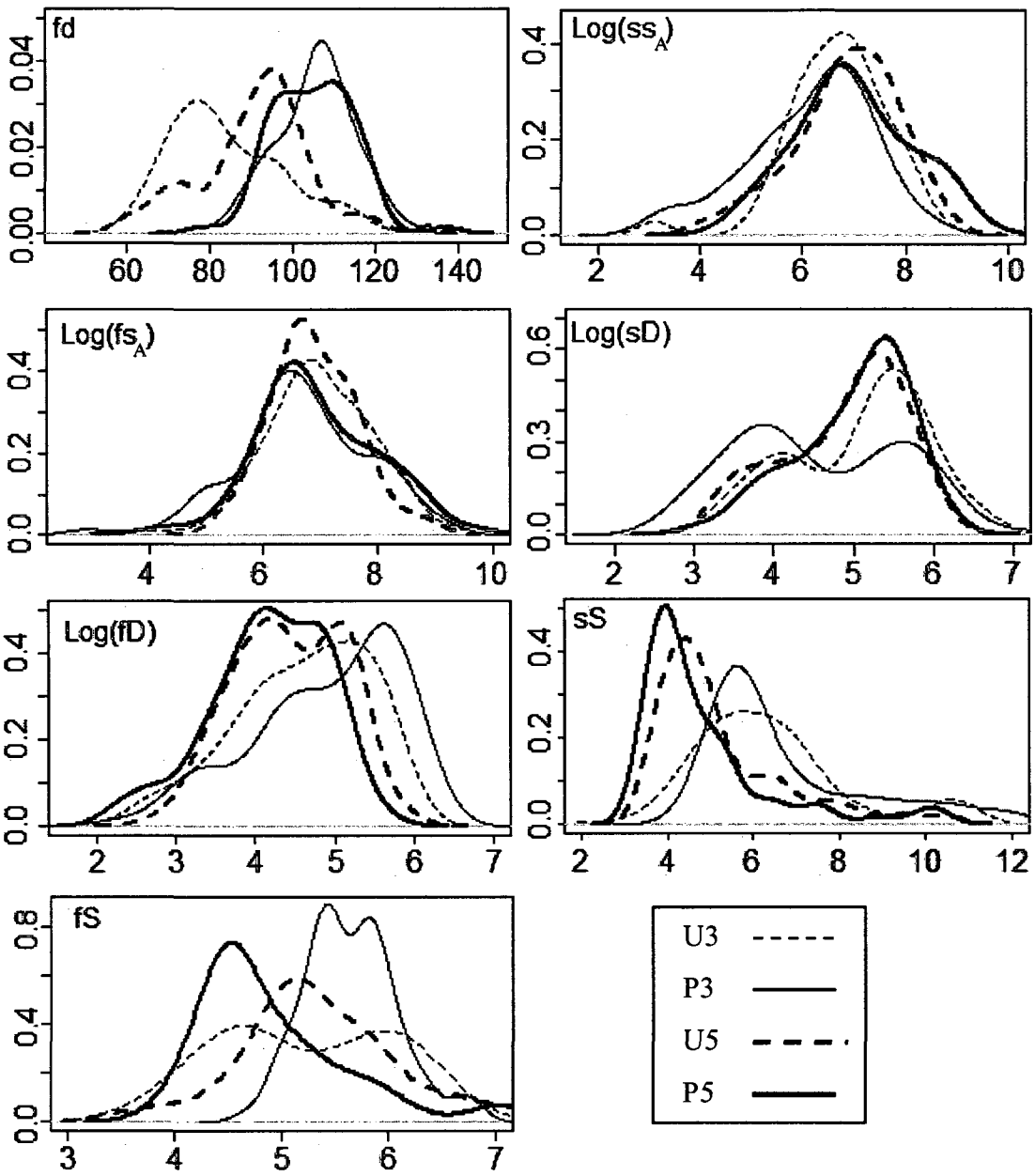

Figure 4.5. Frequency distributions of the fishing variables for two areas (U, P) in 2003 and 2005 (3, 5). *fd*–fishing depth, ss_A–fish density during search, fs_A–fish density during fishing, *sD*–searching duration, *fD*–fishing duration, *sS*–searching speed and *fS*–fishing speed. Four of the variables were log-transformed as indicated.

Chapter 5

Catch depletion analysis using DeLury method for walleye pollock (*Theragra chalcogramma*) in the eastern Bering Sea[1]

Abstract

Walleye pollock (*Theragra chalcogramma*) support the largest single species fishery. The decline of the western population of Steller sea lions over the last few decades raised concerns about the competition between pollock fishery and sea lions predation. Our study focuses on the spatial and temporal scales of fisheries impacts on endangered species, especially in areas around sea lion critical habitat. Observer data from 2002 to 2006 were stratified to investigate the local fisheries impacts after standardization using a generalized linear mixed model. DeLury depletion models were fitted to standardized catch and effort data in each area to study the depletion based on the trend of catch per unit effort. Statistically significant depletion was detected in some Steller sea lion conservation areas from 2002 to 2006. Post hoc analysis indicated that the depletion is more likely to be detected in areas with low pollock biomass, catch and effort. Finally, different Bayesian methods were used to fit the data with hierarchical structure and spatial structure among parameters. The best model using deviance information criterion is the non-spatial hierarchical Bayesian model using different variances among areas. Compared to frequentist methods, Bayesian models resulted in significantly less depleted areas during 2002–2006. Because of its "borrowing strength", the hierarchical model provided more consistent and precise estimates than the frequentist methods.

[1] Shen, H., Quinn, T.J., II, Dorn, M.W., and Wespestad, V. Catch depletion analysis using DeLury method for walleye pollock (*Theragra chalcogramma*) in the eastern Bering Sea. Prepared for submission to the Canadian Journal of Fisheries and Aquatic Sciences

5.1 Introduction

Walleye pollock (*Theragra chalcogramma*) is well known as a valuable commercial fish, which support the largest single species fishery in the world. Walleye pollock catch has averaged about 1.48 million tons in the eastern Bering Sea (EBS) during 2002–2006 (Ianelli et al. 2008). Since the 1990s, the fishery has had two seasonal components. The winter "A season" focuses on pre-spawning aggregations from January 20th to early-mid April. The summer/fall "B-season" opens on June 1st and extends through late October (Ianelli et al. 2008). During the A-season in 2002–2006, pollock were mainly exploited north and west of Unimak Island which is also the location of the Steller sea lion conservation area (SCA).

In addition to its economic importance, walleye pollock is also a key component of the EBS ecosystem as a major prey species for other marine fish, marine mammals and birds (Livingston 1993). With increasing concern about endangered species, some studies have been conducted to investigate whether pollock fisheries affect ecosystem function and bring adverse impacts on sea lion populations. Due to the sea ice cover and weather conditions, the A-season fishery is confined to north and west of Unimak Island. The pollock catch in SCA accounted for about 49% of the catch during A-season (Ianelli et al. 2008). Thus the spatial and temporal scales of fisheries impacts are more important to examine, rather than general impacts in the whole EBS.

The observer program provides data with great coverage of the EBS pollock fishery in space and time which can be used to investigate the fishery impacts at different temporal and spatial scales. The observer program currently deploys observers based on vessel length and type of fishery operations in the EBS pollock fishery. Observer duties include sampling all hauls for species composition. Catcher-processor (C/P) vessels are required to carry two observers 100% of the time. Catcher-only vessels over 125 ft length overall (LOA) and larger are required to carry one observer at all times. There is 30% observer coverage of their fishing days on vessels of 60 to 125 ft LOA. Catcher vessels are not required to carry observers if they deliver their catch to either shoreside

processors or floating processors operating in the Exclusive Economic Zone (EEZ) (C/Ps or motherships) because the catch will be recorded by observers onboard the processors. Vessels under 60 ft LOA are not required to carry observers but they account for only a small proportion of the walleye pollock catch. The observer program provides data with greater coverage in space and time and lower cost than data collected by fishery-independent surveys. Based on the collected catch and effort data, catch per unit effort (CPUE) can be obtained and used as the relative index of underlying resource abundance in stock assessments.

Although there are many debates about the nature of the relationship between catch rates and underlying resource abundances (Harley et al. 2001), many fisheries still use the abundance indices based on catch and effort data as the integral part of the stock assessment process (Quinn and Deriso 1999). Observed CPUE is affected by changes of year, season, vessel, area of fishing and various environmental factors; therefore, CPUE needs to be standardized. In recent years, many statistical methods have been used to standardize CPUE to account for such variations. These methods include generalized linear models (GLM), generalized additive models (GAM), generalized linear mixed models (GLMM) and others (Xiao et al. 2004). Pollock are exploited by vessels of various sizes and functionality. Besides these differences among vessels, catch rates also vary according to changes in seasonal and spatial patterns of both fishing effort and the stock and changes in stock abundance itself. Therefore, it is important to standardize CPUE among and within vessels as well as for spatiotemporal differences. Fixed effects models assume that all observations are independent of each other. However, the haul information of one vessel was repeatedly recorded over a short period and the functionality of one vessel is assumed to be similar which results in some correlations among collected data. The random effects can be added into models to account for the correlation of the data. So the CPUE is standardized using generalized linear mixed models (GLMM).

Since Steller sea lions were listed as an endangered species in 1997, there have been substantial concerns about the potential competition between commercial fishery and predation of sea lions. The competition occurs only during fishing seasons in sea lions habitat areas, which have relatively small temporal and spatial scales. The depletion estimation approach provides the methodology to determine if the removals of the fishery potentially cause the decline of prey availability of sea lions. DeLury (1947) and Leslie and Davis (1939) developed depletion-based population estimators which are typically employed to estimate the initial biomass from a series of removals (Polovina 1986, Quinn 1987). Further details about the depletion estimation approach can be found in Seber (1982) and Battaile and Quinn (2006).

In some areas, the CPUE data sets are too short and too highly variable to provide reliable estimates. Hierarchical modeling allows borrowing information from informative areas to improve the estimates for areas with poor data (Gelman et al. 2004). Considering the tendency of the pollock population to aggregate (Wilson et al. 2003, Barbeaux et al. 2005), pollock biomass may be positively correlated in nearby areas, and also some parameters of stock assessment. Hierarchical modeling uses a common population or prior distribution to model possible dependence among parameters which are treated as random samples drawn from the common distribution. Both frequentist and Bayesian methods can be used for fitting hierarchical models. Bayesian statistics are becoming increasingly popular because they can explicitly quantify uncertainty in both population estimators and data inputs, and are free of fitting models with many parameters and complicated forms (Gelman et al. 2004). Here the hierarchical Bayesian models (HBM) are used to improve the estimators in Alaska Department of Fish and Game (ADF&G) areas with poor data quality.

In HBMs, the parameters can be treated as independent and identically distributed variables because their joint distribution is invariant to any possible permutation of their locations (Su et al. 2004). Thus, there is no temporal or spatial structure included in HBMs. To include spatial correlation among DeLury estimators, the HBMs can be

extended to explicitly include spatial structure into parameter estimation in the Bayesian models. Some studies in epidemiology and geography have demonstrated the importance of incorporating spatial structure in data (Moura and Migon 2002). The spatial structure is modeled by imposing dependence (i.e., the spatially correlated prior distribution) on area-specific parameters. Prior distributions allow the models to use information from nearby areas to improve estimates of parameters for individual areas (Banerjee et al. 2004). In this study, several alternative Bayesian models were developed by specifying different plausible prior distributions for depletion estimators. Then the models were compared using the deviance information criterion (DIC) for choosing the best models (Spiegelhalter et al. 2002).

5.2 Materials and Methods

5.2.1 Data preparation

We only used the observer data from "A" fishing season (January to March) during 2002–2006 which is consistent with the acoustic data used in previous chapters. From January to March, the fishing fleet mainly operated around north of Unimak Island and in waters around the Pribilof Islands. In the observer data, effort is measured as haul time in minutes. The pollock catch is measured in kilograms.

The data were stratified by the Alaska Department of Fish and Game (ADF&G) statistical areas (Figure 5.1), which is used for Alaska fishery management and generally consist of 30×30 nautical mile blocks. Some other procedures were also conducted to reduce extraneous variability in the data. First, we eliminated hauls with less than 90% pollock catch to exclude non-targeting hauls because most hauls have very high (>90%) percentage of pollock (Figure 5.2). Second, some outlier hauls were eliminated if the CPUE was very low as to not indicate targeted fishing. Third, the ADF&G areas were excluded if there were less than 20 hauls. Figure 5.3 showed all ADF&G areas with enough data for analysis during 2002–2006.

5.2.2 CPUE standardization

CPUE was calculated by dividing total catch by effort. Due to its variability, CPUE needs to be standardized, as shown by Battaile and Quinn (2004). First, the haul-by-haul CPUE data were normalized using the natural logarithm transformation, which is a standard transformation for CPUE data. Exploratory data analysis (EDA) revealed that among-vessel differences were large, especially for daytime hauls (Figure 5.4). As pre-spawning pollock are more tightly aggregated during daytime (Shen et al. 2008), the CPUE may be higher than at night (Figure 5.5). Thus this factor should also be included in CPUE standardization. The factor "Diel" was calculated by retrieving the sunrise and sunset time for the latitude, longitude, time zone in relative to GTM/UTC, daylight saving, and date of the haul using the algorithm provided by NOAA (http://www.srrb.noaa.gov/highlights/sunrise/sunrise.html). All hauls were grouped into day or night hauls based on the middle time of each haul.

The haul data of area 645501 in 2004 are used to illustrate the procedure of CPUE standardization. The standardization was conducted with a generalized linear mixed model (GLMM) fitted using 'nlme' package of **R** (http://www.r-project.org/). Because the observations from same vessel tended to be correlated, the random vessel effects were added into the regression models to account for the correlation of the data. In the full models, the interaction terms were also included because there were lower CPUEs during daytime than nighttime for some vessels. So the full model was constructed as,

$$\ln U_i = \alpha + \beta_i * VesselID + g * Diel + b_i * (VesselID: Diel) + \varepsilon_i \quad ,$$

where subscript i is for i^{th} vessel, U_i represents CPUE, α and g are fixed effects, and the β_i and b_i are random (vessel-specific) effects with a normal distribution: $N(0, \sigma_\beta^2)$ and $N(0, \sigma_b^2)$ respectively. The model error term ε_i is distributed as $N(0, \sigma^2)$.

The optimal model was chosen using the following steps: 1) Using fixed-effects ANOVA to fit data and finding the functional form of the model using the stepwise regression method; 2) For building mixed-effects models after step 1, it is important to

choose which parameters in the model, if any, should have a random-effect component included to account for between-group variation ('lmList' function in **R**); 3) Random effects were added into models in step 2. The models were fitted by restricted maximum likelihood. Finally, the mixed-effects model and fixed-effects model were compared to find the best model.

5.2.3 DeLury depletion model

After CPUE standardization, the total daily effort was obtained by dividing total daily pollock catch by the mean standardized CPUE for each ADF&G area. The cumulative effort was calculated from the daily effort values for depletion analysis.

The DeLury (1947) depletion method was used here to investigate the fishery caused depletion. The DeLury method has three assumptions: 1) closed population except for fishing removal, 2) constant catchability, and 3) independent and additive effort. Battaile (2005) demonstrated that these assumptions can be approximately satisfied for pollock fishery in the EBS for the short periods during the A season.

DeLury (1947) model defines

$$U_t = \frac{C_t}{f_t} = qB_t \quad ,$$

where U_t is the CPUE, C_t is the catch, f_t is the fishing effort at time t; B_t is the biomass at time t. q is the catchability coefficient (Quinn and Deriso 1999). Given the survival equation $B_t = B_0 e^{-qE_t}$, the above formula can be rewritten as

$$U_t = qB_0 e^{-qE_t} \quad ,$$

where the E_t is the cumulative effort up to time t, $E_t = \sum_{i=1}^{t-1} f_i - \frac{1}{2} f_i$.

And taking the natural logarithm, the formula can be rewritten as

$$\ln U_t = \ln(qB_0) - qE_t .$$

Natural mortality can be easily included if it is available (Seber 1982),

$$\ln U_t = \ln(qB_0) - qE_t - Mt .$$

To reduce confounding between parameters, the constant M=0.3 was used here according to the SAFE report (Ianelli et al. 2008). The two parameters, q and B_0, can be estimated through linear regression based on the paired catch and effort data. The more negative slope can be considered as the sign of stronger fishery-caused depletion. In each ADF&G area, the depletion estimators were obtained and tested for statistical significance.

The objective of depletion analysis is to examine the potential competition between fishery and sea lion predation. Therefore, the areas inside SCA and surrounding areas (Figure 5.3) were chosen to investigate which fishery characteristics were related to the magnitude of depletion using generalized linear models (GLM). As suggested by Battaile and Quinn (2006), cumulative depletion (D_{cum}) was introduced as the other dependent variable calculated by

$$D_{cum} = \frac{CPUE_0 - CPUE_t}{CPUE_0},$$

where $CPUE_t$ represents the CPUE at time t, $CPUE_0$ represents the CPUE at the beginning of the fishing season. A larger D_{cum} suggested greater cumulative depletion. The slope of depletion estimates indicates the speed of depletion occurring, while cumulative depletion indicates the overall final effects of fishing. Some explanatory variables were used to include temporal and spatial characteristics of the fishery, and other variables included information related to sea lions. The variables included categorical variables, such as year and if the ADF&G area is in SCA, and continuous variables, such as total catch, total effort, estimated initial biomass and distance to sea lion protected areas. Each variable was used to examine the main effects individually. In

this part, the depletion analysis was conducted using R. ArcGIS software was used to display the results of depletion analysis.

5.2.4 Bayesian models

Here we only used the data of ADF&G areas inside and near SCA (Figure 5.3). All the estimation in this part was conducted using WinBUGS software. The models were developed by increasing complexity from area-specific models, to hierarchical Bayesian models, and then to spatial hierarchical Bayesian models. And the optimal models were found based on the deviance information criterion (DIC) (Spiegelhalter et al. 2002).

5.2.4.1 Area-specific Bayesian model

For the DeLury estimations, the parameters were still treated without correlation and estimated based exclusively on the data for each ADF&G area. It is just like the frequentist method to estimate parameters without borrowing information occurs from different areas. The basic form of DeLury model is

$$y_{i,t} = b_{0i} - q_i E_{i,t} + \varepsilon_{i,t},$$

where $y_{i,t}$ =lnCPUE$_{i,t}$, which denotes the logarithm of CPUE in the ith ADF&G area at time t; $b_{0i} = \ln(q_i B_{0i})$; q_i denotes the catchability in ith area; the model error term $\varepsilon_{i,t}$ is distributed as $N(0,\sigma_i^2)$; and σ_i^2 is the variance of the error term. In these models, either same ($\sigma_i^2 = \sigma^2$) or different variances were used across areas. For the area-specific, nonhierarchical model, noninformative priors were assigned for all parameters: $b_{0i} \sim U(0,10)$, $q_i \sim N(0,1)$, $\sigma_i^2 \sim$ IG(0.001,0.001) as suggested by Battaile (2005). IG indicates the inverse gamma distribution which is proper prior distribution specified for variance parameters (Gelman et al. 2004).

5.2.4.2 Hierarchical Bayesian models (HBM)

The estimates from DeLury models varied among ADF&G areas, which may be caused by different biological factors and fishing behavior. In hierarchical models, the

parameters are assumed to be similar from area to area and are treated as random samples drawn from a population of parameters, such as a normal distribution used in this study. These parameters are exchangeable in this sense and can be treated as independent and identically distributed (iid). Therefore, there is no temporal and spatial structure considered in these models.

The intercept (b_{0i}) and catchability (q_i) were assumed similar across areas and were drawn from higher-level population distributions (i.e., normal distribution). They were modeled as follows:

$$b_{0i} \sim N(\mu_b, \sigma_b^2); \qquad q_i \sim N(\mu_q, \sigma_q^2).$$

And the hyperpriors were assigned for hyperparameters by:

$$\mu_b \sim U(0,10); \quad \sigma_b^2 \sim \text{IG}(0.001, 0.001);$$

$$\mu_q \sim N(0,1); \quad \sigma_q^2 \sim \text{IG}(0.001, 0.001).$$

The model parameters to be estimated were the intercepts b_{0i}'s, the catchabilities q_i's, and the variances of the data σ_i^2's which had the same prior distribution as area-specific models. In these models, either same or different variances were used across areas too. The hyper-parameters to be estimated were μ_b, μ_q, σ_b^2 and σ_q^2. Combining the priors, population distributions and likelihood, the joint distribution of all parameters for the hierarchical Bayesian models was

$$p(q_i, b_{0i}, \sigma_i^2, \mu_q, \mu_b, \sigma_b^2, \sigma_q^2 \mid D) \propto p(\mu_q)p(\mu_b)p(\sigma_b^2)p(\sigma_q^2)\prod_{i=1}^{I} p(\sigma_i^2)$$
$$\prod_{i=1}^{I} N(b_{0i} \mid \mu_b, \sigma_b^2)\prod_{i=1}^{I} N(q_i \mid \mu_q, \sigma_q^2)\prod_{i=1}^{I}\prod_{t=1}^{n_i} N(\ln \text{CPUE}_{i,t} \mid E_{i,t}, M, q_i, b_{0i}, \sigma_i^2)$$

5.2.4.3 Spatial hierarchical Bayesian models (SHBM)

While the parameters were assumed to be spatially similar across all areas and were treated as random draws from a common distribution in HBM, spatial HBM assumed a

smaller scale correlation that neighboring areas were more similar than areas farther away from each other. In SHBM, the spatial correlated prior distribution was specified based on the Gaussian conditional autoregressive (CAR) structure (Besag et al. 1991). Generally speaking, the correlation between the nearest neighbors is the highest and then successively decreases as the distance between two points increase. The ADF&G reporting areas were constructed as a lattice network (Figure 5.6). Then, the correlation structure was discrete such that only the bordering areas affect each other (Figure 5.6). WinBUGS provides map-tools to create an adjacency matrix for a spatially correlated prior distribution. The weight of each neighbor is the inverse of total number of neighbor areas. The differences between HBM and SHBM are the prior distributions of the intercepts. Here the SHBMs intercepts had a spatially correlated prior distribution based on a Gaussian CAR structure with $\tau_{car} \sim G(0.5, 0.0005)$ according to the suggestion of GeoBUGS user manual authors (Thomas et al. 2004).

For each year, a total of 6 different models were formed for comparison by combining the different data-level model assumptions (i.e. DeLury depletion model, and σ_i^2 being the same (or not) across areas) and the different assumptions for prior probability distributions defined above. All these Bayesian models were compared by the deviance information criterion (DIC) proposed by Spiegelhalter et al. (2002) as follows.

DIC = 'goodness of fit' + 'complexity'

The 'goodness of fit' was measured via the expectation of deviance $D(\boldsymbol{\theta}) = -2 \log L(y|\boldsymbol{\theta})$, or $\overline{D} = E_{\boldsymbol{\theta}|y}[D]$. 'Complexity' was measured by estimate of the effective number of parameters: $p_D = E_{\boldsymbol{\theta}|y}[D] - D(E_{\boldsymbol{\theta}|y}[\boldsymbol{\theta}]) = \overline{D} - D(\overline{\boldsymbol{\theta}})$; i.e. posterior expectation of deviance minus deviance evaluated at the posterior expectations of the parameters. The DIC was then defined analogously to AIC as: $\text{DIC} = D(\overline{\boldsymbol{\theta}}) + 2p_D = \overline{D} + p_D$. The model with smaller value of DIC was considered as a better-fitting model. In WinBUGS, deviance was automatically calculated and DIC could be calculated automatically too.

5.3 Results

In the 2002–2006 "A" fishing seasons, pollock catch data was quite clean, with a small percentage of non-targeting hauls (2.7% – 9.7%) based on the 90% pollock catch threshold and very low value of CPUE. After removing inappropriate data, 92% – 96% of total pollock catch was available for standardization (Table 5.1). There were a total of 44 ADF&G areas with enough data (Figure 5.3).

5.3.1 CPUE standardization

According to the results from stepwise regression, the interaction terms were not significant, so they were not included. The functional form of the model included two main effects: VesselID and Diel. Differences among the individual confidence intervals in Figure 5.7 gave a clear indication that a random effect was needed to account for vessel-to-vessel variability in the intercept. For the mixed-effect models, the random effects (Vessel effects) were used to account for the between-group variation of the intercepts. Obviously, the estimates from the mixed-effects model tended to shrink toward the fixed effects (Figure 5.8), which was due to the compromise of mixed-effect estimates between the coefficients from the individual fits and fixed effects estimates, associated with the population average. The fixed-effects model and mixed-effects model were compared through a likelihood ratio test. The low p-value of the test revealed that the mixed-effects model provided a much better description of the data than the fixed-effects model ($p<0.001$). In most of strata (103 of 118 strata), the mixed-effects models fitted the data better. So, we used the mixed-effects models to standardize CPUE for all areas during 2002–2006. The fitted models only explained an average of 17% –25% of the total sum of squares (Table 5.2). Of the two factors, VesselID explained more variability (16% –25%) than Diel (0.7% –1.2%).

There were large differences in model coefficient values among areas as illustrated by relatively large inter-quartile range in some years (Figure 5.9). Compared to other years, there were lower values with a larger range of intercepts in 2003. The signs of Diel

were generally positive for hauls during daytime which demonstrated the higher CPUE during daytime. In 2002, the among-vessel variation was higher than that in other years.

5.3.2 Depletion analysis

The linear relationship in the DeLury model is illustrated in Figure 5.10 with data from area 685600 in 2005. As cumulative effort increased, the lnCPUE decreased slowly. Although the R^2 value was very low, the decrease of lnCPUE was very significant (p= 0.03) which may suggest some depletion due to the fishery.

A total of 118 slopes ($-q$) were estimated using the DeLury model. The estimated slopes ranged from –0.00027 to 0.00016 and mostly ranged from –0.0001 to 0.0001 (108 of the 118 slopes). There were 51 positive slopes (indicating increasing CPUE) and 11 of them were significantly positive at $\alpha < 0.05$ level (Table 5.3). There were 67 negative slopes (indicating depletion) and 12 of them were significantly negative at $\alpha < 0.05$ level (Table 5.3). The significant depletion mainly occurred areas inside SCA or close to SCA (Figure 5.11). In 2002, there were two areas with significant negative slopes (Table 5.3). There were 3 ADF&G areas with significant negative slopes in 2003, 2005 and 2006, respectively (Table 5.3). In 2004, there was only one area with significant negative slope (Table 5.3). In 2004, there was the greatest percentage of positive and significantly positive slopes. The pooled data also indicated both significantly more negative and positive slopes (Table 5.3).

Table 5.4 showed the dependence of depletion estimators on different explanatory variables in areas around SCA (significant at $\alpha < 0.05$ level). Using all slopes ($-q$) can help to detect the factors which cause the decrease of the slopes, and even negative slopes. Because our focus is detected depletion (negative slopes), using negative slopes can help to find which factors can make depletion more severe. There was a significant difference in cumulative depletion (D_{cum}) between areas inside or outside SCA (Table 5.4). The negative sign for areas inside SCA suggested that there were more cumulative depletions in areas inside SCA. There were no significant relationships between depletion

slope ($-q$) with temporal and spatial variables related to fishery characteristics, as well as variables related to sea lions (Table 5.4). However, the DeLury depletion slopes ($-q$) were significantly correlated with three variables: $\ln(B_0)$, total catch and effort (Table 5.4). Harvesters chase fish and catch them, thus there is low probability of high catch in areas with less biomass. The estimated slopes decreased (more negative) with the decrease of initial biomass, total catch and effort, which suggested that the depletion was more likely to occur in areas with lower biomass.

5.3.3 Bayesian models

There were a total of 85 strata with enough data for DeLury models from 2002 to 2006 in areas around SCA. Both frequentist and Bayesian methods resulted in more negative slopes than positive slopes. Bayesian models resulted in fewer significant negative slopes, fewer significant positive slopes, and more non-significant slopes than frequentist models (Table 5.5). Using the frequentist method, 66 of 85 models did not find any significant relationship, 9 showed a significant increase in lnCPUE, and 10 indicated significant depletion (Table 5.5). The Bayesian models had 4–8 areas with significant negative slopes and 2–7 areas with significant positive slopes (Table 5.5).

The data from 2006 were used to illustrate the procedure of analysis and some results. One advantage of using spatial hierarchical Bayesian models is that they can automatically provide the spatial display of estimates with the "Map" tools of WinBUGS. The estimated q_i's and intercepts are shown in Figure 5.12 using the areas with enough data. Box plots of q_i's from models 1–6 indicate that most estimates tended to be positive (suggesting depletion) (Figure 5.13). Generally speaking, models using the same variances resulted in less variation of 95% CI's for q than models using the different variances.

The Bayesian models were compared in terms of DIC and the effective number of parameters (p_D) (Table 5.6). Key results emerged from comparing our 6 models. First, the hierarchical models using the same variances did not perform better than their area-

specific counterparts (i.e. Models 1 versus Models 3 or 5). But the non-spatial hierarchical models using different variances performed better than their area-specific counterparts (Model 4 versus Model 2). Second, models using different variances (Models 2, 4 and 6) had better fit to the data than comparable models using the same variance (Models 1, 3 and 5) (Table 5.6). Third, the best model was HBM using different variances. The spatial models did not improve model fit ($\overline{D}$) and had similar p_D to HBM models, so that SHBM had a higher DIC in most cases (Table 5.6).

Further insight was attained by comparing the number of nominal parameters, N_p, with the effective number of parameters, p_D. For area-specific models (Model 1 and 2), the values of N_p were either equal to or smaller than p_D which suggested that there was no borrowing of information in these models (Table 5.6). For the case of year 2002, there were two area-specific parameters for each of the 19 areas plus a single common σ^2 for residuals in Model 1, so N_p was 39; p_D also turned out to be 39. In contrast, most of p_D values of hierarchical models were less than the corresponding N_p (Table 5.6, models 3–4), suggesting borrowing of information for these hierarchical models.

One advantage of Bayesian methods is that the variability of estimations can be reduced if some areas have poor data sets because Bayesian methods can borrow information from other areas with good data (Gelman et al. 2004). The frequentist methods generally tended to have a higher standard error for q than Bayesian methods (Figure 5.14). In areas with small sample size, there were larger differences between frequentist and Bayesian estimators of q and standard error of q (Figure 5.14). This indicated that HBMs substantially reduced the uncertainty of estimators of q in these areas. Figure 5.15 compares estimated depletion slopes ($-q$) and its 95% probability intervals from the best Bayesian model (Model 4) and frequentist method. The Bayesian method resulted in less variable estimates than the frequentist method. There were large variances in some areas (e.g. areas 3, 4, 11 and 12) between the two methods. In most areas, the HBM resulted in smaller variances compared to results of the frequentist method.

The posterior distributions of the hyperparameter μ_q exhibited a typical normal distribution (Figure 5.16). Four different hierarchical models (Model 3–6) did not show much difference in posterior distributions which centered about zero with a relatively dispersed distribution compared to the q values themselves (Figure 5.13). The posterior distribution of hyperparameters of intercepts indicated some differences among models 3–6 (Figure 5.17). Although HBM and SHBM had similar estimates, the spatial models had smaller probability intervals because some variation was explained by the spatial structure of SHBM. The comparison of models using DIC indicated that the spatial models did not improve the fit which suggests that the intercepts working with spatial structure provided similar functional effects with the intercepts of models without spatial structure (Figure 5.18).

5.4 Discussion

The ADF&G reporting areas were used to stratify the catch and effort data. This stratification may have been a statistical artifact which was not based on any biological information. However, the unequal spatial distribution of catch data may not have been adequately captured by these management areas. This may be one of the reasons that our models did not explain much of the variability of the data. The explained variances (17–25%, Table 5.2) of our models were relatively lower than the results of 36–48% by Battaile and Quinn (2004). Another two factors (percentage of pollock catch and hauling speed) were included in their models which may result in higher explained variances than our models. On the other hand, the temporal and spatial factors were generally included in a single model for CPUE standardization (e.g. Quinn 1987 and Large 1992). Here the standardization was separately conducted for each time/space stratum. This stratification definitely can remove substantial variability of data when there were significant differences among different areas. The stratification method was the same one as Battaile and Quinn (2004) which suggested that 23% of variability was removed by the

stratification procedure. Their results can also explain why our models obtained low variances of the data after stratification.

Fishery data were generally standardized using fixed-effects models to account for variations mainly due to vessel effects. In fixed-effect models, the catch data were treated independently of each other. However, there should have been some correlations between the catches from the same vessel because of its fishing efficiency and skipper efficiency. The correlations were included in the standardization procedure by adding random vessel effects. Treating vessel as a random effect was justified in this case. After stratification, each area only had data from some vessels, not all. So the sampled vessel in each area could be reasonably considered as a random sample from a population of total vessels. Our results also demonstrated that the mixed effects models fitted the data better in most of the strata (103 of 118 strata).

In the two factors, the VesselID factor seems to account for much more variation in the data than the Diel factor. The results were not surprising, because variation in CPUE is primarily dependent on vessel characteristics. Battaile and Quinn (2004) indicated that VesselID accounted for the majority of the explained sum of squares (average about 29%), while the vessel factor only explained about 19% of the variation on average in our models (Table 5.2) which may be the result of considering vessel factor as a random effect in the models. Although pollock tended to form schools and targeting schools can produce high CPUE, the increased empty space can result in lower CPUE. In other cases, pollock may form less dense layers or clouds, but have large spatial coverage. Therefore, there may have been higher daytime CPUE in areas with more schools, or there may have been lower daytime CPUE in where there are few schools with increased empty space between fish schools because the harvester have to increase haul time to catch more fish.

The fishery removed some portion of the pollock population and caused a decrease of pollock abundance in some areas. Depletion happens when removals occur faster than the recruitment or growth of the population. CPUE is generally used as the index of underlying abundance in stock assessment. Based on DeLury model, significant depletion

means the significant decrease of CPUE during fishing. Steller sea lions perform some predation by diving, thus sea lions have to dive longer to find enough food when pollock abundance decreases. Longer diving means more energy consumed which could have substantial influence on the predation process, especially for sea lion pups, and then affects the growth or potential mortality of pups. The reproduction can also be affected if adults fail to get enough food.

In previous decades, the EBS pollock stock has been successfully managed and supported a sustainable fishery. However, there is still some detectable within-season local depletion in some areas which suggested some potential competition between pollock fishery and sea lions. During 2002–2006, the detected significant depletion occurred in areas inside SCA and around SCA (Figure 5.11) which held a high percentage of pollock biomass and were the main operating areas of the winter fishing season. Some depleted areas (area 635530, 655430 and 655409) were close to the critical habitat area of sea lions (Figure 5.11) which may result in adverse impact on the sea lion population. There were more areas (4–9 areas in each year) around SCA with significant negative slopes during 1995–1998 in Battaile and Quinn (2004) than our results (1–3 areas in each year) during the winter fishing season. This suggested that management measures put into place in 1999 may have been effective in spreading fishing effort out in space and time. However, more management measures may be needed to shift the fishing effort away from critical habitat areas of sea lions.

The results here are not conclusive because many random variations in the data can hide the signal in depletion analysis. The DeLury analysis examined the depletion related to the trend of CPUE. However, pollock form different kinds of aggregations which can result in the hyperstable relation between CPUE and abundance because the nets are set on relatively large concentrations of fish (Harley et al. 2001). This hyperstability can hide the signal of depletion analysis using fishery catch data. Including search time may remedy this problem. However search time was not currently recorded in the observer

data. Therefore, the hyperstable relationship between CPUE and abundance can result in errors which cause finding less depletion.

Another problem in detecting depletion is that the depletion signal can be detected only when a large enough proportion of the population is removed to cause the significant decrease of fish density. During 2002–2006, approximately 15% of age 3^+ pollock biomass was removed each year from the EBS (Ianelli et al. 2008), although this may be concentrated in some areas. In areas with high biomass, the proportion of removal can be less than 15% although there was high catch and effort. In contrast, the catch from areas with less biomass may have been small but it could have accounted for a large percent of the total biomass in these areas so that the fish density could decrease significantly. Therefore, the results are biologically meaningful that there are high correlations between depletion estimators and initial biomass. The areas with less fish are more susceptible to depletion even with less total catch and effort.

Bayesian models are generally used to account for the uncertainty of estimators and data sets. The hierarchical Bayesian models have been successfully used in meta-analysis (Myers 2001) and improving estimates in fisheries where data quality is not good (Adkison and Su 2001, Su et al. 2001). In the frequentist method, each area was treated separately which is prone to failure in areas with poor data (Gelman et al. 2004). The hierarchical Bayesian models, which treated the parameters as random samples from a common population, can borrow information from areas with good data to improve the estimates in areas with poor data. In our example, there were some areas with poor data due to small sample size or high variability. The HBM resulted in more consistent and more precise estimates of DeLury depletion analysis which can be seen from Figure 5.14 and Figure 5.15. The HBM gave smaller standard errors of q, especially for areas with small sample sizes (Figure 5.14). For areas with high variations, the HBM brought shrinkage of point estimates to their local means (Figure 5.15). Because the parameters were random draws from a common population, the HBM resulted in more consistent

estimates compared to the frequentist method (Figure 5.15), which may explain less significant negative slopes from Bayesian models (Table 5.5).

Some studies have demonstrated the importance of explicitly modeling spatial structure in data (Moura and Migon 2002, Su et al. 2004). Rather than thinking parameters are independently random draws from the common distribution, spatial HBM considered the correlations between parameters in areas and their neighbors and the correlations were modeled using Gaussian CAR specification. However, including spatial structure in our models did not improve the fit to data in most cases (Table 5.6). The spatial HBM provided a worse fit (higher $\overline{D}$) than the non-spatial HBM (Table 5.6). Therefore, the spatial dependences among neighbors may not have been significant enough to affect the estimates of the depletion parameters in our cases.

If some spatial structure did exist, it may not have followed the spatial scale used in our models. ADF&G areas are set based on the lattice of longitude and latitude. There is little ecological information in this assignment. The eastern Bering Sea has a complex oceanographic structure. The ADF&G areas may bisect some natural boundaries and fragment the natural spatial structure of pollock. Also, the CAR prior distribution may not fit the potential spatial autocorrelation among areas. The comparisons of intercepts in HBM and their counterparts in SHBM also demonstrated the similar performance of spatial models and non-spatial models (Figure 5.18). Of course, there were little differences of the estimates of q between spatial HBM and HBM (Figure 5.13).

The posterior distribution of μ_q was quite a bit larger compared to individual q values. For instance, the 95% probability intervals of μ_q ranged from –0.00662 to 0.00662 in year 2006. However, the individual q values of each area were generally in the 10^{-5} to 10^{-6} range. The absolute value of the largest catchability was of the order of 10^{-4}. The sensitivity of the prior of μ_q was explored with variances of 0.01 and 0.001 for the normal distribution. There were no changes among the posterior distributions with different prior distributions. Therefore, the results for μ_q were much less sensitive to the prior specifications. And our estimates of μ_q were robust across model assumptions.

Our final goal was to investigate the potential competition between commercial fishery and Steller sea lion predation around the sea lion conservation area. Both frequentist methods and Bayesian methods indicated that there were statistically significant depletions occurring in some areas around SCA, even in areas very close to the critical habitat areas of sea lion (Figure 5.11). There are many factors which can hide the signal of depletion related to the trend of CPUE. The lack of records of searching time and the potential hyperstabilities of CPUE could make it difficult to find a significant depletion when it was indeed present. Considering all these factors, the results here should be considered conservative because of erring on the side of finding less depletion. In spite of the problems in depletion analysis, some key results need to be pointed out. One is that the depletion is more likely to be detected in areas with lower biomass. This relation between biomass and depletion can be inferred from the results in Table 5.4. The other one is that some depleted areas were close to the critical habitat areas of sea lion. So some management measures are needed to shift the fishing effort away from the sea lion critical habitat. In the last decade, there has been much research about the adverse impact of the fishery on sea lions and management measures have been implemented to prevent the adverse effects of fishery. However, it remains quite difficult to quantify the effectiveness of current measures and the linkage between the fishery and sea lion decline. It remains unknown what percentage of the decline of the Steller sea lion population change is due to the fishing.

5.5 Acknowledgments

The observer data were provided by Alaska Fisheries Science Center. Special thanks to Ren Narita for helping put the data together. The research is sponsored by a grant from the Pollock Conservation Cooperative Research Center to the University of Alaska Fairbanks (UAF). Additional funds for student support were provided by the Alaska Fisheries Science Center, through the Cooperative Institute for Arctic Research (NA17RJ1224) at UAF.

5.6 References

Adkison, M.D., and Su, Z. 2001. A comparison of salmon escapement estimates using a hierarchical Bayesian approach versus separate estimation of each year's return. Can. J. Fish. Aquat. Sci. 58: 1663–1671.

ADF&G (Alaska Department of Fish and Game). 2006. ADF&G chart series, Bering Sea 2006. http://www.cf.adfg.state.ak.us/geninfo/statmaps/charts.php.

Banerjee, S., Carlin, B.P., and Gelfand, A.E. 2004. Hierarchical modeling and analysis for spatial data. Chapman and Hall –CRC, Boca Raton, Fla.

Barbeaux, S.J., Dorn, M., Ianelli, J., and Horne, J. 2005. Visualizing Alaska pollock (*Theragra chalcogramma*) aggregation dynamics. ICES Document CM 2005/U: 01. 12 pp.

Battaile, B.C. 2005. A walleye pollock (*Theragra chalcogramma*) depletion estimator for the eastern Bering Sea, Ph.D. dissertation, University of Alaska, Fairbanks.

Battaile, B.C., and Quinn, T.J., II. 2004. Catch per unit effort standardization of the eastern Bering Sea walleye pollock (*Theragra chalcogramma*) fleet. Fish. Res. 70: 161–177.

Battaile, B.C., and Quinn, T.J., II. 2006. A DeLury depletion estimator for walleye pollock (*Theragra chalcogramma*) in the eastern Bering Sea. Nat. Resour. Model. 19: 655–674.

Beseg, J., York, J., and Mollie, A. 1991. Bayesian image-restoration, with 2 applications in spatial statistics. Ann. Inst. Stat. Math. 43: 1–59.

DeLury, D.B. 1947. On the estimation of biological populations. Biometrics. 3: 145–167.

Gelman, A., Carlin, J.B., Stern, H.S., and Rubin, D.B. 2004. Bayesian data analysis. 2nd ed. Chapman and Hall – CRC, London, UK.

Harley, S.J., Myers, R.A., and Dunn, A. 2001. Is catch-per-unit-effort proportional to abundance? Can. J. Fish. Aquat. Sci. 58: 1760–1772.

Ianelli, J.N., Barbeaux, S., Honkalehto, T., Kotwicki, S., Aydin, K., and Williamson, N. 2008. Assessment of walleye pollock stock in the eastern Bering Sea. In: Stock assessment and fishery evaluation report for the groundfish resources of the Bering Sea/Aleutian Islands regions. North Pac. Fish. Mgmt. Council, Anchorage, AK, section 1: 47–136.

Large, P.A. 1992. Use of multiplicative model to estimate relative abundance from commercial CPUE data. ICES J. Mar. Sci. 49: 253–261.

Leslie, P.H., and Davis, D.H.S. 1939. An attempt to determine the absolute number of rats on a given area. J. Anim. Ecol. 8: 94–113.

Livingston, P.A. 1993. Importance of predation by groundfish, marine mammals and birds on walleye pollock *Theragra chalcogramma* and Pacific herring *Clupea pallasi* in the eastern Bering Sea. Mar. Ecol. Prog. Ser. 102: 205–215.

Moura, F.A.S., and Migon, H.S. 2002. Bayesian spatial models for small area estimation of proportions. Statistical Modeling, 2(3): 183–201.

Myers, R.A. 2001. Stock and recruitment: generalizations about maximum reproductive rate, density dependence, and variability using meta-analytic approaches. ICES J. Mar. Sci. 58: 937–951.

Polovina, J.J. 1986. A variable catchability version of the Leslie model with application to an intensive fishing experiment on a multispecies stock. Fish. Bull. 84: 423–428.

Quinn, T.J., II. 1987. Standardization of catch-per-unit-effort for short-term trends in catchability. Nat. Res. Mod. 1: 279–296.

Quinn, T.J., II, and Deriso, R.B. 1999. Quantitative Fish Dynamics. Oxford University Press, New York.

Seber, G.A.F. 1982. The estimation of animal abundance, 2nd edition. Griffin, London.

Shen, H., Quinn, T.J., II, Wespestad, V., Dorn, M.W., and Kookesh, M. 2008. Using acoustics to evaluate the effect of fishing on school characteristics of walleye pollock. In: Resiliency of gadid stocks to fishing and climate change. Alaska Sea Grant, University of Alaska Fairbanks: 125–140.

Spiegelhalter, D.J., Best, N.G., Carlin, B.P., and van der Linde, A. 2002. Bayesian measures of model complexity and fit. J. R. Stat. Soc. [Ser B] (Stat. Method.) 64: 1–34.

Su, Z., Adkison, M.D., and Van Alen, B.W. 2001. A hierarchical Bayesian model for estimating historical salmon escapement and escapement timing. Can. J. Fish. Aquat. Sci. 58: 1648–1662.

Su, Z., Peterman, R.M., and Haeseker, S.L. 2004. Spatial hierarchical Bayesian models for stock–recruitment analysis of pink salmon (*Oncorhynchus gorbuscha*). Can. J. Fish. Aquat. Sci. 61: 2471–2486.

Thomas, A., Best, N., Lunn, D., Amold, R., and Spiegelhalter, D. 2004. GeoBUGS user manual. http://www.mrc-bsu.cam,ac.uk/bugs.

Wilson, C.D., Hollowed, A.B., Shima, M., Walline, P., and Stienessen, S. 2003. Interactions between commercial fishing and walleye pollock. Alaska Fish. Res. Bull. 10: 61–77.

Xiao, Y.S., Punt, A.E., Miller, R.B., and Quinn, T.J., II. (*Editors*). 2004. Models in fisheries research: GLMs, GAMs and GLMMs. Fish. Res. 70: 137–428.

Table 5.1. The tonnage of pollock and the number of hauls available for standardization after removal of catch data for two reasons listed in text.

			Elimination			
Year		Total Pollock catch	Pollock Non target	<20 hauls	Available data	% of total
2002	tons	255,850	5,631	4,608	245,610	96.0%
	Hauls	3,248	118	73	3,057	94.1%
2003	tons	258,078	4,436	6,051	247,590	95.9%
	Hauls	3,574	117	100	3,357	93.9%
2004	tons	258,785	15,301	4,988	238,494	92.1%
	Hauls	3,526	343	77	3,106	88.1%
2005	tons	257,582	6,744	5,757	245,079	95.1%
	Hauls	3,222	142	80	3,000	93.1%
2006	tons	262,061	4,151	5,025	252,884	96.4%
	Hauls	3,104	85	66	2,953	95.1%

Table 5.2. The averaged percentage of total sum of squares explained by the whole standardization procedure and by each factor used in the model.

Year	Average Explained	Vessel ID	Day
2002	25.2	24.5	0.7
2003	20.1	19.3	0.8
2004	17.4	16.2	1.2
2005	17.7	16.8	0.9
2006	17.2	16.1	1.1

Table 5.3. Chi-square test for expected proportions of positive and negative slopes and significant and non significant slopes given the null hypothesis of no depletion.

	2002	2003	2004	2005	2006	Pool
# significant neg	2	3	1	3	3	12
# non significant	19	22	20	20	14	95
# Significant pos	2	3	4	0	2	11
χ^2 (Pearson's)	7.43	15.91	19.04	10.96	19.23	52.34
df	2	2	2	2	2	2
p value	0.02	<0.001	<0.001	0.004	<0.001	<0.001
# negative slopes	12	16	9	15	15	67
# positive slopes	11	12	16	8	4	51

Table 5.4. The *p* values of linear relationship between depletion estimators and some explanatory variables using ADF&G areas inside SCA and surrounding areas. The data from 2002 and 2006 were pooled to conducted fixed effect analysis. The "+" in brackets means a positive relationship. The "–" in brackets means a negative relationship. Dummy variables (0, 1) were used to indicate whether an area is inside or outside the BSPRA or SCA, in which case a "1" indicates an area is inside.

Dependent variables	Slopes		Cumulative depletion	
DeLury slope type	All	Negative	All	Negative
Year	0.15	0.29	0.47	0.85
ADF&G area	0.87	0.59	0.38	0.75
Inside BSPRA	0.41	0.98	0.32	0.74
Inside SCA	0.41	0.09	0.35	**0.01(1 is –)**
ln(Initial Biomass)	**0.003(+)**	**<0.001(+)**	0.76	0.75
Total Catch	**0.03 (+)**	**0.02(+)**	0.21	0.59
Total Effort	**0.01(+)**	**0.02(+)**	0.29	0.80
Distance to Dutch Harbor	0.20	0.45	0.59	0.58
Unalaska Island	0.27	0.55	0.39	0.64
Akutan Island	0.15	0.39	0.88	0.49
Akun Island	0.12	0.34	0.65	0.34
Unimak Island	0.14	0.27	0.40	0.38
Amak Island	0.77	0.69	0.14	0.53

Table 5.5. The estimated slopes ($-q$) from different models and significant slopes at α=0.05 level.

		Bayesian Models					
	Frequentist	1	2	3	4	5	6
Non-significant slope	66	74	72	72	73	72	79
Significant positive slope	9	5	5	6	7	6	2
significant negative slope	10	6	8	7	5	7	4
Positive slope	36	40	40	39	41	39	41
Negative slope	49	45	45	46	44	46	44

Note: Model 1 is the Area-specific model with same variance across all areas. Model 2 is the Area-specific model with different variances. Model 3 is the HBM with same variance across all areas. Model 4 is the HBM with different variances. Model 5 is the SHBM with same variance across all areas. Model 6 is the SHBM with different variances.

Table 5.6. Model-checking quantities for the alternative models with the DeLury depletion modles as the data-level structure for area around SCA.

Year	Model	Quantity σ^2	$\overline{D}$	$\hat{D}$	N_p	p_D	DIC
2002	Area-specific	Same	104	65	39	39	143
		Diff	–91	–153	57	62	–29
	HBM	Same	105	67	43	37	142
		Diff	–92	–151	61	60	–32*
	SHBM	Same	106	69	43	37	143
		Diff	–76	143	61	66	–10
2003	Area-specific	Same	–161	–196	35	35	–126
		Diff	–252	–308	51	58	–192
	HBM	Same	–161	–195	39	34	–127
		Diff	–252	–196	55	56	–196*
	SHBM	Same	–160	–195	39	35	–125
		Diff	–247	–306	55	59	–188
2004	Area-specific	Same	–244	–283	39	39	–205
		Diff	–332	–395	57	63	–269
	HBM	Same	–244	–282	43	38	–206
		Diff	–333	–394	61	61	–272*
	SHBM	Same	–243	–281	43	38	–205
		Diff	–330	–392	61	62	–268
2005	Area-specific	Same	–140	–171	31	31	–109
		Diff	–206	–258	45	52	–154
	HBM	Same	–139	–170	35	31	–108
		Diff	–207	–255	49	48	–159*
	SHBM	Same	–139	–169	35	30	–109
		Diff	–204	–253	49	49	–155
2006	Area-specific	Same	–217	–248	31	31	–186
		Diff	–342	–394	45	52	–290
	HBM	Same	–217	–248	35	31	–186
		Diff	–340	–386	49	46	–294*
	SHBM	Same	–216	–247	31	31	–185
		Diff	–324	–380	49	56	–268

Note: σ^2, variance of residuals; Same, same value for all ADFG areas; Diff, different values for each ADFG area; No., the model number referred to in the text; $\overline{D}$, the posterior average of deviance; $\hat{D}$, point estimate of deviance at the posterior expectations of parameters; N_p, the nominal number of parameters in the model; p_D, the effective number of parameters; DIC, deviance information criterion. *The case with the best fit or lowest deviance information criterion (DIC) of the six models.

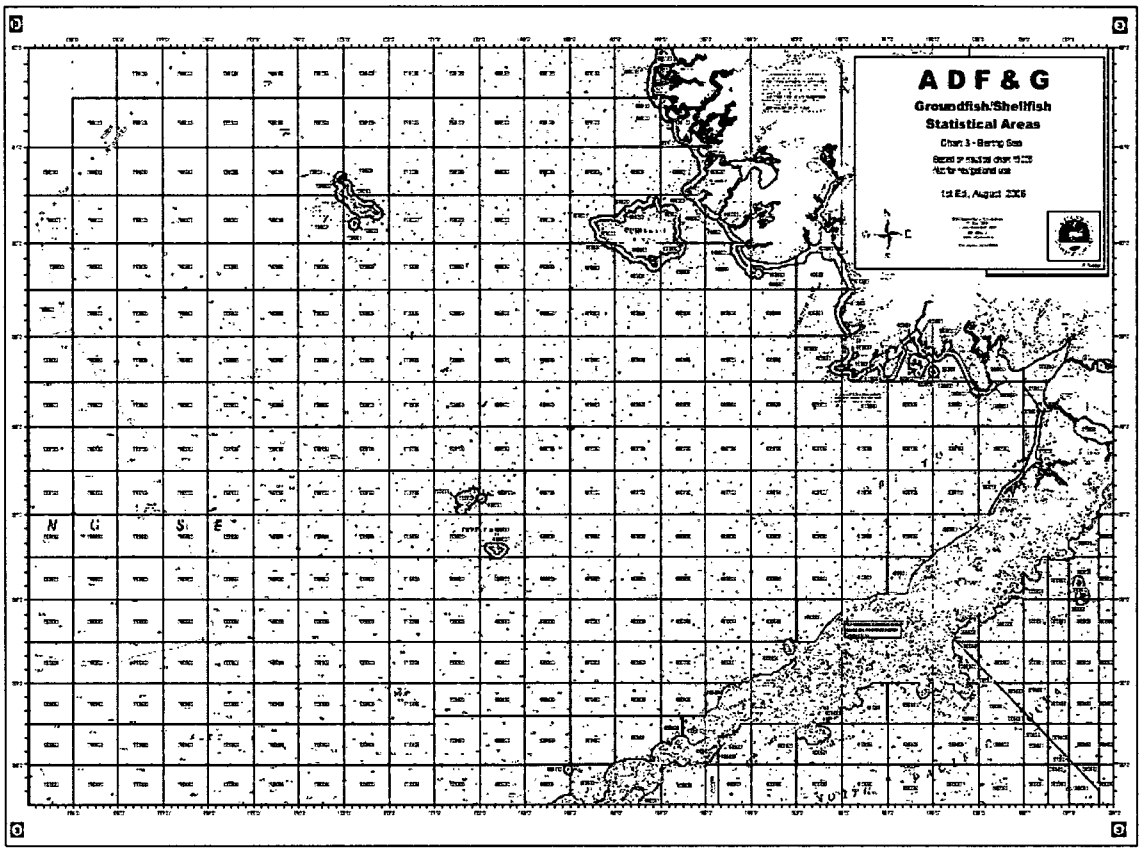

Figure 5.1. Maps of the Bering Sea/Aleutian Islands showing the Alaska Department of Fish and Game statistical areas (ADF&G, 2006).

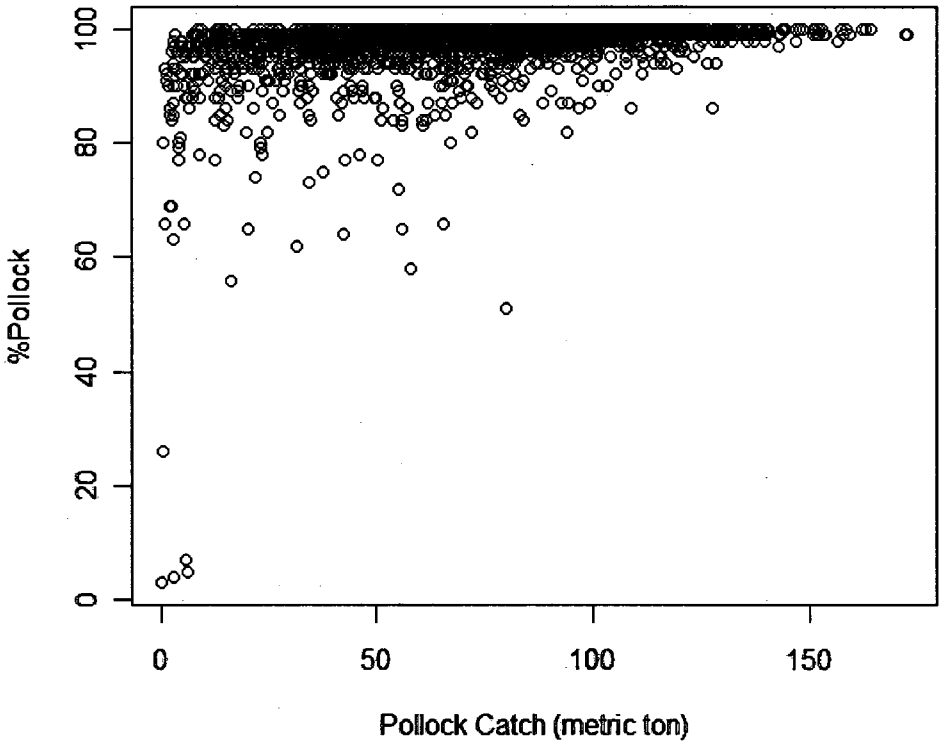

Figure 5.2. Percentage of pollock in haul versus haul weight for 2003.

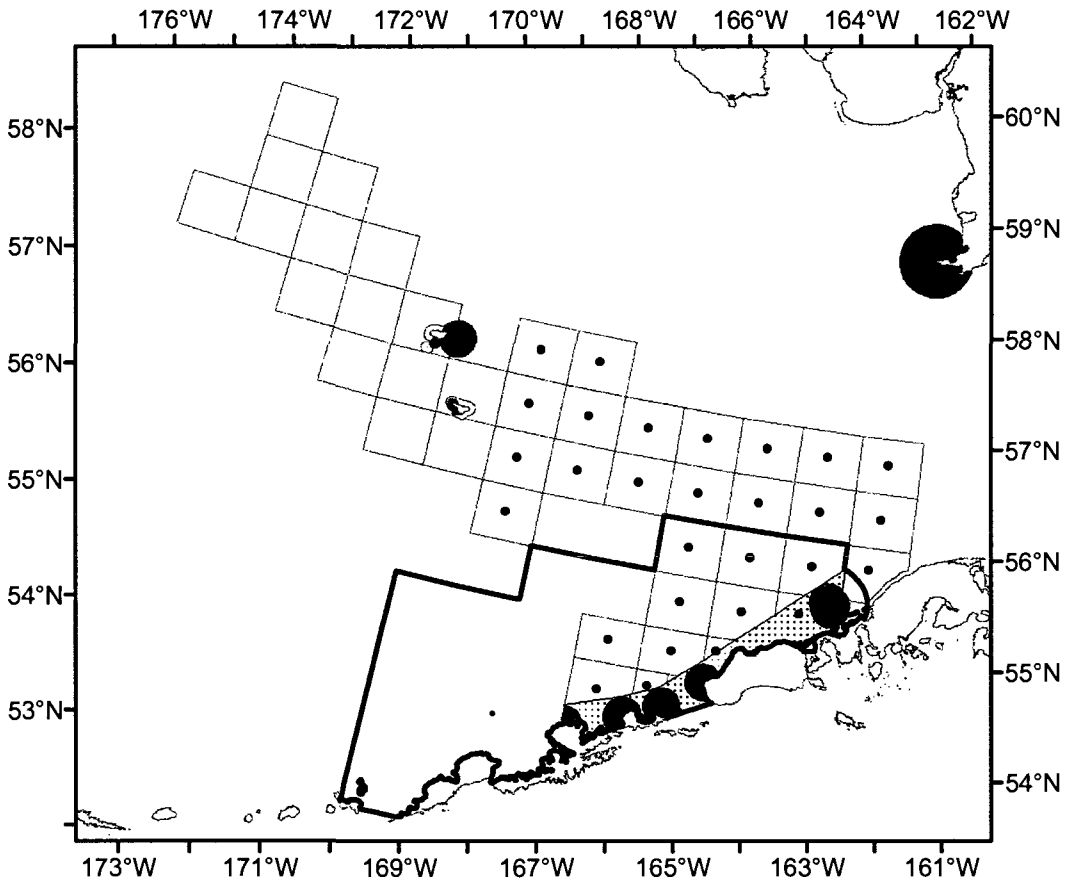

Figure 5.3. Map of southeastern Bering Sea showing the Steller sea lion conservation area (SCA, outlined in bold), the Bering Sea Pollock Restricted Area in dot shading and Critical habitat areas (hatched circles) surrounding sea lion haulouts and rookeries within the BSPRA. ADF&G areas (blocks) shown are the focus of much of the analysis in this chapter. Blocks with centroid dots show the areas inside SCA and surrounding areas.

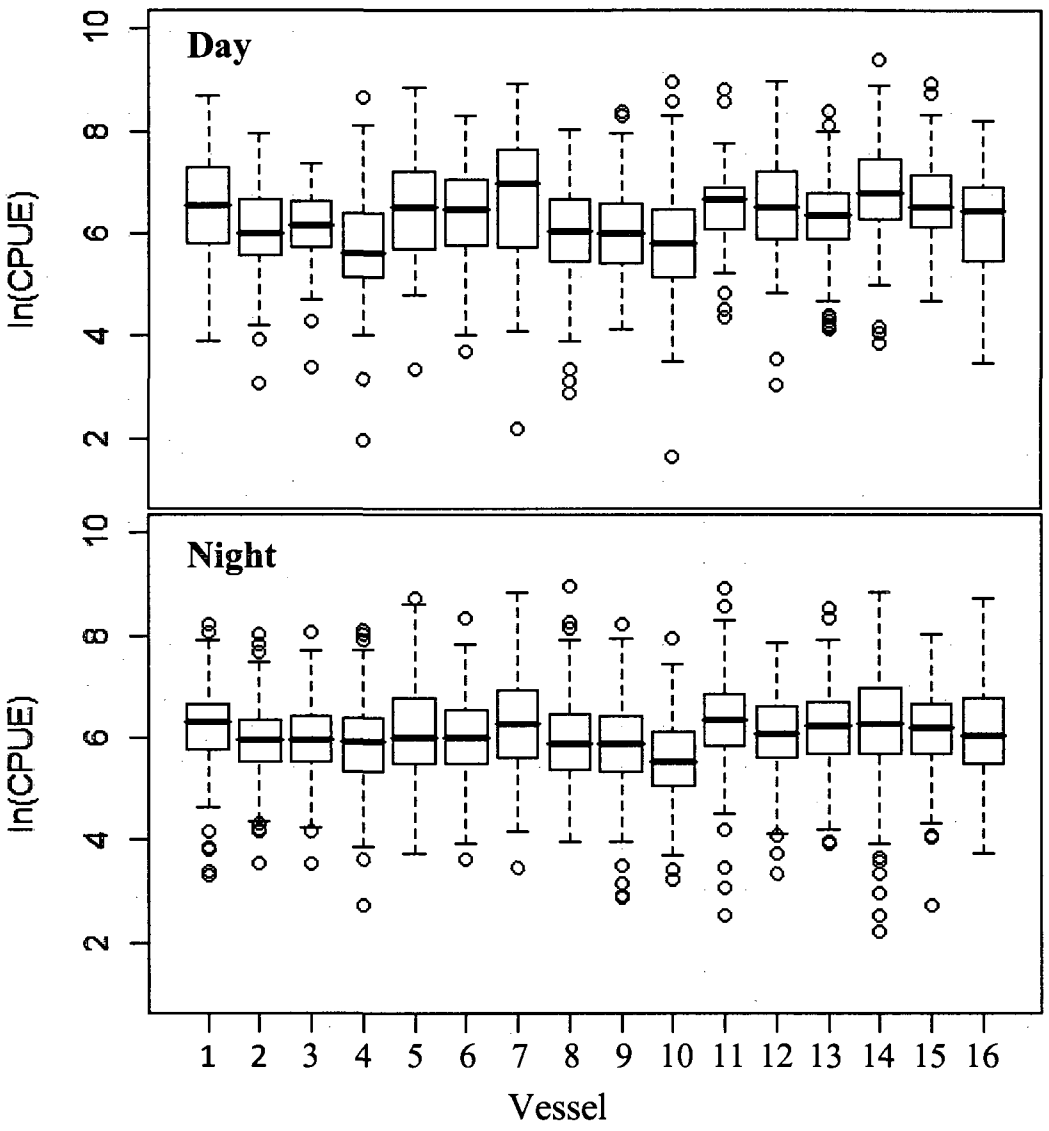

Figure 5.4. The box plots of ln(CPUE) of different vessels. The upper panel displays lnCPUE in daytime and bottom panel displays the ln(CPUE) at nighttime (using data in year 2003).

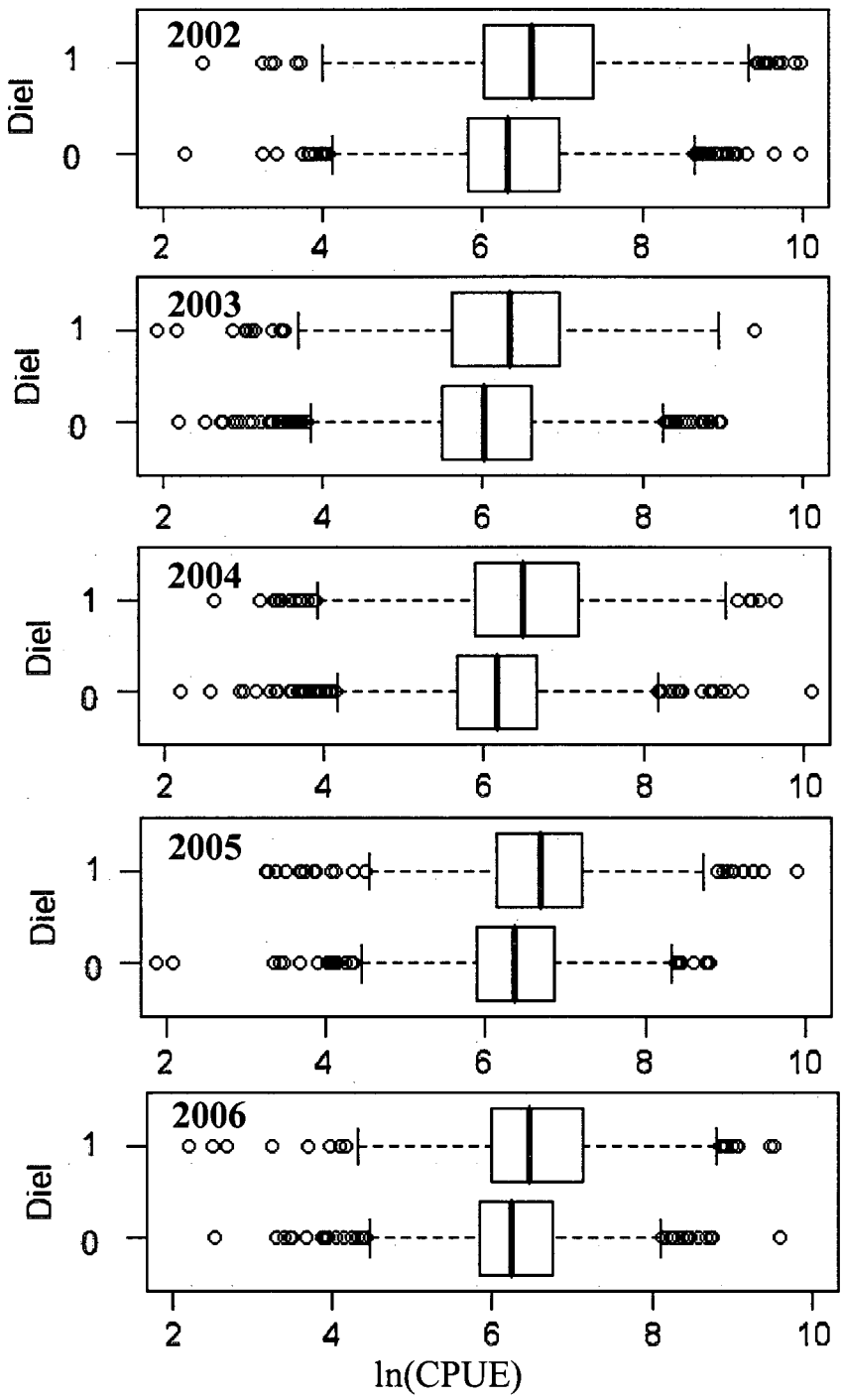

Figure 5.5. The box plots of ln(CPUE) in daytime and nighttime from 2002–2006 (top to bottom). On y-axis, "1" represents hauls in the daytime, and "0" represents hauls at nighttime.

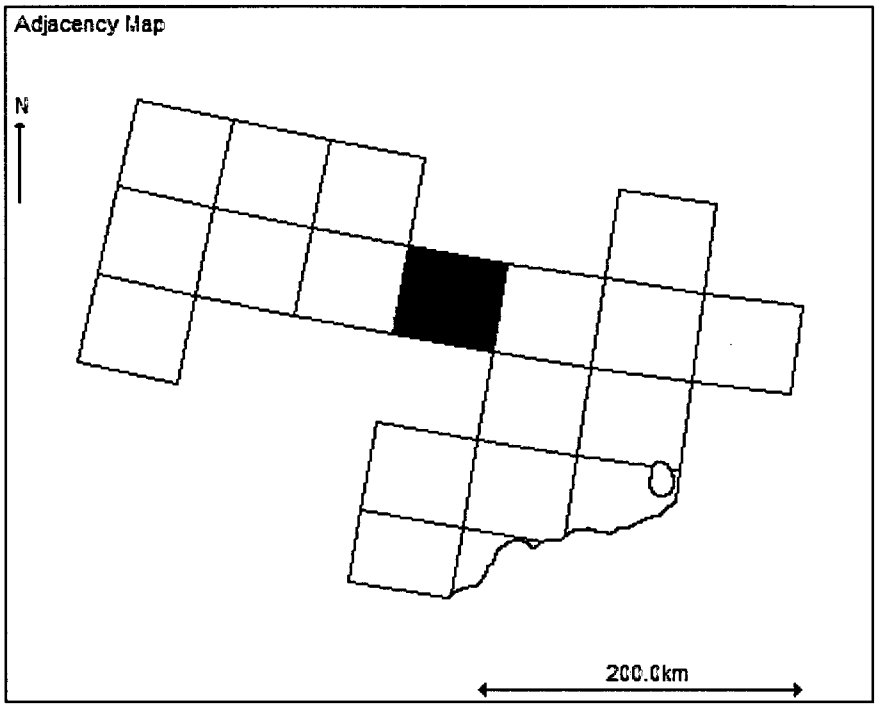

Figure 5.6. The rough map of 19 ADF&G areas inside or close to SCA in 2002, showing what are considered as adjacent areas (lightly gray shading) to area 655600 (black shading).

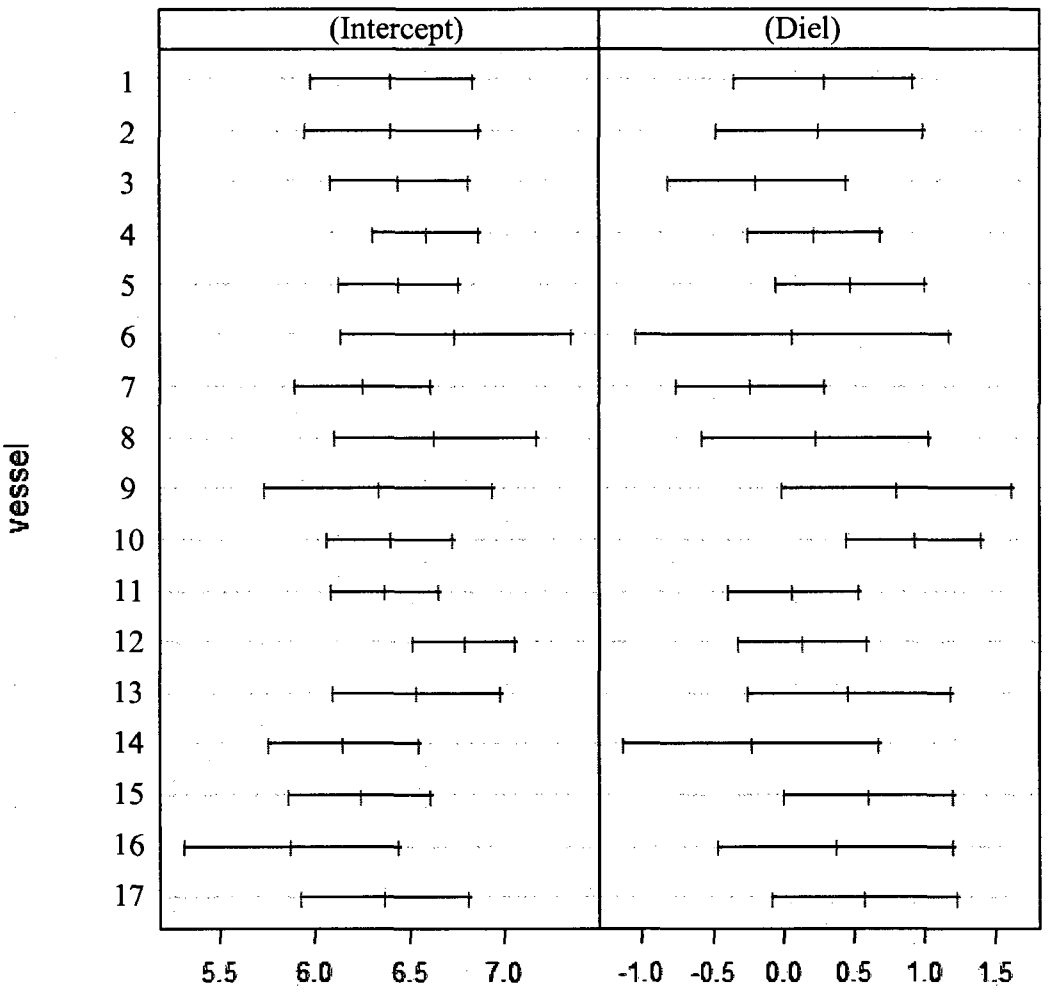

Figure 5.7. Ninety-five percent confidence intervals of intercepts and slopes for each vessel in the data using data of area 645501 in 2004.

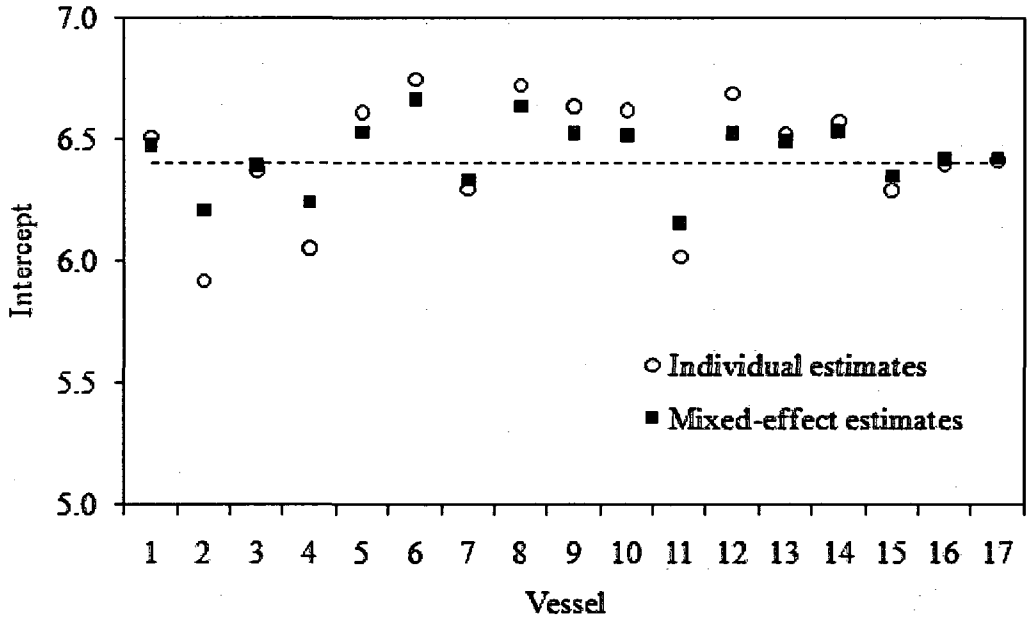

Figure 5.8. The estimated intercepts using fixed-effect individual models and mixed-effect model. The dash line indicated the fixed effects in mixed-effects estimates.

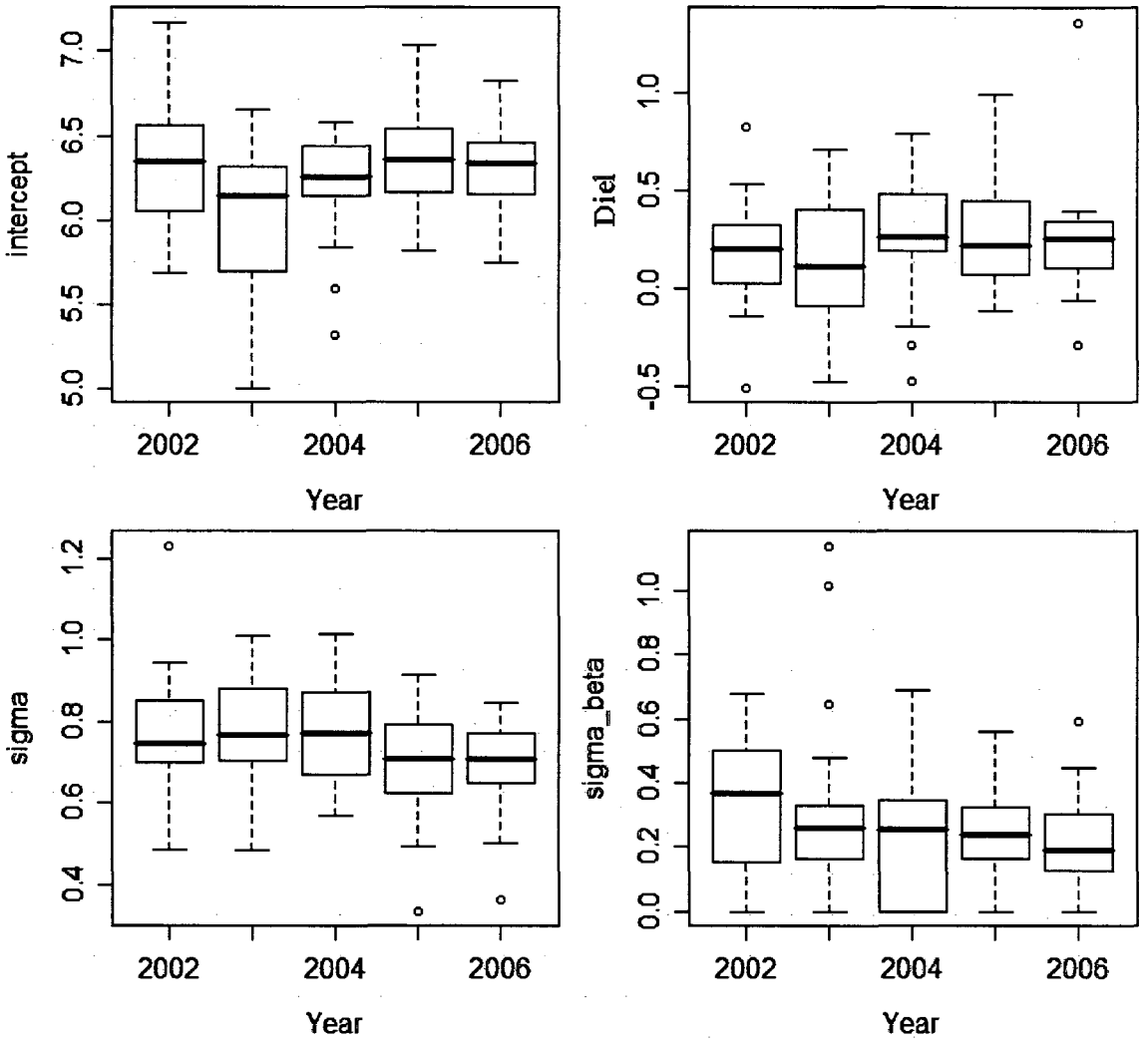

Figure 5.9. Box plots of estimated coefficients for all factors during 2002–2006. Sigma is the within-vessel variation and Sigma_Beta is the among-vessel variation.

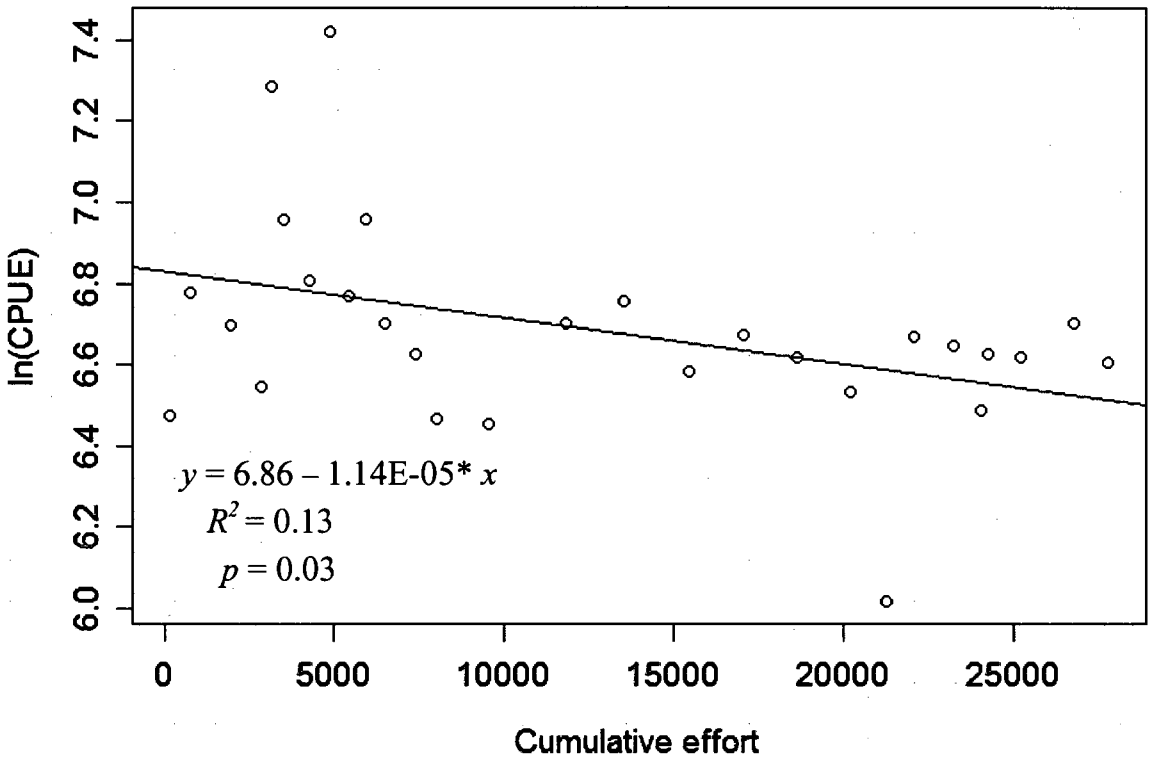

Figure 5.10. An example illustrating the linear relationship between natural log-transformed CPUE and cumulative effort in the DeLury model.

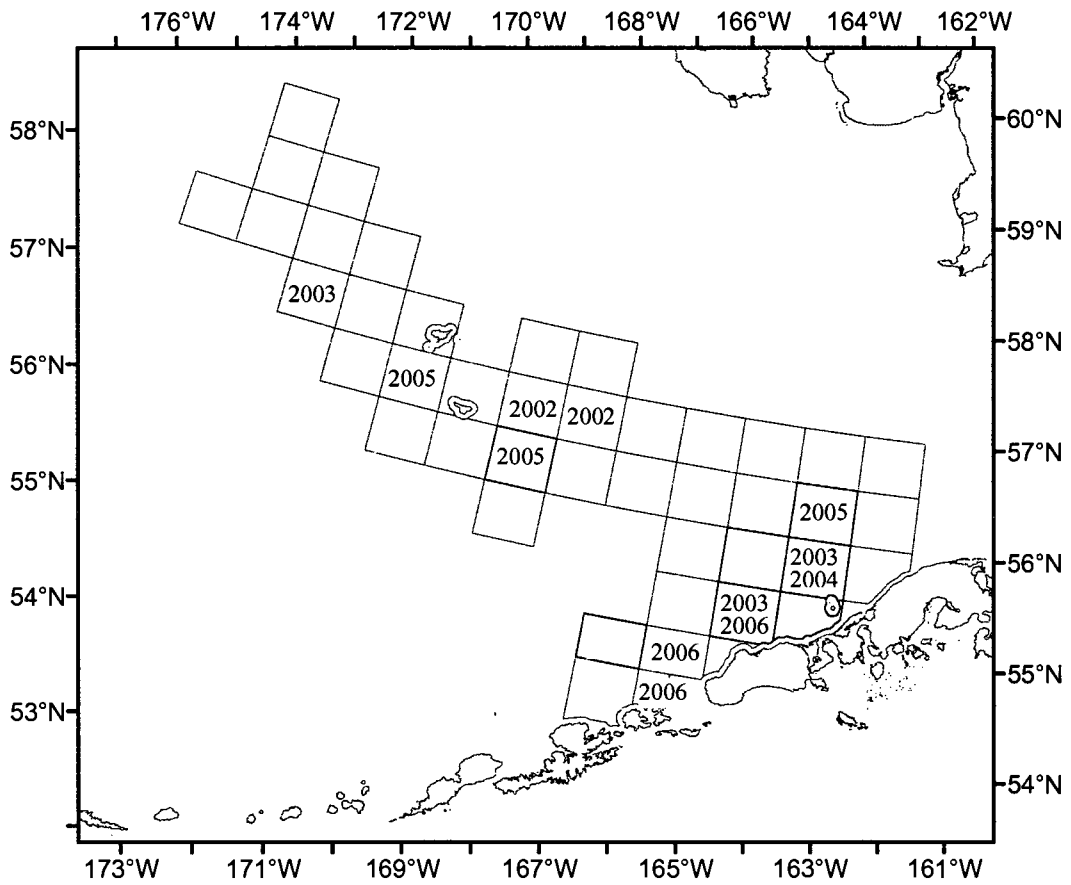

Figure 5.11. Map of the EBS showing the ADF&G areas with enough data for analysis. The years where significant depletion occurred are shown in the quadrats.

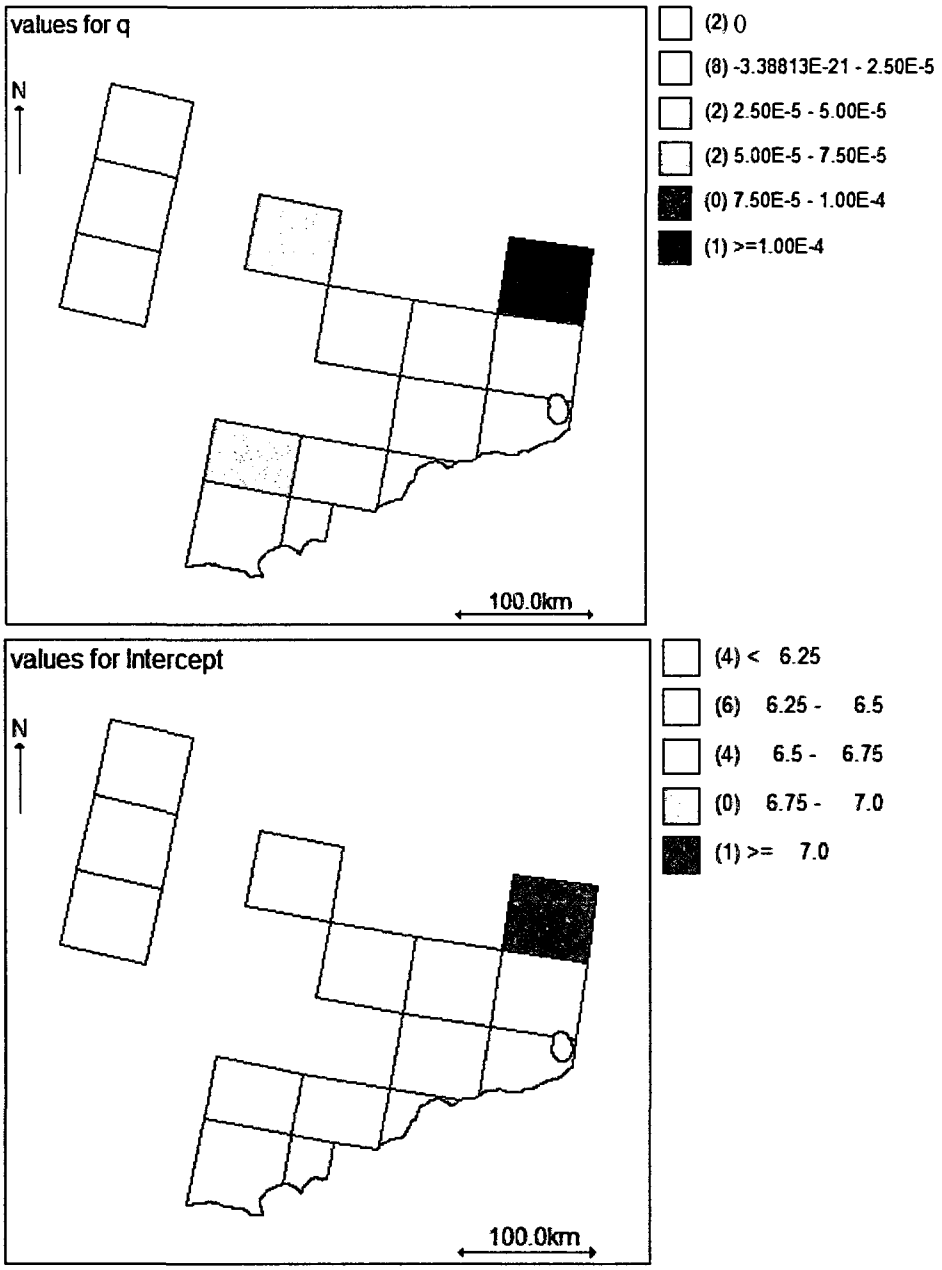

Figure 5.12. The spatial distribution of estimated values of q (upper panel, more positive value means more depletion) and intercepts (lower panel) from the spatial hierarchical Bayesian model using same variance across all areas.

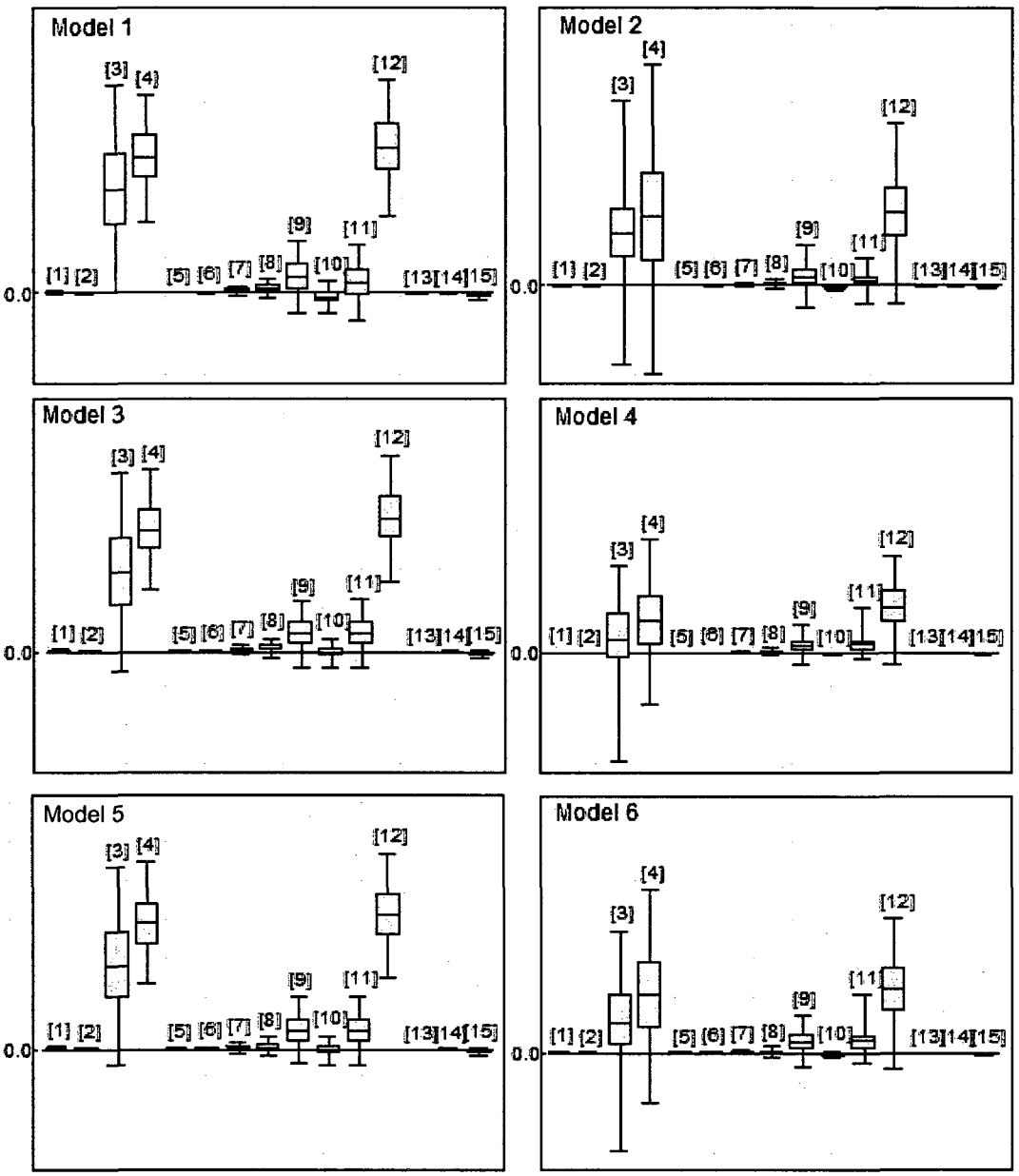

Figure 5.13. Box plots of posterior inferences of q_i's (median and 95% probability intervals), obtained from the Models 1–6 in 2006.

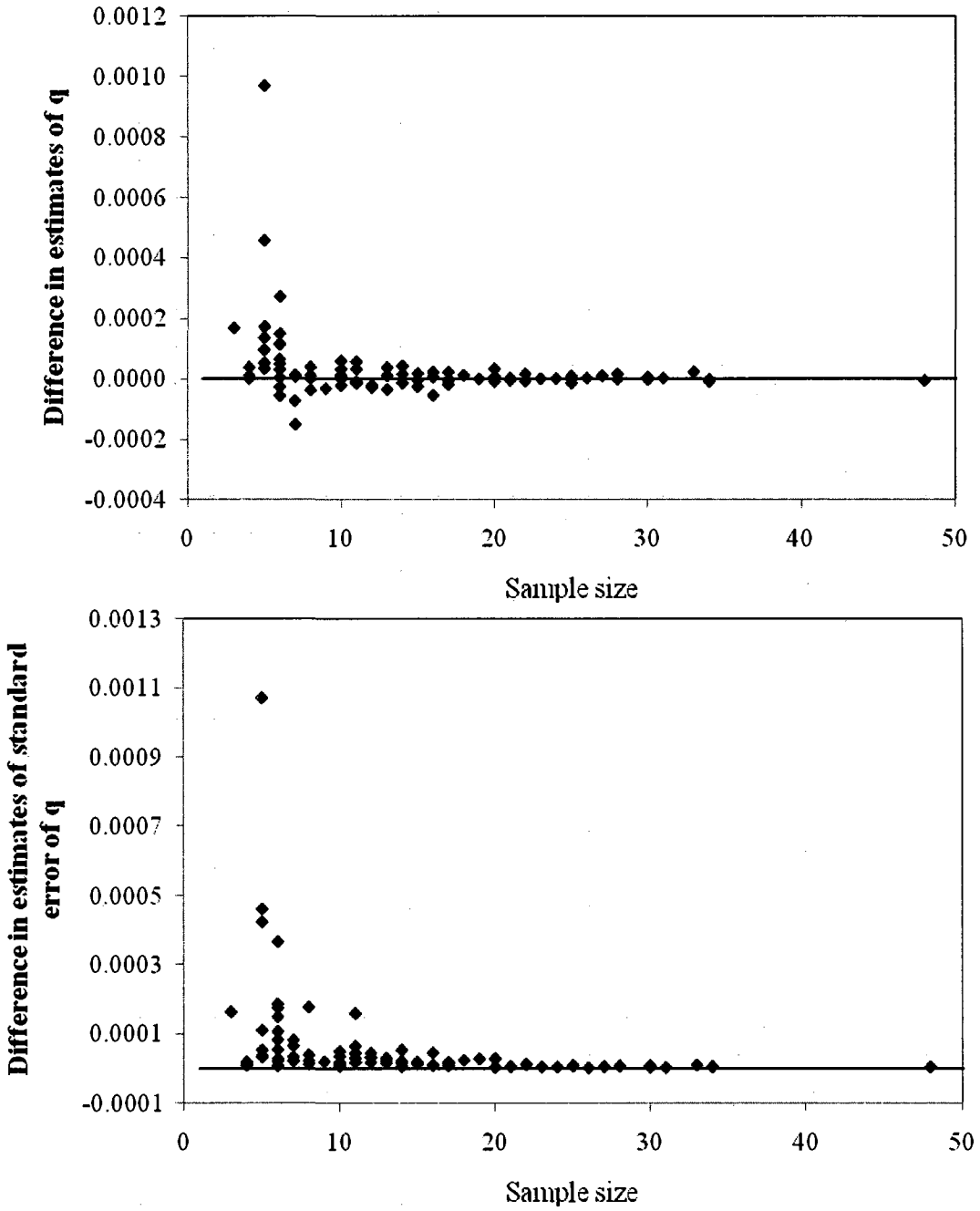

Figure 5.14. Differences between frequentist and hierarchical Bayesian model (Model 5) estimates of cathcability q and its associated standard error relative to the sample size.

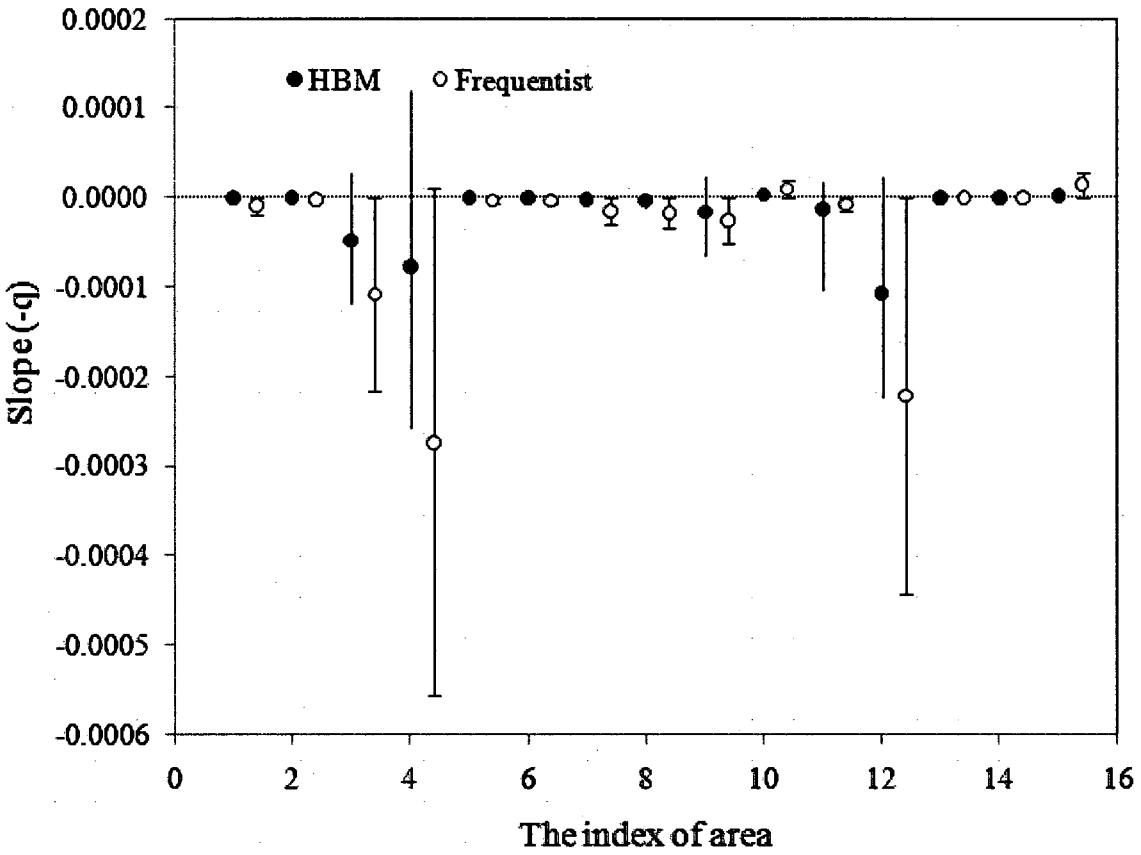

Figure 5.15. Posterior inferences (median and 95% probability intervals) of depletion slopes ($-q_i$'s), obtained from the hierarchical Bayesian model (Model 4) and frequentist method using data in 2006.

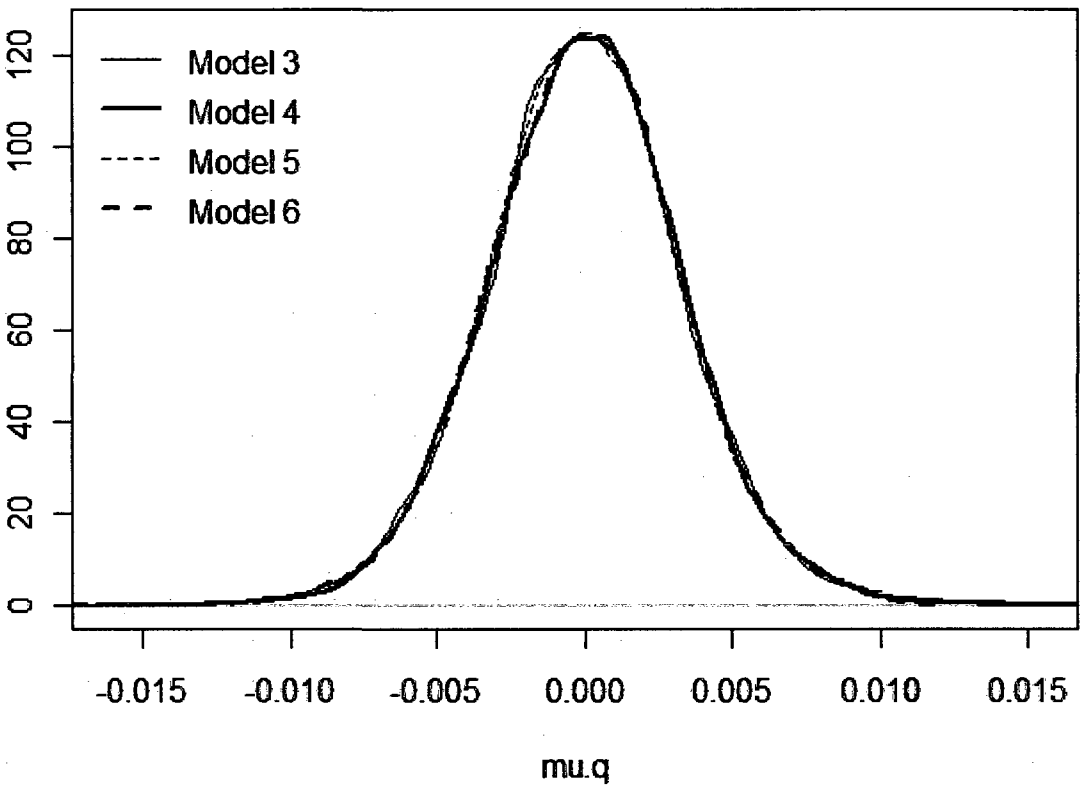

Figure 5.16. Posterior density of μ_q for Models 3–6, year 2006.

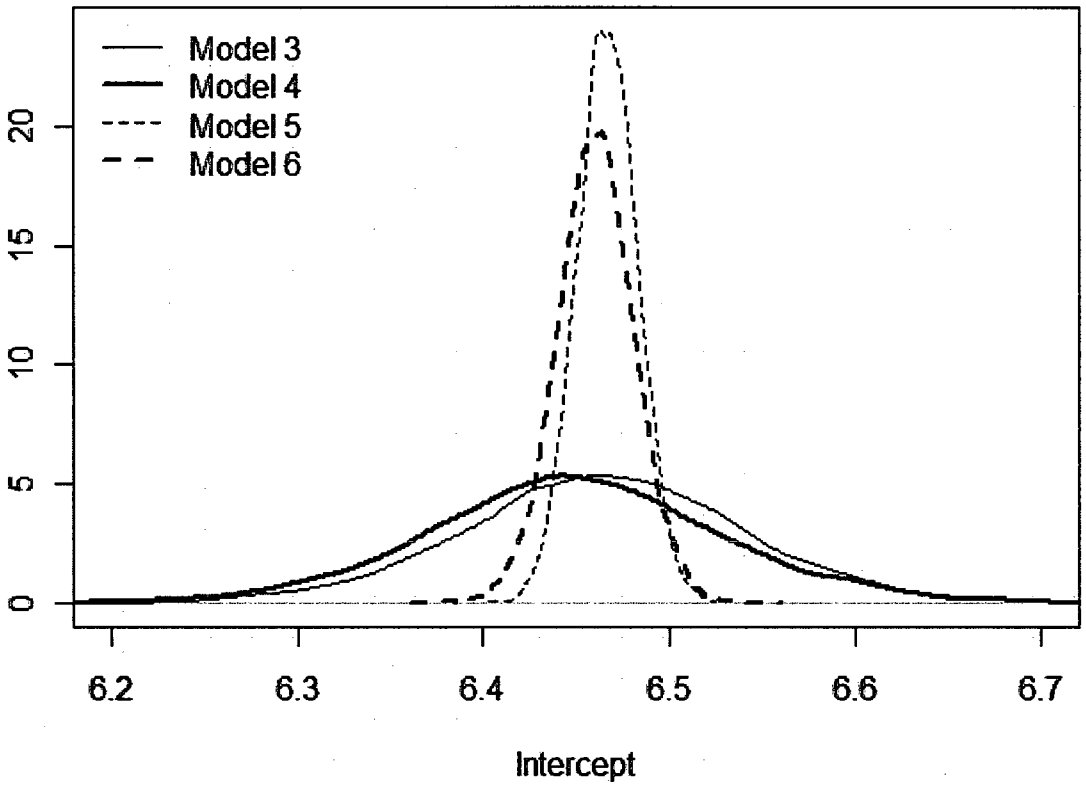

Figure 5.17. Posterior densities of hyperparameters of intercepts for Models 3–6, year 2006.

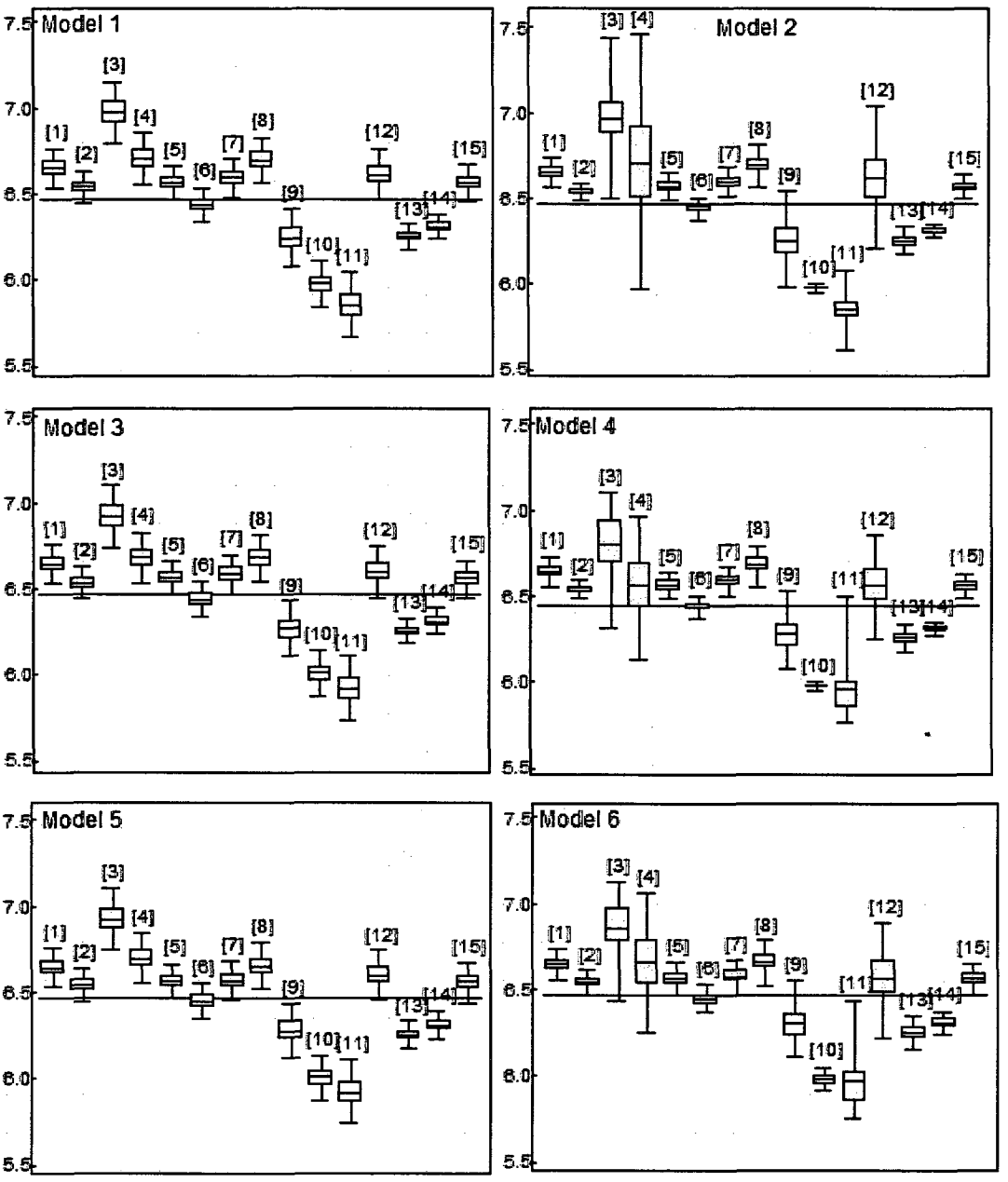

Figure 5.18. Box plots of posterior distributions of intercepts (median and 95% probability intervals), obtained from the Models 1–6 in 2006.

General Conclusions

There has been increasing concerns since 1990 about the ecological impact of the commercial fishery on walleye pollock (*Theragra chalcogramma*) in the eastern Bering Sea (EBS). Pollock form persistent mid-water and near-bottom schools during the spawning season. This schooling behavior can exaggerate the fishing impact because harvesters are skilled at finding fish aggregations using search strategies aided by technology. Although there are many scientific surveys in the EBS, there are few surveys conducted in winter when the first major fishing season occurs, which has made it difficult to explore pollock distribution and fishing impact in this season. To better understand the mechanism of pollock abundance and distribution in winter, we must rely on the information from the commercial fishery, such as observer data collected since 1990. This project started in 2001 to explore the feasibility of collecting acoustic data using commercial fishing vessels. The acoustic data provided information about pollock distribution as well as vessel distribution in the winter fishing season. This dissertation focused on investigating pollock distribution related to the fishery and environmental factors using fisheries acoustic data and observer data.

The first stage of this work (chapter 1) investigated the changes in school characteristics of pollock during a short period. Spawning pollock distribution has a strong diel cycle with dense schools during the daytime and sparser layers during the nighttime. Schools also aggregate into clusters, even clusters of clusters. After some days of fishing, pollock spatial distribution changed at different scales over a short time (about one month). Pollock schools became denser, smaller and smoother. The spatial distribution of schools became sparser, as evidenced by the lower frequency of schools per elementary distance sampling unit and the increase in average next neighbor distances (NND). The increased estimates from variography also indicated some changes at scales larger than 1 nautical mile. It is interesting to note that the average NND between schools within a cluster and the average abundance of clusters did not change significantly. Therefore, the increased overall NND was caused by an increase in inter-cluster distance

and in distance between solitary schools. Although the changes in aggregation pattern were found during fishing, it is still difficult to determine whether these changes are due to the fishery or biological changes in behavior and movement related to environmental factors and the end of the spawning season.

To further investigate the mechanisms explaining pollock spatial distribution, three environmental factors were used to uncover the relationship between pollock distribution and physical conditions as well as spatial autocorrelation in the winter fishing season (chapter 2). Daytime environmental data and fish density from acoustics were used in this chapter. Models were constructed to describe the relation between pollock density and environmental factors, as well as to incorporate spatial autocorrelation. For each data set from different months and years, the best model was selected according to AIC values. It turned out that temperature and wind were important in pollock distribution at different scales. It is obvious that pollock avoid cold water; the general distribution of pollock was limited to the south of St. George Island in cold years (e.g., 2002 and 2006). The dome-shaped relationship between temperature and pollock density indicated that pollock density was not only influenced by cold water but also relatively high temperature which has not been mentioned before. Pollock density was relatively higher in waters with temperature 3.5 ~ 4.0°C. Because wind speed changed at a daily scale, wind speed tended to affect pollock density at a small scale. There was a negative relationship between pollock density and wind speed. After accounting for the influences of environmental factors, the spatial pattern differed in February from January, although pollock distributed in similar areas of north Unimak Island. From examination of the variograms, the increased ranges indicated that the spatial correlation among pollock extended to greater distances. And the decreased partial sill suggested that the fishery may smooth out the spatial structure and cause the decrease of the variation among pollock density.

Compared to little information about pollock in winter, there are plenty of data about vessel distribution from Vessel Monitoring Systems (VMS) and data collected from the observer program. Harvesters search for fish aggregations and catch them;

therefore, the vessel distribution can reflect the underlying fish distribution if harvesters search the entire range of pollock. The linkage between vessel and fish distribution could allow inferences to be made about pollock distribution when actual fish information is not available. The third stage of this work (chapter 3) was to classify the searching behavior of harvesters and its relation to pollock distribution. Harvester behavior was examined using the Lagrangian approach which utilizes trajectories of the harvester's movement. The searching pattern was reasonably described by a Levy flight process, one kind of random walk model. Rather than correlated to the spatial concentration of pollock distribution, harvester behavior was strongly associated with the fractal dimension of pollock distribution which indicates the degree of clustering of fish. Therefore, the movement parameter of vessels can be considered as a good indicator of fish spatial distribution at a large scale, and it might contribute to real-time monitoring of the EBS pollock fishery.

Instead of vessel trajectories, the observer data were used to explore the fishing behavior related to pollock distribution at a smaller scale (chapter 4). A principal component analysis with instrumental variables was carried out to evaluate the effect of schooling pattern on fishing behavior in two fishing grounds: north Unimak Island and near the Pribilof Islands, in 2003 and 2005. There were significant differences in school descriptors among areas and years due to different abundance and physical conditions. Because harvesters chase fish aggregations, the different aggregation patterns have influences on fishing behavior. Our results indicated that school density had a greater effect than school size on fishing behavior. When they encountered less dense aggregations, the harvesters tended to fish with longer tows at higher speeds.

In previous chapters, the removals from the population were not explicitly considered. The fishery disproportionally removes fish in different areas which can cause local depletion. To examine the local depletion in the southern EBS, the DeLury model was used to conduct catch depletion analysis, especially in ADF&G areas inside or close to the Steller sea lion conservation area (SCA). The first step was to prepare data for

depletion analysis to avoid the large variation in observer data caused by other factors. A mixed effects model was found to be better than a fixed effects model for catch per unit effort (CPUE) standardization using two important factors: Vessel ID and haul during day or night. Then the frequentist method was used to estimate the depletion estimators. Significant depletion was detected in some areas from 2002 to 2006. Post hoc analysis indicated that the depletion is more likely to be detected in areas with low pollock biomass, catch and effort. Finally, different Bayesian models were used to investigate the local depletion with hierarchical structure and spatial structure. The best model was found to be the non-spatial hierarchical Bayesian model using different variance among areas. The "borrowing strength" of hierarchical Bayesian models improved the estimates by using frequentist methods. Compared to the results of previous study, there were fewer areas being significantly depleted by the pollock fishery. This suggests that management measures put into place in 1999 may have been effective in spreading fishing effort out in space and time and decreased the local depletion during 2002–2006.

In this dissertation, data from the commercial fishery were used to analyze the pollock abundance and distribution in the winter fishing season. The key finding is that there was significant spatial structure in pollock distribution which should be included in stock assessment. It is clear that we have detected some changes in pollock distribution at the school scale and at the larger scales during fishing. And some part of the changes can be attributable to the fishery. The significant correlation between fish and harvesters suggested that vessel distribution can be used as an indicator of fish distribution when there is no information about fish. Finally, the catch depletion analysis confirmed that there appeared to be less local depletion in recent years compared to years before 1999.

Generally speaking, the opportunistic acoustic data collected from fishing vessels can be used to investigate pollock abundance and distribution related to the fishery and physical condition at different temporal-spatial scales. This project has indicated that these data can substantially augment and enhance data collection and resource management in the Bering Sea. However, there are still some questions to be addressed.

Acoustic data are voluminous (terabytes) and its collection, storage and retrieval are time-consuming. Some programs need to be created to automatically process the raw data and extract the useful information. More help is needed from crews and researchers to see that proper maintenance and servicing of on-board data storage devices is done. The data loggers worked well when instructions were followed, but there were a number of occasions when the data loggers did not produce any information because of minor technical problems. This work is continuing and better data can be collected with proper cooperation and communication in the future. Research like this are going around the world, as shown in the proceedings of the international ICES SEAFACTS meeting in Berge, Norway, 2007, published as volume 66, number 6 of the ICES Journal of Marine Science. Furthermore, the opportunistic acoustic data (OAD) are much cheaper and have larger spatiotemporal coverage than a dedicated scientific survey. The increase of OAD of good quality can help augment the information about fish distribution and improve fisheries management.

Appendix

List of Symbols and Acronyms

Chapter 1

D_{clus}	Distance to the next cluster
D_{soli}	Next-neighbor distance among solitary schools
EDSU	Elementary distance sampling unit
h	Lag distance
I_{abun}	Abundance index
I_{clus}	Abundance index of cluster
I_{soli}	Abundance index of solitary school
L_{clus}	Length of cluster
L_{tr}	Track length
m	Number of EDSUs
n_i	Number of schools of ith EDSU
$\overline{n}$	Average number of schools in an EDSU
N_{clus}	Number of clusters
N_s	Number of schools per cluster
N_{soli}	Number of solitary schools
N_{tot}	Total number of schools
$N(h)$	Number of pairs with a distance h apart
$NASC$	Nautical area backscattering coefficient (m^2/nm^2)
nm	Nautical mile
NND	Next-neighbor distance
s_i	Location of ith observation
s_L	Line backscattering coefficient (m)
s_v	Volume backscattering coefficient (linear measure)
S_v	Volume backscattering strength (dB re 1 m^{-1})

V_D	Vertical distribution (m)
$z(s_i)$	Value of school descriptor s_v at location s_i
$\gamma(\cdot)$	Semivariogram
ρ_{clus}	Number of schools per unit cluster length

Chapter 2

C_k	The kth environmental variables measured
D_E	Depth of the Ekman layer
$N(h)$	Number of pairs with a distance h apart
$S(x_i)$	Stationary Gaussian process
W	Wind speed
β	Regression coefficents
$\gamma(\cdot)$	Semivariogram
$\mu(x_i)$	Mean effect
ρ	Correlation coefficient
σ^2	Sill
τ^2	Nugget effect
ϕ	Range
φ	Latitude

Chapter 3

a	Parameter of exponential function
b	Parameter of exponential function
C	Normalization constant, $C = (\mu - 1) l_{\min}^{\mu-1}$
D	Fractal dimension
EDSU	Elementary distance sampling unit
l	Move length

l_{min}	Minimum value of move length l
m	Slope at the origin of a log-log semivariogram
n	Number of moves
R_n^2	Net squared displacement
s_A	Nautical area backscattering coefficient (m^2/nm^2)
Ss	Spatial concentration index
x	Cumulative fraction of s_A
y	Cumulative fraction of EDSU
α	Parameter characterizing diffusive process
μ	Exponent of power law distribution

Chapter 4

A	Area of pollock school
D	Depth of pollock school
E	Elongation of pollock school
F	Fractal dimension of pollock school
fd	Fishing depth
fD	Fishing duration
fS	Fishing speed
fs_A	Fish density during fishing
L	Length of pollock school
P	Perimeter of pollock school
P3	Pribilof Islands in 2003 (class)
P5	Pribilof Islands in 2005 (class)
PCAIV	Principal component analysis with instrumental variables
s_A	Nautical area backscattering coefficient (m^2/nm^2)
sD	Searching duration

sS	Searching speed
ss_A	Fish density during search
S_v	Volume backscattering strength (dB re 1 m^{-1})
T	Thickness of pollock school
U3	Unimak Island in 2003 (class)
U5	Unimak Island in 2005 (class)

Chapter 5

b_0	Intercept, $\ln(qB_0)$
B_0	Initial biomass
C	Catch
D	Deviance
D_{cum}	Cumulative depletion
E	Cumulative effort
f	Fishing effort
M	Natural mortality
N_p	Nominal number of parameters
p_D	Effective number of parameters
q	Catchability
U	Catch per unit effort (CPUE)
y	Logarithm of CPUE
ε	Error term
$\boldsymbol{\theta}$	Posterior of parameter
μ_b	Mean of intercept
μ_q	Mean of catchability
σ^2	Variance